

Structure-Property Relationships to Understand Comprehensive Rejuvenation Mechanisms of
Aged Asphalt Binder

by

Amirul Islam Rajib

A Dissertation Presented in Partial Fulfillment
of the Requirements for the Degree
Doctor of Philosophy

Approved July 2020 by the
Graduate Supervisory Committee:

Elham Fini, Chair
Huiming Yin
Kamil Kaloush
Mahour Parast
Michael Mamlouk
Mounir El Asmar

ARIZONA STATE UNIVERSITY

August 2020

ABSTRACT

This research focused on the structure-property relationships of a rejuvenator to understand the comprehensive rejuvenation mechanism of aged asphalt binder. Aged asphalt such as recycled asphalt shingles (RAS) and reclaimed asphalt pavement (RAP) contain various amounts of asphalt binder. However, the asphalt binder in RAS and RAP is severely aged and inferior in properties compared to a virgin binder. To address this issue, liquid additives have been used under the general title of rejuvenators. That poses an additional challenge associated with the lack of clear metrics to differentiate between softeners and rejuvenators. Therefore, there is a need for a thorough study of rejuvenators. In this study, diverse-sourced rejuvenators have been used in RAS and RAP-modified binders as well as laboratory-prepared aged binders. The properties of the rejuvenated aged binder were characterized at a macro-level and molecular level. The study showed that the performance of the RAS-modified binder was significantly improved after bio-modification by a bio-rejuvenator.

This study further evaluated laboratory-prepared aged asphalt rejuvenated with different rejuvenators. The results found that oxidized bitumen became soft after adding rejuvenators, regardless of their source. Molecular dynamics simulation showed that the effective rejuvenator restored the molecular conformation and reduced the size of asphaltene nanoaggregates.

The study results showed that due to the specific chemical composition of certain rejuvenators, they may negatively impact the durability of the mixture, especially about

its resistance to moisture damage and aging. Computational analysis showed that while the restoration capacity of rejuvenators is related to their penetration into and peptizing of asphaltene nanoaggregates, the durability of the restored aged asphalt is mainly related to the polarizability values of the rejuvenator. Rejuvenators with lower polarizability showed better resistance to aging and moisture damage.

In summary, this study develops the rheology-based indicators which relate to the molecular level phenomenon in the rejuvenation mechanism. The rheology-based indicators, for instance, crossover modulus and crossover frequency differentiated the rejuvenators from recycling agents. Moreover, the study found that rejuvenation efficiency and durability are depended on the chemistry of rejuvenators. Finally, based on the learning of chemistry, a chemically balanced rejuvenator is synthesized with superior rejuvenation properties.

DEDICATION

I dedicate this dissertation to my parents, Md. Billal Hossain, and Minora Begum and to my family for their love and encouragement.

I also want to dedicate this dissertation to all my teachers who taught me directly or indirectly from primary education all the way to doctoral education.

ACKNOWLEDGMENTS

I would like to express my deepest gratitude to my advisor, Dr. Elham Fini, for her guidance, support, and encouragement throughout my graduate studies. Her profound wisdom and experience helped me to accomplish my research goals.

I also appreciate the financial support of the National Science Foundation through my adviser's CAREER award.

I would like to thank Dr. Michael Mamlouk, Dr. Kamil E. Kaloush, Dr. Mounir El Asmar, Dr. Mahour M. Parast, and Dr. Huiming Yin for being a part of my dissertation committee, and providing guidance.

I am also thankful to my colleagues and friends and specially our lab manager Jeffrey Long. I am thankful to Dr. Ajit Kelkar, Dr. Lifeng Zhang, and Karen Courtney from Joint School of Nanoscience and Nanoengineering, NCA&T as well as Daniel Oldham, Shahrzad Hosseinnezhad, Alireza Samieadel, and Faisal Kabir with Arizona State University for their continued supports.

Special thanks to Samia Jahan, and Mahmud Shahed, for their love and support and for always being there for me.

TABLE OF CONTENTS

	Page
LIST OF TABLES	IX
LIST OF FIGURES	XI
CHAPTER	
1 GENERAL INTRODUCTION.....	1
1.1 Background.....	1
1.2 Recycled Asphalt Shingles (RAS).....	2
1.3 Reclaimed Asphalt Pavement (RAP)	3
1.4 RAS and RAP Binder Rejuvenation.....	3
1.5 Research Objectives	4
1.6 Organization of Dissertation.....	5
1.7 References	7
2 INVESTIGATING THE PROPERTIES OF SEVERELY AGED ASPHALT (RAS) WITH RECYCLING AGENTS	9
2.1 Abstract.....	9
2.2 Introduction	10
2.2 Materials and Methods	15
2.3 Results and Discussion.....	21

CHAPTER	Page
2.4 Conclusions	43
2.5 Acknowledgments	45
2.6 References	46
3 THE EFFECT OF CHEMICAL COMPOSITION OF RECYCLING AGENTS ON REVITALIZING OXIDIZED ASPHALT	50
3.1 Abstract.....	50
3.2 Introduction	51
3.3 Materials and Method.....	55
3.4 Results and Discussion.....	68
3.5 Conclusion.....	90
3.6 Acknowledgments	92
3.7 References	93
4 EVALUATING SOURCE DEPENDENCY OF REJUVENATORS	98
4.1 Abstract.....	98
4.2 Introduction	99
4.3 Materials and Methods	103
4.4 Results and Discussion.....	117
4.5 Conclusion.....	132
4.6 Acknowledgments	134

CHAPTER	Page
4.7 References	135
5 INVESTIGATING MOLECULAR-LEVEL FACTORS THAT AFFECT THE DURABILITY OF RESTORED AGED ASPHALT BINDER.....	139
5.1 Abstract.....	139
5.2 Introduction	140
5.3 Experiment Plan	145
5.4 Materials and Methods	145
5.5 Results and Discussion.....	155
5.6 Conclusion.....	172
5.7 Acknowledgment.....	174
5.8 References	175
6 ECONOMIC STUDY.....	179
6.1 Size of the Asphalt Global Market.....	179
6.2 Market for Recycled Asphalt.....	180
6.3 Asphalt Recycling Agents	181
6.4 A Bio-based Sustainable Rejuvenator	182
6.5 References	186
7 CONCLUSIONS AND RECOMMENDATIONS	188

CHAPTER	Page
7.1 Rejuvenation Mechanism of Severely Aged Asphalt.....	188
7.2 Effect of Chemical Composition of Recycling Agents	189
7.3 Source Dependence of a Rejuvenator's Efficacy	190
7.4 Durability Study of Rejuvenated Aged Asphalt.....	191
7.5 Recommendations	191
REFERENCES	193
APPENDIX	
A PREVIOUSLY PUBLISHED WORK.....	206
B COAUTHOR PERMISSION FOR PREVIOUSLY PUBLISHED WORK.	209
BIOGRAPHICAL SKETCH	211

LIST OF TABLES

Table	Page
2-1 Recycled Asphalt Shingles Gradation	16
2-2 Viscosity-Based Aging Index.....	22
2-3 Rutting Performance.....	27
2-4 Fatigue Cracking Performance	28
2-5 Aged Stiffness and m-Value Results at 60 Seconds.....	35
3-1 Chemistry and Source of RA.....	55
3-2 Selected Molecules for Molecular Simulation to Study the Effect Of RA A and C on Self-Interaction of Oxidized Asphaltene Molecules.....	63
3-3 Slope Value Calculated Using Power Fit for All Samples.....	71
4-1 Literature Review of Indicators Used to Measure Rejuvenator Performance.....	102
4-2 Selected Binder Properties (PG 64-22)	104
4-3 Sources of Rejuvenators.....	104
4-4 Molecules Selected for Molecular Dynamics Simulation	113
4-5 Crossover Modulus and Frequency Values	118
4-6 Dry and Wet Peak Tensile Strength, and Moisture Susceptibility Index	119
4-7 Glass Transition Temperature (Tg) for All Samples	122
4-8 SARA Fractions of Blended Samples and Pure Rejuvenators	123
4-9 Colloidal Stability Index for All Samples	124
4-10 Measured Number of Gyration for Mixture Samples	130

Table	Page
4-11 Crossover Modulus and Frequency Values for Field Aged Samples.....	132
5-1 General Asphalt Binder Properties for PG 64-16 Used in This Study.....	146
5-2 Description of Rejuvenated Samples.....	146
5-3 DFT-Based Polarizability Values for Molecular Species Identified in Rej-Al, Rej-SO, and Rej-Swilgae.....	170
6-1 Types of Rejuvenators (NCAT, Spring 2014).....	181

LIST OF FIGURES

Figure	Page
2-1 Surveyed Factors Limiting the Use of RAS (Williams et al., 2018).....	12
2-2 Viscosity Values for RAS and BMS Specimens; (a) Unaged and (b) Aged.....	21
2-3 Average Shear Susceptibility for RAS And BMS Specimens at 5-25 Rpm: (Left) Unaged and (Right) Aged.....	23
2-4 Viscosity vs. Inverse Temperature for RAS and BMS Specimens	24
2-5 Complex Modulus Results for 5 and 40% RAS and BMS at 64° C for Unaged (a) and Aged (b)	26
2-6 Crossover Modulus and Frequency Results for Aged BMS and RAS.....	30
2-7 Change in (Delta) Crossover Modulus and Frequency Results for Aged BMS and RAS.....	31
2-8 Crossover Temperature Results for BMS and RAS Samples: (a) Unaged and (b) Aged.....	32
2-9 BBR Stiffness Results for Unaged BMS and RAS Samples at -12°C	33
2-10 BBR Stiffness Results for Aged BMS and RAS Samples at -12°C	34
2-11 Delta Tc Results for BMS and RAS Using the BBR	36
2-12 Unaged Creep-Deflection Curves at -18°C for Control, 40% RAS, and BMS	38
2-13 The m-value Results for 40% BMS and 40% RAS at -18°C: (a) Unaged and (b) Aged.....	39

Figure	Page
2-14 Unaged Time-Dependent Creep Load Deflection for 40% BMS and 40% RAS at -18°C	40
2-15 Failure Strain for RAS and BMS at -12°C: (a) Unaged and (b) Aged	41
2-16 Failure Strain for 40% RAS and 40% BMS Samples at -18°C (a) Unaged and (b) Aged.....	42
2-17 Fracture Energy for 40% BMS and 40% RAS Samples at -18°C: (a) Unaged, (b) Aged.....	43
3-1 Moisture Conditioning Apparatus for Contact Angle Measurement.....	60
3-2 The Initial Simulation Box after Addition of RA A's Molecules	66
3-3 $G^*/\sin(\delta)$ Value for All Samples at 64° C	69
3-4 $G^*\sin(\delta)$ Value for All Samples at 46° C	70
3-5 Complex Shear Modulus (G^*) Master Curves for All Samples.....	71
3-6 Phase Angle Plot for All Samples	72
3-7 Crossover Modulus Values Estimation for Sample C	73
3-8 Crossover Modulus Values for All Samples	74
3-9 Crossover Frequency Value for All Samples	75
3-10 (a, b) FTIR Spectra of All Samples	77
3-11 SARA Fractions of Pure RA and All Other Samples.....	79
3-12 Colloidal Stability Index for All Samples	80
3-13 Molecular Size Distribution.....	82

Figure	Page
3-14 Dry and Wet Contact Angle for Neat Binder	83
3-15 Unconditioned and Conditioned Contact Angle Measurements at 23° C	84
3-16 Contact Angle Moisture Susceptibility Index Values at 23° C	85
3-17 Aggregation Study of Oxidized Asphaltene Molecules with and Without the Presence of RAs' A and C Molecules.....	86
3-18 Radial Distribution Function Plot for the Last Five Seconds of the Simulation Shown in Figure 3-17.....	88
3-19 Snapshots of Simulation: Top- Subsequent Snapshots Showing Deagglomeration Process of Oxidized Asphaltene Molecules with the Presence of RA A; Bottom- Formation of a Large Agglomerate of Oxidized Asphaltenes after Supplying RA C's Molecules.....	89
4-1 The Initial Simulation Box after Addition of Rejuvenator's Molecules.....	116
4-2 Complex Modulus (G*) vs. Phase Angle Data.....	117
4-3 Binder Residue from Bitumen Sample R (Left) Adhering to the Glass Surface in Dry Condition; (Right) after Adhesive Failure Following 2 hr Water Conditioning.	120
4-4 Measurement of Glass Transition Temperature at the Second Heating Cycle with Exothermic Down Positive	121
4-5 The Molecular Size Distribution of All Samples	126
4-6 Oxidized Asphaltene and Oxidized Asphaltene Plus Rejuvenator A Molecules Average Aggregation Number Plot	127

Figure	Page
4-7 RDF Plot for the Last Five Seconds of the Simulation Shown in Figure 4-6	129
4-8 C* vs. Crack Growth Rate (a*) Plot for Control and Control +5%Rej. Samples	131
5-1 Experiment Plan of the Study.....	145
5-2 (Left) Glass Beads Used to Mix with Bitumen; (Middle) Sample Before Water Conditioning; (Right) Sample after Water Conditioning.....	154
5-3 Complex Modulus Master Curves.....	155
5-4 Graphs of Phase-Angle Value Versus Reduced Frequency	156
5-5 Crossover-Modulus Values for All Samples.....	157
5-6 Crossover Frequency for All Samples.....	158
5-7 Shear Strain Versus Time at 3.2 Kpa	159
5-8 (a, b) Stiffness and m-Value Results for All Samples at -6 °C	161
5-9 Delta T _c Values for all Samples.....	161
5-10 Carbonyl Index Value for All Samples Measured with FTIR.....	163
5-11 Aging Index Values for All Samples From 50 hours to 200 Hours	164
5-12 Hamburg Wheel-Tracking Test Results for All Samples.....	165
5-13 Viscosity Versus Shear Rate for Dry and Wet Specimens of (a) Rej-Al, and (b) Rej- Swilgae.....	166
5-14 MISTI Values for Rejuvenators Rej-Al and Rej-Swilgae	167
5-15 Polarizability Values for the First 6 Compounds of Each of Rej-Al, Rej-SO, and Rej-Swilgae.....	172

Figure	Page
6-1 Size of Global Asphalt Market: Data for 2019-2020; Projections for 2021-2026 (Reports And Data, 2019).....	180
6-2 Reported Use of RAP, RAS, and GTR Across the U.S. (NCAT, Spring 2014)	180
6-3 A Freshwater Harmful Algal Bloom Turned Lake Erie a Bright Blue Green (NSF Media, 2018).....	183
6-4 Algae Blooms Across the U.S. (EWG, 2020)	184

CHAPTER 1 GENERAL INTRODUCTION

1.1 Background

The Federal Highway Administration (FHWA) and the National Asphalt Pavement Association (NAPA) share a common goal of sustainability in road construction through use of recycled materials. It was reported that the crude oil price is highly volatile, and the price fluctuates due to several factors including political, economic, environmental factors (Bajpai, 2020). Moreover, the production of asphalt binders has been reduced since the advent of coking technology and advanced refining processes allowing for conversion of heavy residue to synthetic fuel (Khan et al., 2017). To enhance sustainability in pavement construction, it is necessary to promote use of recycled materials and limit the dependency on new materials including but not limited to virgin asphalt binder and stone aggregates for which supplies, and natural resources are shrinking. In terms of asphalt binder, the recycled alternatives are recycled asphalt shingles (RAS), reclaimed asphalt pavement (RAP), ground tire rubber (GTR), end of life polymers and plastics (Hosseinnezhad et al., 2019; Kabir et al., 2020; Li et al., 2019). This approach not only conserves raw materials but also reduces overall construction costs (Williams et al., 2018). Among these recycled materials, RAP and RAS usage has increased rapidly in new-pavement construction recently (Oldham et al., 2019; Fini et al., 2020). It should be noted that use of RAP and RAS in new-pavement construction should not compromise the pavement performance and durability (Rajib et al., 2020).

1.2 Recycled Asphalt Shingles (RAS)

Recycled asphalt shingles are the roofing shingles that go to landfills after their service life. RAS is an excellent source of asphalt binder with an average asphalt content ranging from 15%-35% (Gevrenov, 2008). RAS can be sourced from the manufacture's waste (post-manufacture) or from tear-off waste (post-consumer). Both sources of RAS contain a high amount of asphalt binder, and they can be processed and partially replace virgin binder. The use of RAS in virgin binder has showed significant environmental and economic benefit. The amount of RAS usage has increased significantly from 701,000 tons in 2009 to an estimated 1,053,000 tons in 2018. It is estimated that the cost savings on materials (asphalt binder and aggregate) from the use of RAS were approximately \$0.079 billion and \$0.107 billion, respectively, in the 2017 and 2018 construction seasons (Williams et al., 2019). Recycled materials should not only provide environmental and economic benefits, they should also provide engineering benefits. RAS usage can be detrimental in new pavement due to stiffer binder properties if the proper characterization of RAS (amount, properties, and quality of available asphalt binder) is not accurately identified. Thus, the guiding principles for using RAS in asphalt mixture are: 1) meet the same requirements as asphalt mixtures with all virgin materials, and 2) perform equal to or better than asphalt mixtures with all virgin materials (Williams et al., 2019). To follow the guiding principles, it is necessary to ensure the quality of RAS with proper treatment such as application of recycling agents or rejuvenators.

1.3 Reclaimed Asphalt Pavement (RAP)

According to NAPA, RAP is extracted from existing pavement when it is necessary to undergo pavement milling operations (NAPA, 1996). Milling operations are typically conducted to maintain curbs and structural clearance for bridges and overpasses by grinding a specified depth of existing pavement to allow new pavement layers during pavement rehabilitation (Elkashef, 2017). Typically, RAP contains 5%-6% asphalt binder that is stiffer compared to the base virgin binder. The application of RAP in new pavement construction is increasing; nearly 97% of RAP is put back into new-pavement construction, and the remaining 3% is used in other civil-engineering applications such as unbound aggregate bases (Williams et al., 2019). This amounted to a total of 82.2 million tons of RAP in 2018, a 46.8% increase from 2009. Using RAP saves approximately 4.1 million tons (23 million barrels) of asphalt binder and more than 78 million tons of aggregate, with a total estimated value of more than \$2.8 billion. With growing interest in using RAP, it is important to understand the side effects of using RAP with virgin binder and propose guidelines on what measures to take to minimize detrimental effects.

1.4 RAS and RAP Binder Rejuvenation

Many researchers have used different type of recycling agents or rejuvenators to help restore the physical and chemical properties of the aged asphalt binder in RAS and RAP (Ahmed & Hossain, 2020; Oldham et al., 2015; Zadshir et al., 2019; Zhang et al., 2019; Ziari et al., 2019). Typical rejuvenators balance the lost maltene fractions of aged asphalt

and help the dispersion of asphaltenes by preventing them from agglomerating or possibly deagglomerating existing nano-aggregates. It is important to accurately measure a rejuvenator's performance and define proper indicators to call it a “comprehensive rejuvenator”. Some rejuvenators may act as softening agents rather than comprehensively rejuvenating the aged asphalt. To identify a comprehensive rejuvenator that will help to increase the recycling rate of RAS and RAP, it is necessary to understand the rejuvenation mechanisms on macro-level properties (such as viscosity, stiffness, and modulus) and molecular-level properties (such as deagglomeration, polydispersity, molecular weight). Identification of comprehensive rejuvenators by developing novel indicators of comprehensive rejuvenation for aged asphalt may help road authorities to differentiate recycling agents from comprehensive rejuvenators. This approach may help develop effective modifiers to rejuvenate aged asphalt that will facilitate the recycling and reuse of aged asphalt binder found in RAS and RAP.

1.5 Research Objectives

The objectives of the study and the corresponding hypotheses and research questions of each objective are stated below:

- Investigate the properties of severely aged asphalt (RAS) with recycling agents.
Question: “Does the presence of certain recycling agent “comprehensive rejuvenators” decrease the intermolecular interactions of oxidized asphaltenes to cause deagglomeration?”

- Investigate the properties of aged asphalt (RAP) with recycling agents.

Question: “Does the extent of deagglomeration of nano-aggregates correlate with rheological parameters?”

- Study the durability of a chemically balanced rejuvenated asphalt.

Question: “Does the specific chemical composition of a rejuvenator negatively impact the durability of restored aged asphalt binder?”

- Study the economic viability of a comprehensive rejuvenator.

Question: “How is the comprehensive rejuvenator relevant to the asphalt market?”

1.6 Organization of Dissertation

In this dissertation, each chapter is formatted as a standalone technical paper with minimal references to other parts of the study. This format hypothesizes that a technical paper will result or has resulted from each chapter; therefore, each chapter possesses its own conclusions and references.

Chapter 2 focuses on the first objective of this study: investigating the properties of bio-modified RAS in virgin binder. A viscosity-based aging index, shear susceptibility, and the activation energy of bio-modified and non-modified RAS are discussed. In addition, the fracture energy, physical hardening, and fatigue resistance of RAS are investigated in detail.

Chapter 3 discusses the role of the chemical composition of different recycling agents in rejuvenating laboratory-prepared aged asphalt binder. Rheological indicators based on the

crossover modulus and crossover frequency are developed to differentiate recycling agents that can accurately be called rejuvenators.

Chapter 4 demonstrates the source dependence of a rejuvenator's efficacy in revitalizing aged bitumen and RAP bitumen mixtures. Rejuvenation efficacy is characterized based on micro-level and macro-level investigation. Both laboratory experiments and computational modeling are used to understand the underlying rejuvenation mechanisms.

Chapter 5 focuses on the durability issue of a chemically balanced rejuvenated asphalt binder. The rejuvenator is synthesized from balanced feedstock of lipid and protein. Based on the laboratory experiments and computational modeling, the molecular-level factor is identified that affects the durability of restored aged asphalt binder. Density functional theory is used to quantify the polarizability of a rejuvenator, to measure the durability of the restored aged asphalt.

Chapter 6 studies the economic impact of rejuvenated aged asphalt and how the application of a comprehensive rejuvenator in recycling aged asphalt is a viable solution relevant to the asphalt market.

Chapter 7 summarizes the research output and provides recommendations for future work.

1.7 References

- Ahmed, R. B., & Hossain, K. (2020). Waste cooking oil as an asphalt rejuvenator: A state-of-the-art review. *Construction and building materials*, 230, 116985. doi:<https://doi.org/10.1016/j.conbuildmat.2019.116985>
- Bajpai, P. (2020). Top Factors That Affect the Price of Oil. Retrieved from <https://www.investopedia.com/articles/investing/072515/top-factors-reports-affect-price-oil>.
- Elkashef, M. E. (2017), Using soybean-derived materials to rejuvenate reclaimed asphalt pavement (RAP) binders and mixtures. *Graduate Theses and Dissertations*. 15514. <https://lib.dr.iastate.edu/etd/15514>
- Fini, E., Rajib, A. I., Oldham, D., Samieadel, A., & Hosseinneshad, S. (2020). Role of Chemical Composition of Recycling Agents in Their Interactions with Oxidized Asphaltene Molecules. *Journal of Materials in Civil Engineering*, 32(9), 04020268.
- Gevrenov, J. (2008). Utilization of recycled asphalt shingles in hot-mix asphalt. *Recycling Shingles into Roads, US EPA Perspective. Presentation Made at the Missouri Showcase*.
- Hosseinneshad, S., Kabir, S.F., Oldham, D., Mousavi, M., Fini, E.H., 2019. Surface functionalization of rubber particles to reduce phase separation in rubberized asphalt for sustainable construction. *Journal of Cleaner Production* 225, 82-89.
- Kabir, S.F., Mousavi, M., Fini, E.H., 2020. Selective adsorption of bio-oils' molecules onto rubber surface and its effects on stability of rubberized asphalt. *Journal of Cleaner Production* 252, 119856.
- Khan, M. K., Sarkar, B., Zeb, H., Yi, M., & Kim, J. (2017). Simultaneous breaking and conversion of petroleum emulsions into synthetic crude oil with low impurities. *Fuel*, 199, 135-144.
- Li, J., Xiao, F., Zhang, L., & Amirhanian, S. N. (2019). Life cycle assessment and life cycle cost analysis of recycled solid waste materials in highway pavement: A review. *Journal of Cleaner Production*, 233, 1182-1206.
- NAPA. (1996). Pavements, Recycling Hot-Mix Asphalt National Asphalt Pavement Association (NAPA). Information Series 123.–Lanham (MD), 1996.–28 p.
- Oldham, D. J., Fini, E. H., & Chailleux, E. (2015). Application of a bio-binder as a rejuvenator for wet processed asphalt shingles in pavement construction. *Construction and building materials*, 86, 75-84.

- Oldham, D. J., Rajib, A. I., Onochie, A., & Fini, E. H. (2019). Durability of bio-modified recycled asphalt shingles exposed to oxidation aging and extended sub-zero conditioning. *Construction and Building Materials*, 208, 543-553.
- Rajib, A. I., Pahlavan, F., & Fini, E. H. (2020). Investigating Molecular-Level Factors That Affect the Durability of Restored Aged Asphalt Binder. *Journal of Cleaner Production*, 122501.
- Williams, B. A., Copeland, A., & Ross, T. C. (2018). *Asphalt Pavement Industry Survey on Recycled Materials and Warm-Mix Asphalt Usage: 2017*. Retrieved from
- Williams, B. A., Willis, J. R., & Ross, T. C. (2019). *Asphalt Pavement Industry Survey on Recycled Materials and Warm-Mix Asphalt Usage: 2018*. Retrieved from
- Zadshir, M., Hosseinnezhad, S., & Fini, E. H. (2019). Deagglomeration of oxidized asphaltenes as a measure of true rejuvenation for severely aged asphalt binder. *Construction and building materials*, 209, 416-424.
- Zhang, R., You, Z., Wang, H., Ye, M., Yap, Y. K., & Si, C. (2019). The impact of bio-oil as rejuvenator for aged asphalt binder. *Construction and building materials*, 196, 134-143.
- Ziari, H., Moniri, A., Bahri, P., & Saghafi, Y. (2019). Evaluation of performance properties of 50% recycled asphalt mixtures using three types of rejuvenators. *Petroleum Science and Technology*, 1-7.

CHAPTER 2 INVESTIGATING THE PROPERTIES OF SEVERELY AGED ASPHALT (RAS) WITH RECYCLING AGENTS

A version of this paper published in Journal of construction and Building Materials
Oldham, D. J., Rajib, A. I., Onochie, A., & Fini, E. H. (2019). Durability of bio-modified
recycled asphalt shingles exposed to oxidation aging and extended sub-zero conditioning.
Constr. Build. Mater., 208, 543.

2.1 Abstract

The use of recycled asphalt shingles (RAS) in pavement construction has received significant attention due to its economic and environmental advantages. However, the nature of asphalt binder in RAS is significantly aged and requires modification before application to ensure it does not compromise pavement performance. The paper introduces a novel approach to modify RAS as a means of facilitating its application in new construction while examining the feasibility of rejuvenating RAS via bio-modification. In addition, this study investigates the durability of the modified RAS, referred to as bio-modified shingles (BMS), by exposing BMS to both severe oxidation aging and sub-zero extended conditioning followed by a comprehensive thermo-mechanical characterization. Study results showed the performance of RAS was significantly improved after bio-modification. The performance improvement was reflected in BMS having lower viscosities, stiffnesses, shear susceptibilities, crossover temperatures, while having higher m-values and failure strains compared to RAS asphalt.

It was further observed that the enhancement lasted even after BMS was exposed to severe oxidation aging and 72hr conditioning at -18°C indicating an enhanced durability of BMS. The latter can be attributed to molecular interactions between the bio-modifier and aged asphalt disturbing the molecular packing of asphaltene and wax molecules. Such molecular packing is known as a dominant mechanism for hardening at sub-zero temperatures. This paper contributes to the body of knowledge and practice by providing insight on the merits of revitalizing recycled asphalt shingles to enhance its durability and facilitate its application in construction to promote sustainable construction practices.

Keywords: Rejuvenation, Durability, Recycling, Asphalt Roofing Shingles, Bio-binder, Physical Hardening, Rheology, Oxidation

2.2 Introduction

The price of asphalt binder has increased from nearly \$176 per ton in 2004 to \$455 per ton in 2018 (NCDOT, 2018). Due to the overall increase in the price of asphalt binder and depletion of crude oil sources, substituting a portion of asphalt binder with the binder available in Recycled Asphalt Shingles (RAS) has been promoted (West & Willis, 2014). In the United States, about 14 percent of the total supply of scrap shingles (including both manufacturers' scrap shingles and post-consumer roofing shingles) are reclaimed for use in asphalt pavements (NAPA, 2016). According to a survey conducted by NAPA, in partnership with the Federal Highway Administration (FHWA), RAS usage is widespread with approximately 1.4 million tons of RAS used in asphalt pavement in the

United States. This resulted in a binder cost savings of over \$37.5 million (NAPA, 2016). Moreover, the usage of RAS in asphalt pavement saves a considerable amount of landfill area each year. In addition, it should be noted that the use of RAS reduces the material costs, decreases rutting performance, and promotes more sustainable management practices (Hansen & Newcomb, 2011; Maupin, 2010; Williams et al., 2013; Zhou, 2013). Despite the economic, environmental, and performance benefits of reusing RAS in asphalt pavement construction, it is to be noted that due to the highly aged nature of asphalt found in shingles, use of RAS in new pavement construction may negatively affect pavement performance specially in cold season and low temperature regions. It has been shown that in cold regions the overall performance of the asphalt pavement depends on the binder's low temperature performance. When the temperature drops suddenly, a high thermal stress develops within the asphalt binder. If the stress within the pavement exceeds tolerance, crack initiation will occur. The latter is documented as the main contributor to thermal cracking distresses thus reducing pavement performance. Introduction of an oxidized/aged binder, such as recycled asphalt shingles to the base binder, increases thermal stress development due to the increase in overall stiffness combined with the loss of stress relaxation capability (Maupin, 2010; You et al., 2011). It has been documented that the addition of RAS to virgin binder results in an increase in stiffness and a decrease in the m-value at low service temperatures. Such drawbacks are known as limiting factors for the widespread use of RAS as a partial replacement for virgin asphalt in new pavement construction (Abbas et al., 2013). This issue is reflected in

a recent survey of US State Departments of Transportation on factors limiting the use of RAS in their state (Figure 2-1). The results found that over 67% of the commonly noted factors were related to the performance as 47.3% noted specification limits, 12.7% claimed mixture performance, and 7% listed volumetric requirements (Williams et al., 2018). The response labeled as “other” included responses such as lack of interest, asphalt plant limitations, perceptions of poor performance, and local abundance of RAP.

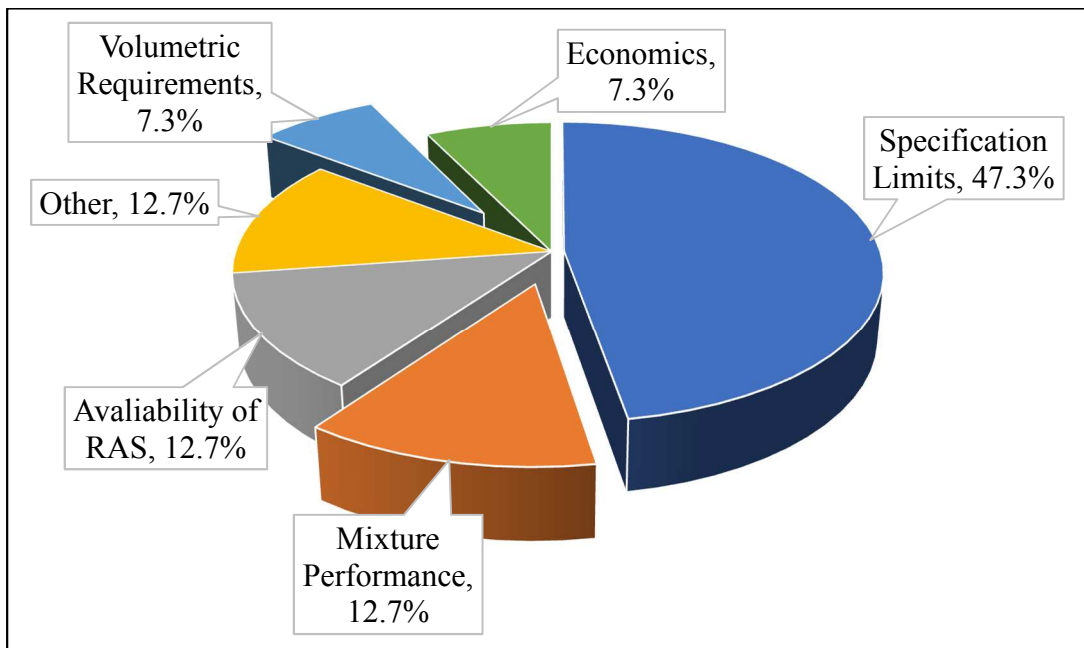


Figure 2-1 Surveyed Factors Limiting the Use of RAS (Williams et al., 2018)

The adverse effects of the RAS on virgin asphalt binder are attributed to its highly oxidized nature as well as a lack of adequate blending between virgin asphalt binder and RAS (Mogawer et al., 2013; Zhao et al., 2015). RAS chemical structure, microstructure, and physical properties are significantly different from those of the virgin asphalt binder;

this in turn, prevents proper blending between RAS and virgin binder. Grinding RAS to an ultrafine particle size has been used to facilitate its blending with asphalt binder; however, this method was not found effective in reducing negative effects of RAS on the low temperature properties of virgin binder at high percentages (Elseifi et al., 2012).

In order to facilitate RAS application and avoid negative effects, certain properties of RAS should be improved by means of proper treatment. Many studies found that rejuvenators and modifiers can be applied to aged asphalt to improve their rheological and mechanical properties (Mousavi et al., 2016; Oldham et al., 2015; Pahlavan, Hung, et al., 2018; Pahlavan, Mousavi, et al., 2018). Several researchers have used both petroleum-based rejuvenators and bio-based rejuvenators. Zeng et al. evaluated the residue from castor oil production as a rejuvenator for aged asphalt binder and found that the addition of the rejuvenators to the aged asphalt restored the viscoelastic properties of the binder (Zeng et al., 2018). At a concentration of 20%, the authors found that thermal-cracking properties of the aged asphalt binder was significantly improved to nearly that of the virgin asphalt binder. Al-Mansoori and his team used encapsulated sunflower cooking oil as a rejuvenator and healing agent in preparing calcium-alginate polymer-based capsules (Al-Mansoori et al., 2018). The authors found that the oil released from the capsules, upon their breakage, resulted in rejuvenating asphalt mastic. Su et al. used microcapsules containing rejuvenator and found improvement through the self-healing mechanism of aged bitumen (Su et al., 2015). Elkashef et al. introduced soybean oil-derived material as a potential rejuvenator for asphalt binder. The authors concluded that

at a very low dosage (0.75% by weight of the asphalt), soybean additive was able to modify the rheological properties of asphalt binder efficiently (Elkashef et al., 2018).

Ongel and Hugener, applied a rejuvenator produced from cashew nut shells, vegetable oil, naphthenic oils to improve the aged bitumen's rheological performance. The authors found that the addition of 6% cashew nut shells or 5% vegetable/naphthenic oil blend to aged asphalt binder decreased the overall binder by two penetration grades from 40/50 to 70/100 (Ongel & Hugener, 2015). Ji et al. used waste cooking vegetable oils-based rejuvenator (corn oil and soybean oil) to recover the aged asphalt, they showed that vegetable oil rejuvenators decreased viscosity and stiffness of the aged asphalt binder effectively and improved fatigue cracking and low-temperature cracking resistance (Ji et al., 2017). Zaumanis and co-workers added waste vegetable grease, organic oil, aromatic extract, waste vegetable oil, distilled tall oil, and waste engine oil to RAP binder and observed that the organic additives required a concentration of 8-11%, while the petroleum additives required higher concentrations of 14-21% to provide a similar softening effect on RAP binder (Zaumanis et al., 2015).

In addition to the above plant-based modifiers, Bio-binder produced from the processing of swine manure was used to modify oxidized asphalt binder (Fini et al., 2011). It has been shown that Bio-binder is able to improve certain asphalt properties such as temperature susceptibility and low temperature cracking even when aged asphalt such as RAP or RAS is present in the mixture (Hill et al., 2013; Mogawer et al., 2012; Zadshir et al., 2018). Rheological and molecular characterization performed on bio-modifier applied

to highly aged asphalt binder such as those found in RAS, showed bio-modification can revitalize aged asphalt (Mousavi et al., 2016; Oldham et al., 2015). However, aforementioned studies did not study performance of the bio-modified samples after aging. Accordingly, this paper not only introduces a novel bio-modifier to treat RAS, but also studies the durability of modified RAS, referred to as bio-modified shingles (BMS) by exposing them to both severe oxidation aging and extended sub-zero conditioning followed by a comprehensive thermo-mechanical characterization.

2.2 Materials and Methods

2.2.1 Materials

Scrap asphalt shingles are commonly categorized into two groups. The first group is called tear-off scrap shingles (TOSS) which is referred to post-consumer products typically recovered after 10-15 years of service life on the roof of a building. The second group is manufactured waste scrap shingles (MWSS) which are shingles discarded during or after manufacturing due to defects. It should be noted that although TOSS is more abundant than MWSS, TOSS has more variability in terms of binder content and gradation compared to MWSS which makes it inferior and less utilized (Marasteanu et al., 2012; Zhou, 2013). This study uses tear-off scrap shingles acquired from S.T. Wooten's Quality Control lab located in Sanford, NC. The gradation of the TOSS after grinding as well as the particle analysis is given in Table 2-1. The final gradation of the shingle batch blended with the binder had an average particle size of 85.5 μm following the procedure reported by Oldham et al., 2015.

Table 2-1 Recycled Asphalt Shingles Gradation

Sieve Size	% Passing
3/8" (9.5 mm)	100.00
No. 4 (4.75 mm)	95.39
No. 8 (2.36 mm)	87.64
No. 16 (1.18 mm)	69.51
No. 30 (600 μm)	47.64
No. 50 (300 μm)	32.23
No. 100 (150 μm)	19.05
No. 200 (75 μm)	6.19

The bio-based binder used for this study was derived from swine manure sourced from a large hog farm in Mt. Olive, NC. The swine manure was converted to Bio-binder following the method developed by Fini et al. 2011. To do so, manure was heated in a sealed stainless canister to 340°C for a specified duration of time before being cooled down to room temperature and processed further by vacuum filtration and distillation. Optimization of the processing time of Bio-binder from swine manure found that increasing residual time increased amide-enriched compounds which in turn enhances the interaction of Bio-binder and asphalt mixtures (Hung et al., 2017). Chemical characterization of the Bio-binder shows the presence of a high content of aromatics and resins as well as a lower molecular weight compared to petroleum-based asphalt binder

which can make it a promising candidate for use with aged asphalt material (Fini et al., 2011, Pahlavan et al., 2018a).

To prepare bio-modified RAS asphalt, the RAS particles were blended directly with the asphalt binder. The RAS particles were added at concentrations of 5%, 15%, 30%, and 40% by mass of binder (PG 64-22) at 180°C for 1 hour at approximately 450 rpm. For the BMS samples, each RAS-modified specimen was blended with 10% Bio-binder by mass at 750 rpm for 30 minutes at 135°C. Each sample was fully re-blended for 5 minutes prior to preparing test specimens. To expose specimens to oxidation aging resembling the field aging process, the RAS and BMS samples were conditioned in a rolling thin film oven (RTFO) and a pressure aging vessel (PAV) following (ASTMD2872-12e1, 2012; ASTMD6521-13, 2013) specifications, respectively. To conduct extended sub-zero conditioning, specimens were placed in an isothermal chamber at -18°C for specified time before testing.

2.2.2 Rheometry

Viscosity measurements were conducted on both RAS- and BMS-modified asphalt samples using the Brookfield Viscometer RV-DV-III Ultra following (ASTMD4402, 2015) at spindle speeds of 5, 10, 20, 25, 50, and 100 rpm and different temperatures ranging from 100-160°C. Based on the viscosity results, an aging index was developed using Equation 1. Moreover, from the viscosity results, shear susceptibility (S.S) was calculated, which is defined as the change in viscosity with the change in shear rate and

was calculated using Equation 2. Lastly, the activation energy was determined for the BMS and RAS samples using Equation 3.

$$\text{Aging Index} = \frac{\text{Aged Viscosity} - \text{Unaged Viscosity}}{\text{Unaged Viscosity}} \times 100 \quad (2-1)$$

$$\text{S.S} = \frac{\text{Log (Viscosity)}}{\text{Log (Speed)}} \quad (2-2)$$

$$\ln \eta = \ln A + \frac{E_f}{R} \frac{1}{T} \quad (2-3)$$

Where:

η is the rotational viscosity of asphalt in Pa·s

E_f is the flow activation energy (KJ. mol⁻¹)

R is the universal gas constant (8.314×10⁻³ KJ.mol⁻¹. K⁻¹)

T is the temperature

K and A are constants.

The elastic and viscous properties of the shingle-modified binders were measured using a Malvern Kinexus dynamic shear rheometer (DSR) according to (ASTMD7175-15, 2015).

The samples were evaluated from 76 to 4 °C at 6-degree intervals using 31 different frequencies ranging from 0.1 to 100 rad/s. To accommodate the torque limit of the instrument, the 25-mm spindle (gap size of 1 mm) was used for the temperatures from 76 to 46 °C, while the 8-mm spindle (gap size of 2 mm) was used for the temperatures from

40 to 4 °C. From the results, the frequency at which the elastic and viscous moduli curves intersect (crossover frequency) was determined.

2.2.3 Three Point-bending Test

The low temperature creep stiffness and stress relaxation capacity (m-value) were determined for the bio-modified shingle specimens using the bending beam rheometer (BBR) following (ASTMD6648-08, 2016) at -12°C. The stiffness and m-value results were calculated using Equation 4 and 5 respectively:

$$S(t) = \frac{PL^3}{4bh^3\delta(t)} \quad (2-4)$$

$$m(t) = |\text{dlog}[S(t)]/\text{dlog}(t)| = |[B + 2C\text{log}(t)]| \quad (2-5)$$

where:

P = applied constant load (100 g or 0.98 N)

L = distance between beam supports (102 mm)

b = beam width (12.7 mm)

h = beam thickness (6.25 mm)

S (t) = asphalt binder stiffness at a specific time *t*

δ (t) = deflection at a specific time *t*

B and C = regression coefficients

t = loading time

In addition to stiffness and m-value, which was calculated using above equations, Delta

Tc (ΔTc) was determined using Equation 6. The Delta Tc is defined as the difference

between the two critical low temperatures determined based on the stiffness and m-value

criteria. The two temperatures correspond to the temperatures at which the specimen's stiffness is 300 MPa, and its m-value is 0.3, (limits specified based on Superpave specification).

To be able to calculate the aforementioned temperatures, the samples were tested at both -12 and -18 °C. The values of T_c (stiffness) and T_c (m-value) were calculated using Equations 7 and 8, respectively.

$$\Delta T_c = T_c(\text{Stiffness}) - T_c(\text{m-value}) \quad (2-6)$$

$$T_c(\text{Stiffness}) = T_1 + \left(\frac{(T_1 - T_2) * (\text{Log}300 - \text{Log}S_1)}{\text{Log}S_1 - \text{Log}S_2} \right) - 10 \quad (2-7)$$

$$T_c(m) = T_1 + \left(\frac{(T_1 - T_2) * (0.300 - m_1)}{m_1 - m_2} \right) - 10 \quad (2-8)$$

2.2.4 Direct Tension Test (DTT)

To determine failure strain and stress values, a direct tension test was performed at -12°C using a displacement rate of 1.00 mm/min following (ASTMD6723, 2012). The fracture energy was also determined by calculating the area under the load versus displacement curve using Equation 9.

$$\text{FractureEnergy} = \sum \frac{\text{Area}_{L-DCurve}}{\text{Area}_{C.S.A}} \quad (2-9)$$

where:

$Area_{L-D.Curve}$ = the area under the load - displacement curve (N.m)

$Area_{C.S.A}$ = the cross-section area of fractures specimen (m^2)

2.3 Results and Discussion

2.3.1 Dynamic Viscosity Results

Figure 2-2 shows the viscosity values for unaged and aged samples at 20 rpm and 135°C. Analysis of the viscosity values for both RAS and BMS samples was performed at different temperatures, shear rates and aging conditions. Viscosity results show consistently lower viscosity for BMS compared to RAS, for both unaged and aged results with smaller differences observed at 30% and 40% specimens especially after long-term aging.

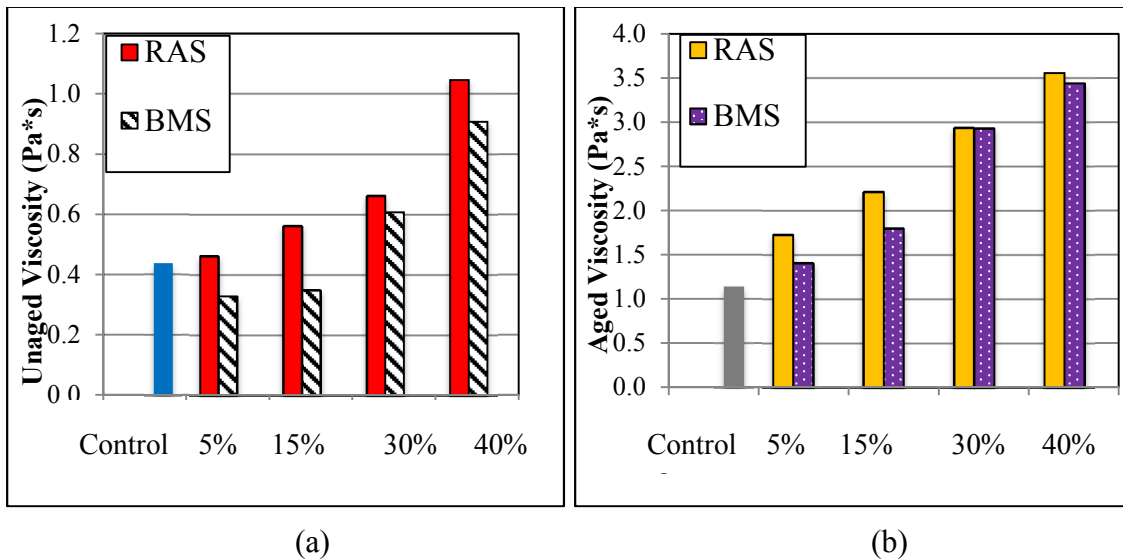


Figure 2-2 Viscosity Values for RAS and BMS Specimens; (a) Unaged and (b) Aged

Table 2-2 shows the values for the viscosity-based aging index, which is developed based on Equation 1. Considering the already oxidized nature of the RAS, the change in viscosity of RAS when exposed to additional aging is expected to be minimal. It can be observed that the presence of Bio-binder in BMS slightly increased the Aging Indices of RAS-modified binder, which could be attributed to the removal of light compounds in Bio-binder as well as increased blending between aged binder and Bio-binder. The slightly increased aging index of BMS does not depict its inability to modify the RAS sample. Since, even after aging the aged BMS still performed better and showed a reduced viscosity result compared to aged RAS samples.

Table 2-2 Viscosity-Based Aging Index

	5% Shingles	15% Shingles	30% Shingles	40% Shingles
RAS	73%	75%	77%	71%
BMS	77%	81%	79%	74%

Using the viscosity results, the shear susceptibility of RAS and BMS modified binder, for both unaged and aged samples at 120°C and 5, 10, 20, and 25 rpm, was calculated using Equation (2) and is shown in Figure 2-3. It was observed that the shear susceptibility increases with the increase of RAS concentration. This phenomenon could be explained

as the RAS content was increased and that overall BMS had a lower shear susceptibility than RAS. The deviation from the Newtonian fluid behavior was found to increase with increase of RAS and BMS, and the specimens showed shear thinning behavior, which was also reported in previous research on RAS modified asphalt (Oldham et al., 2015). The bio-modification may have reduced the intermolecular interaction of asphalt binder which dictates the sample to be less sensitive to shear rate. After bio-modification, the aforementioned effect was alleviated as evidenced by 5 and 15% BMS scenarios showing even lower shear susceptibility than the control asphalt. After aging, the shear susceptibility increased significantly for all samples, however, all BMS maintained a lower shear susceptibility than RAS even after aging. The difference between the RAS and BMS specimens was reduced after aging, and specially at high concentration where the effect of bio-modification was less noticeable.

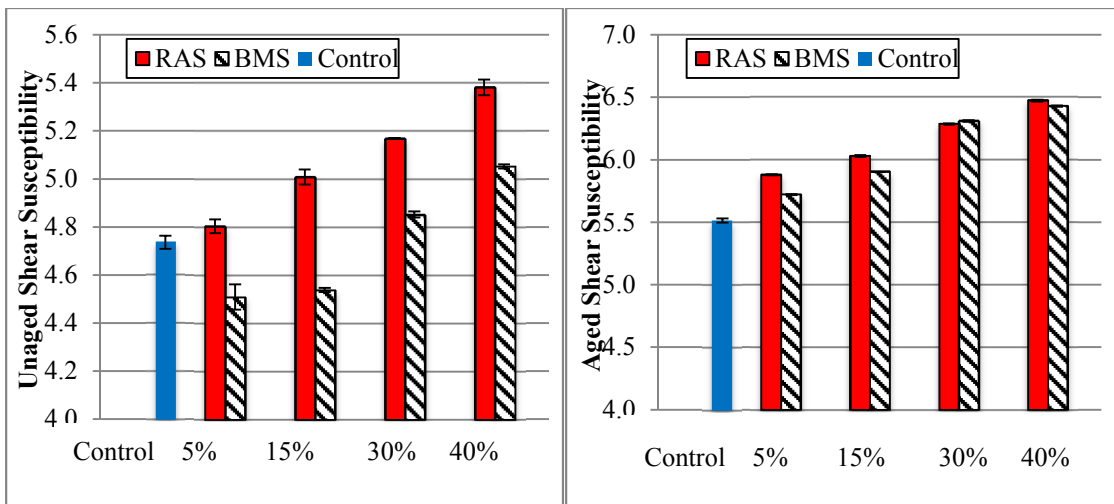


Figure 2-3 Average Shear Susceptibility for RAS and BMS Specimens at 5-25 rpm:
(Left) Unaged and (Right) Aged

To observe the flow activation energy of RAS and BMS samples, the viscosity versus inverse of temperature was plotted (Figure 2-4) and the slope of each curve was referred to as activation energy. The flow activation energy is defined as the energy required to change the resistance to flow. The inclusion of RAS significantly increased activation energy as evidenced by significantly higher slope of all samples containing RAS compared to that of the control. Bio-modification was shown to lower the slope of the RAS samples, for example, in the case of 5% and 15% BMS, the slope was reduced to be closer to that of the control sample.

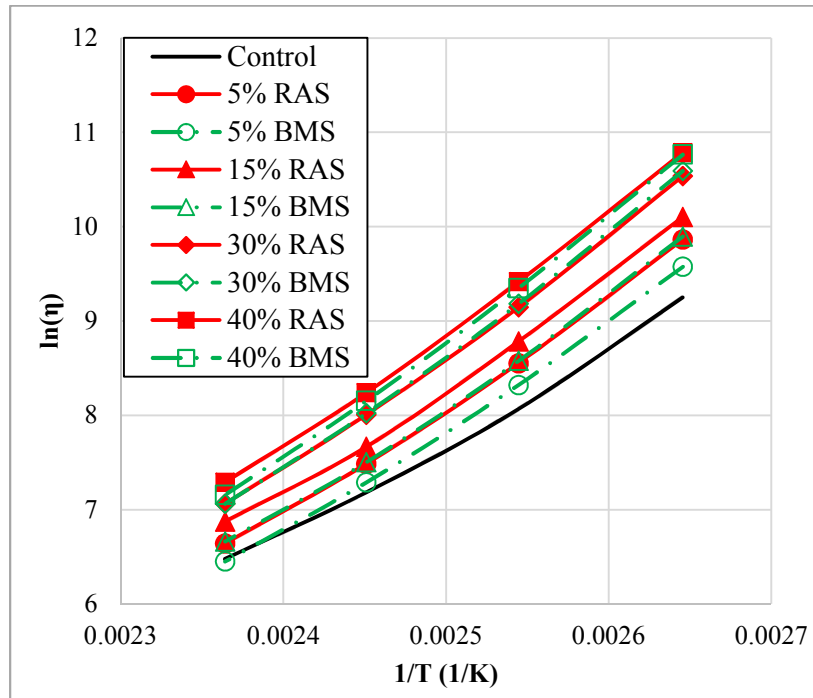


Figure 2-4 Viscosity vs. Inverse Temperature for RAS and BMS Specimens

The observed increase in activation energy in the presence of RAS can be attributed to increased interactions among components of oxidized asphalt increasing their polarity and promoting the formation of agglomerates (Samieadel et al., 2019). This more polar fraction is more likely to continue to agglomerate and increase the overall binder's resistance to flow and activation energy (Zhang et al., 2019). The latter agglomerates may be reduced after bio-modification due to de-agglomeration mechanism induced by biomolecules diffusing into self-assembled structures in asphalt (Pahlavan et al., 2018a).

2.3.2 Dynamic Shear Rheometer Results

Using the dynamic shear rheometer (DSR), the measured viscous and elastic moduli results at 0.1 to 100 rad/s at 64°C were used to calculate the unaged and aged complex shear moduli (Figure 2-5). The unaged RAS and BMS complex moduli show a consistent increase with increasing shingle percentage. Bio-modification resulted in nearly 50% reduction in moduli. After long term aging, the difference between RAS and BMS reduces, however, BMS values were consistently lower than those of RAS.

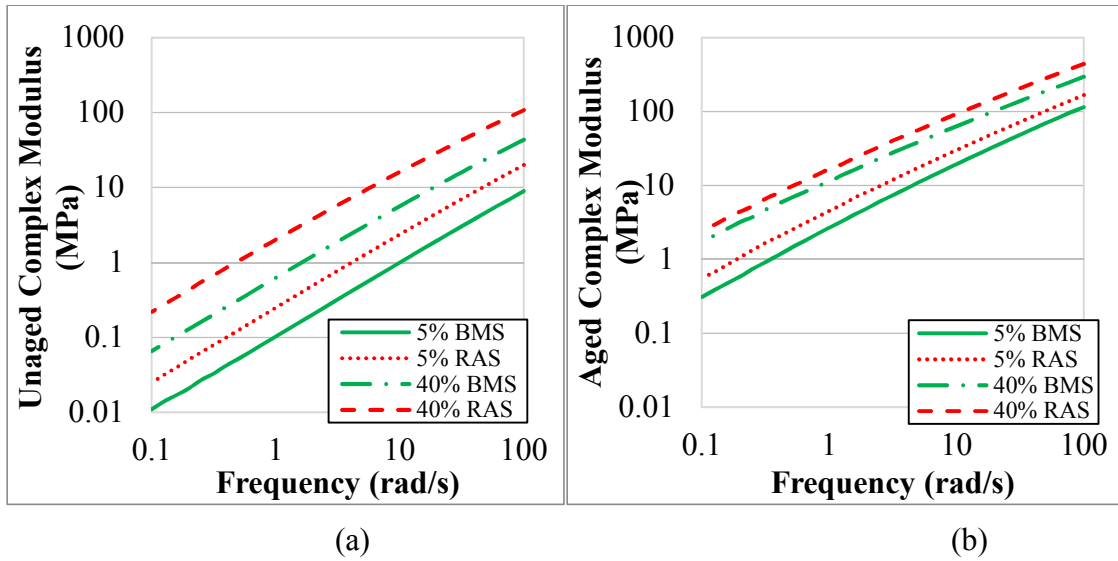


Figure 2-5 Complex Modulus Results for 5 and 40% RAS and BMS at 64° C for Unaged (a) and Aged (b)

From the complex modulus results, the values at 10 rad/s, were determined and used to calculate the Superpave specification parameters as indicators for the material's susceptibility to rutting and fatigue cracking (ASTMD6373-13, 2013). In Table 2-3, the threshold, $G^*/\sin(\delta) > 1.00$ kPa, for the rutting parameter was used to calculate the binder's high temperature grade. The results show that for 5% RAS, the change in the original high grade of 64°C is not noticeable. However, at RAS concentration of 15% and higher, a significant change in passing grade was observed. On the other hand, the inclusion of Bio-binder was shown to maintain the original high grade of 64°C even up to 30% RAS dosage.

Table 2-3 Rutting Performance

	Rutting Parameter $G^*/\sin(\delta)$					Criteria	High Temperature Grade
	58°C	64°C	70°C	76°C			
5% RAS	3.79	1.59	0.72	0.35	> 1.00 kPa	64°C	
5% BMS	1.46	0.65	0.31	0.16		58°C	
15% RAS	5.94	2.49	1.10	0.53		70°C	
15% BMS	3.38	1.69	0.77	0.38		64°C	
30% RAS	6.45	2.75	1.24	0.60		70°C	
30% BMS	2.82	1.32	0.66	0.33		64°C	
40% RAS	29.56	11.91	4.98	2.18		76°C	
40% BMS	3.38	3.93	1.73	0.82		70°C	

The fatigue cracking parameter threshold ($G^*\sin(\delta) < 5000\text{kPa}$) calculated at different temperatures for the aged specimens is given in Table 2-4. According to this threshold,

to avoid fatigue cracking, $G^* \sin(\delta)$ of binders, after being exposed to PAV aging, must be lower than 5000 kPa. This threshold was used to determine low passing temperature grade for each RAS concentration. The results show that even 5% RAS concentration led to a change in low passing temperature grade, indicating that all RAS samples were more susceptible to fatigue cracking. However, bio-modification was able to consistently reduce the $G^* \sin(\delta)$ value for all RAS percentages, indicating that Bio-binder can help improve fatigue cracking performance even after long term aging.

Table 2-4 Fatigue Cracking Performance

	PAV Aged Fatigue Cracking Parameter $G^* \sin(\delta)$						Criteria	Passing Temperature
	34°C	31°C	28°C	25°C	22°C			
5% RAS	2158.41	2874.54	4443.94	6135.87	8368.22	< 5000 kPa	28°C	
5% BMS	1441.66	1880.09	3072.82	4274.63	6061.63		25°C	
15% RAS	2522.63	3387.99	4886.47	6742.44	8962.07		28°C	
15% BMS	1843.17	2417.30	3849.30	5327.31	7407.98		28°C	
30% RAS	2972.57	4000.42	5868.79	8015.94	10689.73		31°C	
30% BMS	2700.62	3574.16	5256.36	7076.94	9493.83		31°C	

40% RAS	4927.79	6624.25	9181.28	12350.81	15983.85		34°C
40% BMS	3224.76	4748.68	6143.13	9066.44	10958.42		31°C

The DSR was also used to measure the viscous (G'') and elastic (G') moduli as a function of frequency as well as determine the crossover values. In Figure 2-6, the G'' and G' are plotted for long term aged 5% and 40% shingle concentration. As shingle percentage increased from 5 to 40%, the crossover frequency (intersection of the G'' and G') reduced, which indicates the materials become stiffer and less compliant. However, after bio-modification both crossover frequency and modulus increased to be closer to that of control specimen.

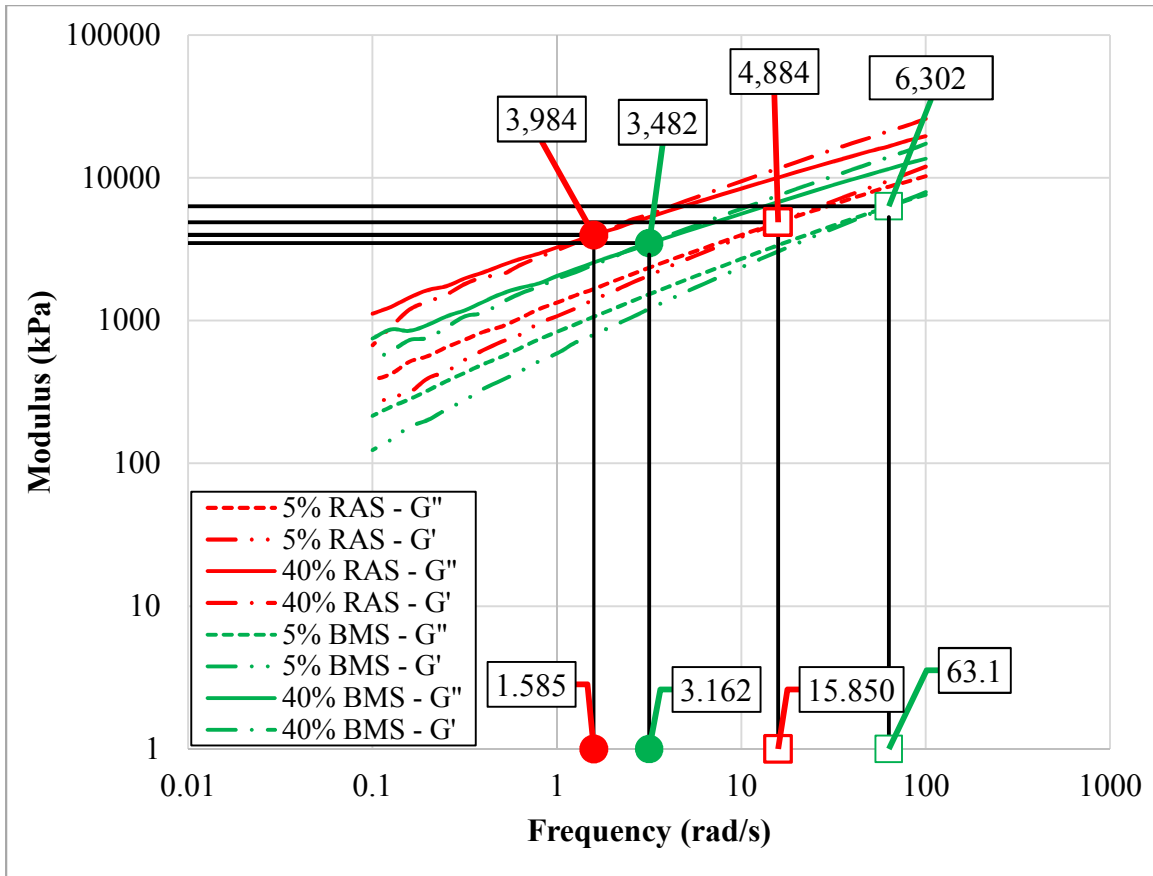


Figure 2-6 Crossover Modulus and Frequency Results for Aged BMS and RAS

In order to examine the effect of bio-modification on crossover modulus and frequency, the difference in crossover values between BMS and RAS were plotted in Figure 2-7. In all scenarios, bio-modification was found to be effective in increasing crossover values. This could be related to the Bio-binder's ability to de-agglomerate oxidized asphalt components which are self-assembled due to the increased polarity during aging. The efficacy of bio-modification in increasing crossover frequency was found to be reduced at higher RAS concentration, with nearly no changes in crossover frequency observed at

40% RAS. Considering that the bio-modification method remained the same for all RAS dosages, the reduced efficacy can be in part due to the reduced ratio of Bio-Binder to RAS; while the dosage of RAS increased, Bio-binder dosage remained constant in the bio-modification process thus making Bio-binder less available per unit of RAS. On the other hand, the difference in crossover modulus was noticeable at all RAS concentration level and was increased at higher concentration, which may indicate decreased polydispersity due to deagglomeration role of Bio-binder breaking larger self-assembled structures to smaller and more uniform clusters thus reducing the particle size distribution.

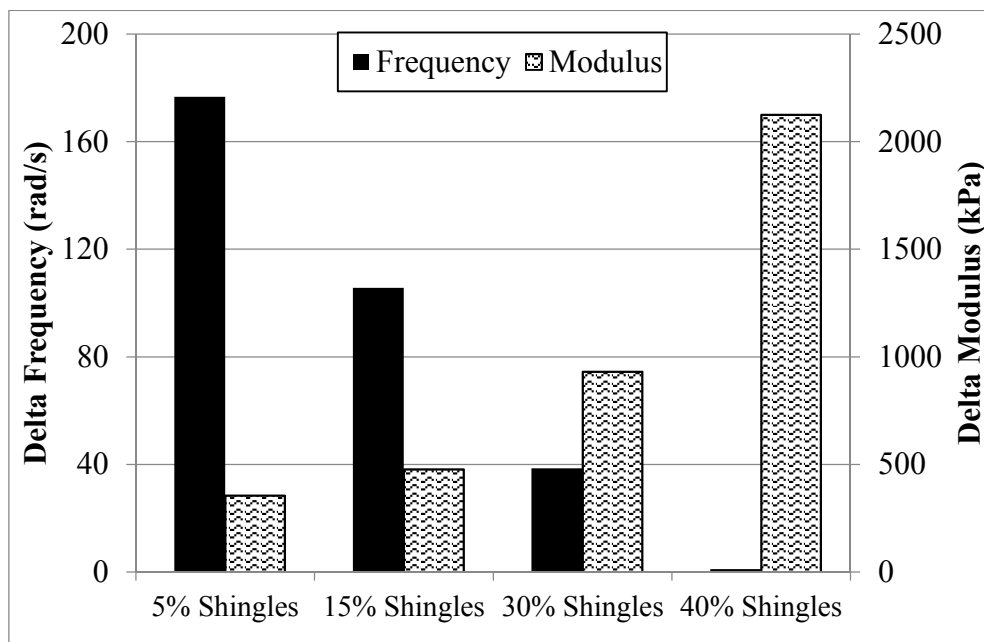


Figure 2-7 Change in (Delta) Crossover Modulus and Frequency Results for Aged BMS and RAS

Figure 2-8 shows the crossover temperatures before and after specimens were exposed to long-term aging. It can be seen that the crossover temperature consistently increased as RAS and BMS concentration increases. However, the BMS values were significantly lower than those of RAS. After bio-modification, the crossover temperature of 5, 15, 30 and 40% RAS was decreased by 29%, 52%, 40%, and 49%, respectively. After the samples were exposed to long-term aging, the difference in crossover temperature between RAS and BMS was found to be 16%, 13%, 14%, and 17% respectively. This in turn indicates that the enhancement effect of bio-modification remains even after long-term aging leading to a more compliant material.

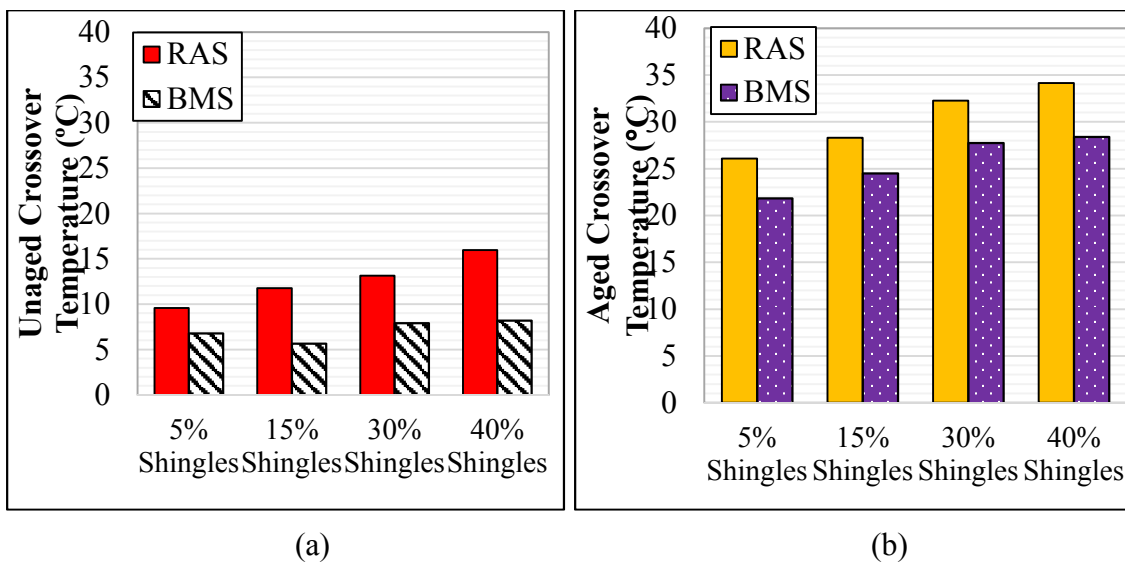


Figure 2-8 Crossover Temperature Results for BMS and RAS Samples: (a) Unaged And (b) Aged

2.3.3 Three-point Bending Test (Bending Beam Rheometer) Results

Deflection of the samples at low temperature under a constant load was measured for each scenario. Equation 4 was used to calculate the stiffness of RAS and BMS samples. For the unaged samples in Figure 2-9, a consistent increase in stiffness was observed with the increase in shingle percentage. After bio-modification, all specimens show reduced stiffness to a point that 40% BMS (bio-modified) had a lower stiffness than 5% RAS (non-modified). The difference between RAS and BMS was reduced after aging, as shown in Figure 2-10, however, the trend remained the same with all BMS samples having lower stiffnesses than RAS.

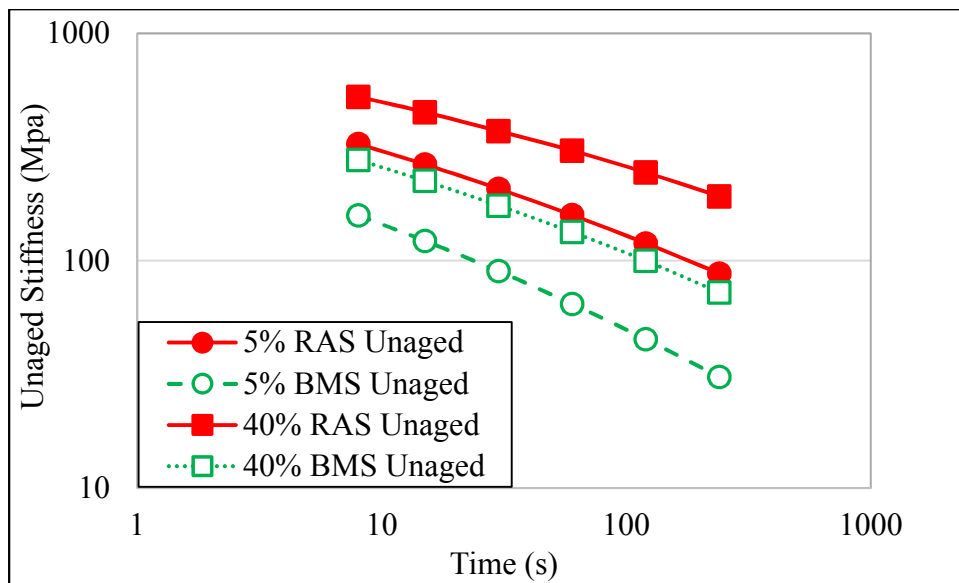


Figure 2-9 BBR Stiffness Results for Unaged BMS and RAS Samples at -12°C

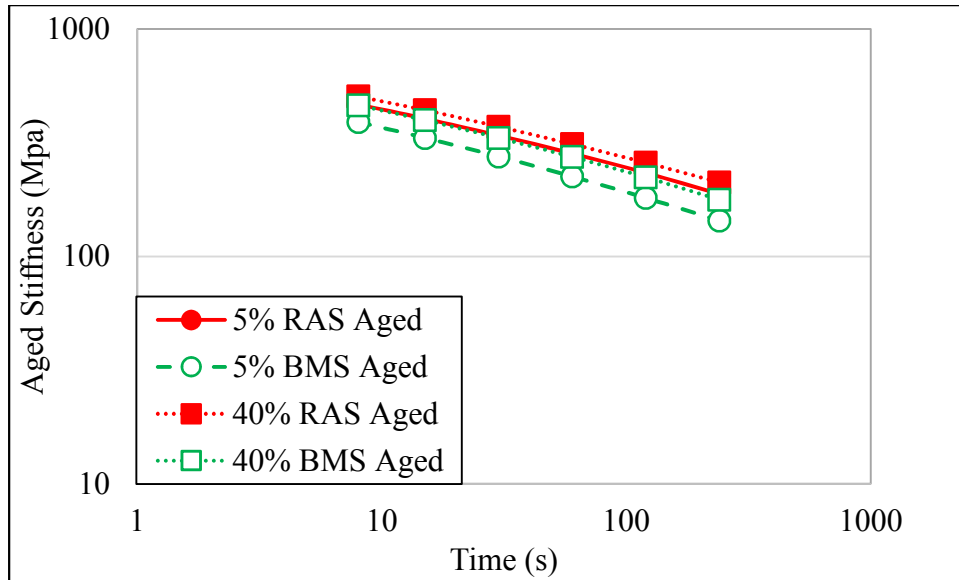


Figure 2-10 BBR Stiffness Results for Aged BMS and RAS Samples at -12°C

The grading parameters (stiffness and m-value at 60 seconds), used by Superpave Performance specification (ASTMD6373-13, 2013) as indicators of binder susceptibility to low temperature cracking, are shown in Table 5. It can be seen that bio-modification decreased stiffness of 5, 15, 30, 40% RAS by 59%, 38%, 37%, and 56%, respectively. The difference between RAS and BMA was reduced to 21%, 14%, 12%, and 12%, respectively after aging. However, all BMS samples showed lower stiffness than RAS. The m-value on the other hand was found to be higher for BMS than for RAS with the difference being 25%, 18%, 10%, and 33% before aging, and 10%, 1%, 9%, and 6% after aging. This indicates that the enhancement effect of bio-modification lasts even after aging and that Bio-binder was able to compensate for some of the stiffening effect of RAS leading to a more compliant material with improved low temperature performance.

It should be noted that without bio-modification, the low temperature grade could not be met even at 5% shingles. Alternatively, bio-modification enabled the RAS sample to meet the low temperature grade up to 30% shingles thus allowing a significant increase in RAS concentration without compromising low temperature performance.

Table 2-5 Aged Stiffness and M-Value Results at 60 Seconds

	5% Shingles		15% Shingles		30% Shingles		40% Shingles	
	-12°C	-18°C	-12°C	-18°C	-12°C	-18°C	-12°C	-18°C
Stiffness (MPa)								
RAS	284	444	291	478	307	497	313	512
BMS	225	405	250	424	271	455	275	471
m-value								
RAS	0.28	0.24	0.29	0.23	0.28	0.25	0.26	0.23
BMS	0.30	0.26	0.30	0.26	0.30	0.24	0.28	0.25

In order to further examine effect of RAS on low temperature properties, the Delta T_c values were calculated and are shown in Figure 2-11. To determine the Delta T_c values, the BBR was used to measure stiffness and m-values at temperatures which will give stiffness and m-value results above and below 300 MPa and 0.3, respectively. Therefore,

the samples were all tested at -18°C in addition to -12°C and the results were used to determine $T_{c,s}$ and $T_{c,m}$ via Equations 5 and 6. Finally, the Delta T_c was calculated as the difference between $T_{c,s}$ and $T_{c,m}$.

From the results, at shingle dosages of 5, 30 and 40%, Delta T_c values were found to be -4.66, -4.73, and -6.14°C for RAS, and -2.67, -1.36, and -5.70°C for BMS respectively.

Previous research documented that an increase in Delta T_c relates to higher levels of aging in asphalt (Anderson, 2017). The lower values of Delta T_c in the BMS specimens may indicate a reduction of the effect of aged asphalt, which can be attributed to Bio-binder's ability to enhance the blending between aged and virgin binder (Figure 2-11). This was especially noticeable at 30% BMS for which the Delta T_c was reduced from -4.73 in RAS to 1.36 in BMS. The latter is in-line with results in previous showing 30% BMS meets low temperature grading of control binder.

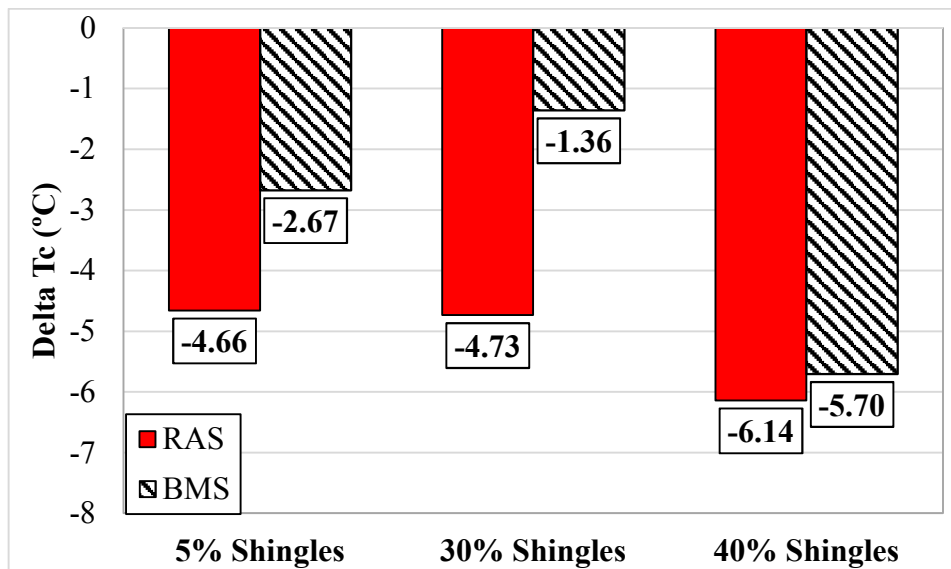


Figure 2-11 Delta T_c Results for BMS and RAS Using the BBR

To further study the durability of BMS, the physical hardening phenomenon was studied using an extended sub-zero conditioning at -18°C followed by BBR testing (Marasteanu et al., 2012). Physical hardening is known to cause time-dependent isothermal changes in mechanical properties. It has been documented that the effect of physical hardening is reversible if the material is heated to room temperature (Hesp & Subramani, 2009). This phenomenon is caused by the isothermal reduction of free volume which occurs at temperatures close to the material's glass transition temperature (Romero et al., 1999). The effect of physical hardening is typically reflected in an increase in the stiffness value and a reduction of the stress relaxation capacity of the asphalt (Anderson et al., 1994; Bahia, 1992). The latter led the specification to require asphalt binder properties be evaluated after both 1hr and 24hr conditioning at a specified temperature (AASHTO-M320-05, 2002). It has been also documented that binder properties measured after extended conditioning correlates better with field performance data due to the accounting for physical hardening effect of binder (Hesp & Subramani, 2009).

Figure 2-12 shows that after bio-modification, the deflection of RAS specimens is closer to that of virgin binder even after extended conditioning. At 0 hours conditioning, the BMS increased the deflection by an average of 4% while the increase was found to be 23% after 72 hrs. As conditioning time increased the difference between RAS and BMS increased indicating a suppressing effect of Bio-binder on physical hardening. The latter could be attributed to the surfactant effect of Bio-binder delaying structuring and crystallization of alkane chains of asphalt binder at sub-zero temperatures.

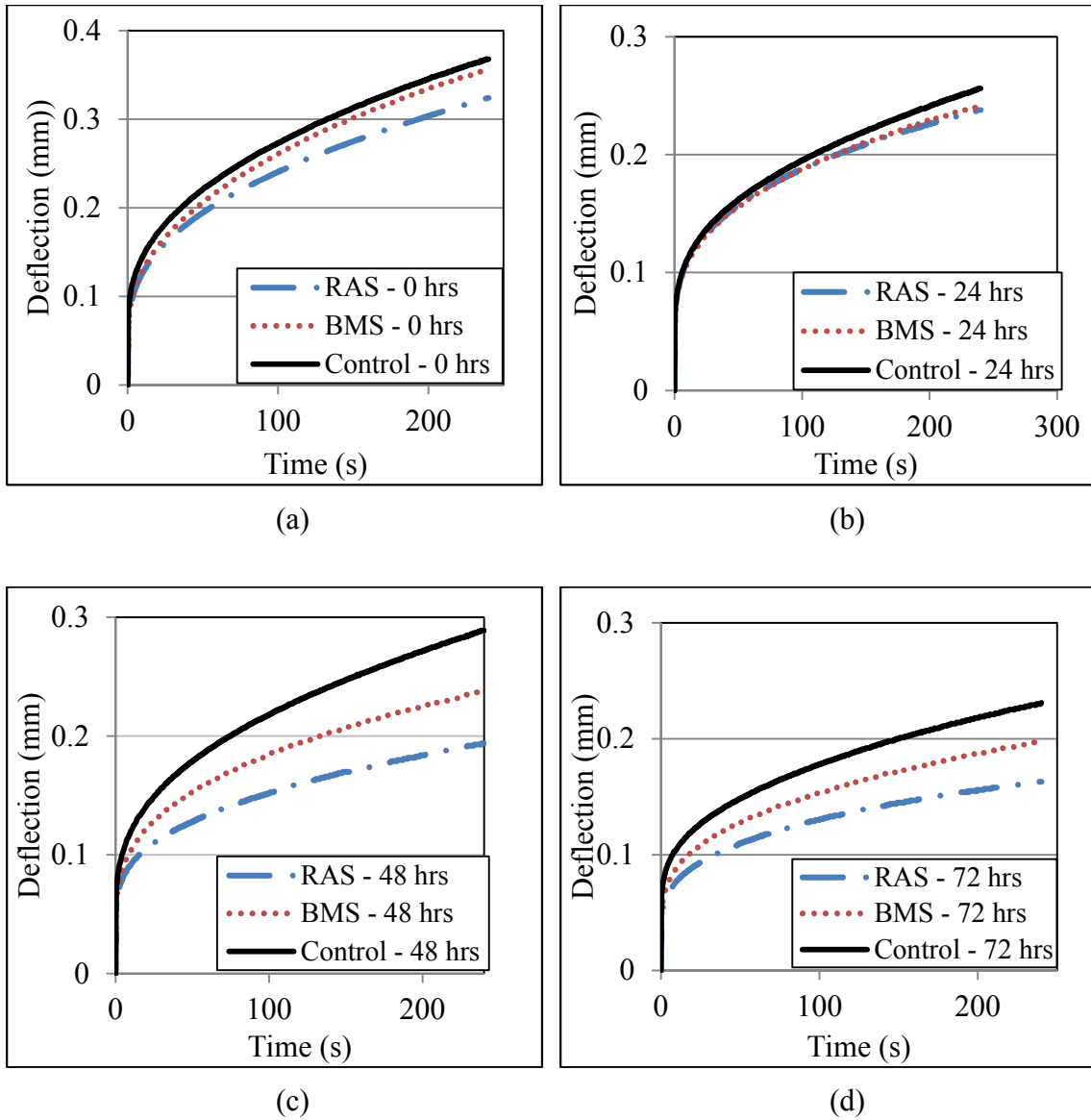


Figure 2-12 Unaged Creep-Deflection Curves at -18°C for Control, 40% RAS, and BMS

Figure 2-13 further demonstrates the relaxation performance of the samples at different conditioning times for both RAS and BMS samples before and after long-term aging.

Overall, BMS had a higher m-value than RAS indicating an increased ability to alleviate

stress within the material. The improvement in stress releasing capacity was even more noticeable after long-term aging. The m-values of BMS at 5, 15, 30 and 40% shingles were found to be 12%, 14%, 21%, and 23% higher than that of RAS, respectively.

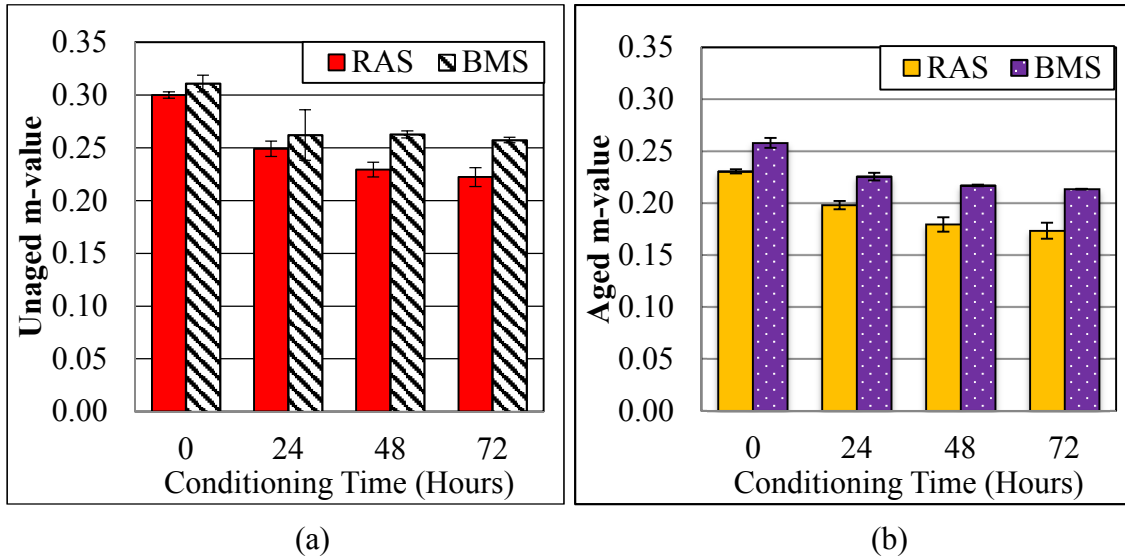


Figure 2-13 The m-value Results for 40% BMS and 40% RAS at -18°C: (a) Unaged and (b) Aged

The creep deflection for the BMS and RAS samples conditioned at 0, 24, 48, and 72 hours at -18°C are shown in Figure 2-14. It can be seen that binder becomes stiffer (less deflection) as the conditioning time increases. It was further observed that by conditioning the RAS samples for 24, 48 and 72 hours, the creep stiffness increased by an average of 25%, 50% and 69%, respectively. However, stiffness of BMS samples for the same conditioning time increased 30%, 32% and 42% respectively. This can be attributed to the Bio-binder suppressing physical hardening by delaying molecular packing and structuring of alkane chains in asphalt at sub-zero temperature.

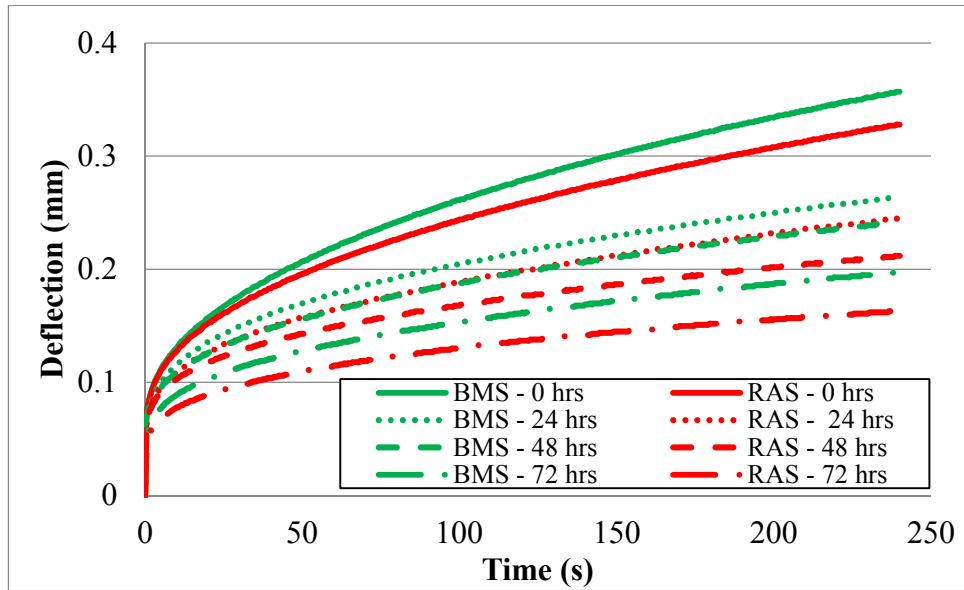


Figure 2-14 Unaged Time-Dependent Creep Load Deflection for 40% BMS and 40% RAS at -18°C

2.3.4 Direct Tension Test Results

The DTT was utilized to determine the failure strain for the RAS and BMS at, 15 and 30% shingles both before and after long-term aging. It was shown that failure strain reduces as the RAS concentration increases. The findings were consistent with those of previous study that showed failure strain decrease with increasing percentages of particles (Wang et al., 2013). Bio-modification was shown to increase the failure strain of RAS by 256% and 288%, respectively (Figure 2-15). The more ductile behavior of BMS samples compared to RAS was observed even after long-term aging as evidenced by BMS having

113% and 838% higher failure strains at 15% and 30% shingle concentrations after aging, respectively.

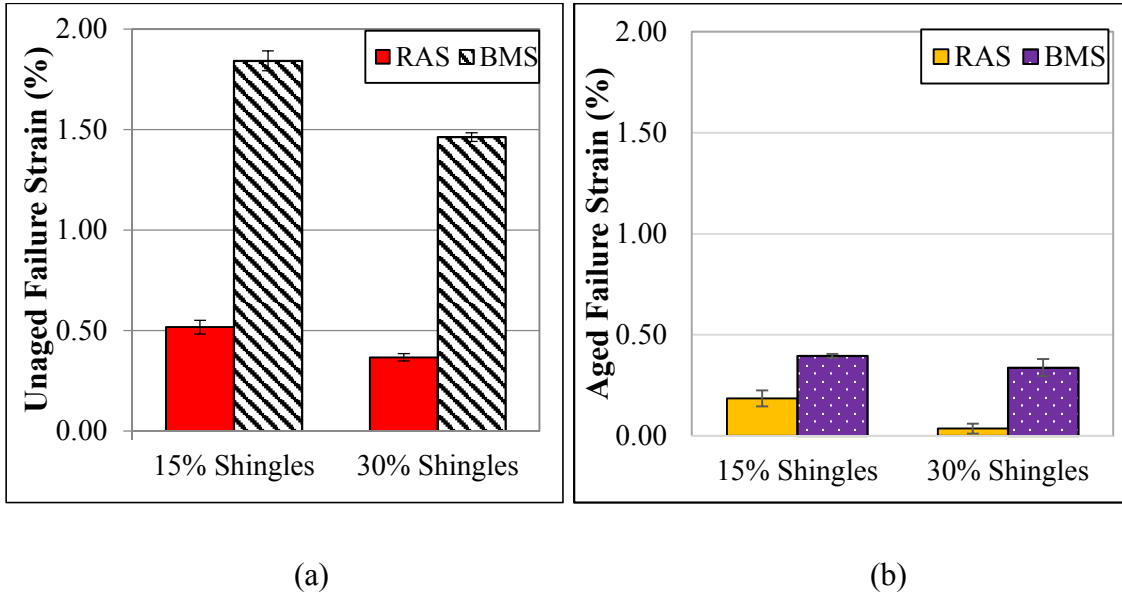


Figure 2-15 Failure Strain for RAS and BMS at -12°C: (a) Unaged and (b) Aged

The phenomenon of physical hardening was also studied by examining failure strain of specimens after extended conditioning at -18°C for both unaged and PAV-aged 40% shingles. Figure 2-16 shows that as conditioning time increases, the failure strain decreases in both RAS and BMS samples. However, BMS had a consistently higher failure strain value compared to RAS even after aging.

For the 40% RAS samples, the failure strain did not significantly change after 48 and 72hr conditioning, which may indicate that the material has already reached its maximum physical hardening.

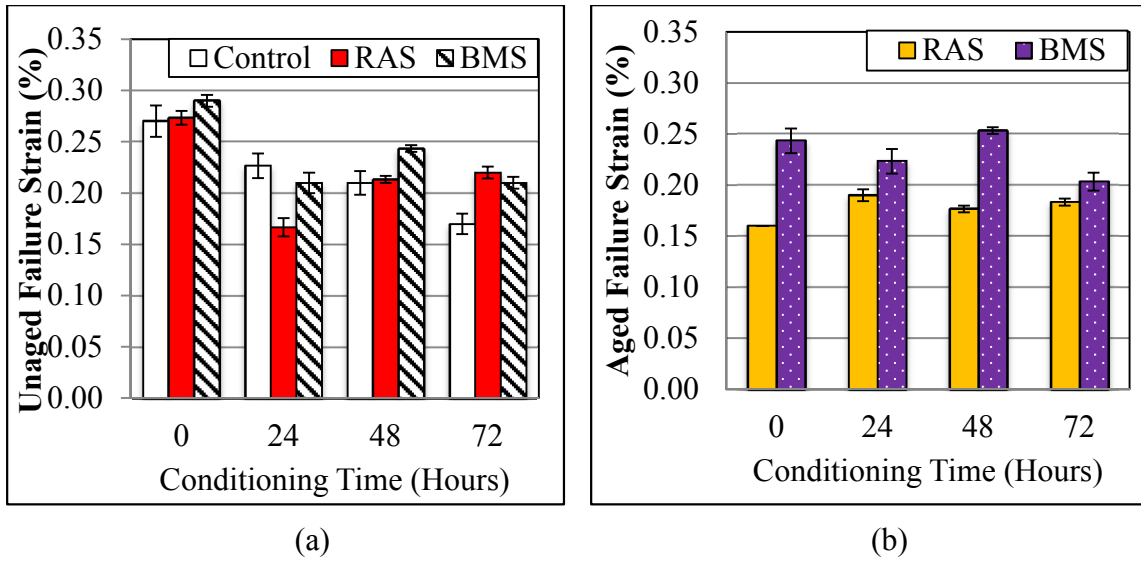


Figure 2-16 Failure Strain for 40% RAS and 40% BMS Samples at -18°C (a) Unaged and (b) Aged

Figure 2-17 shows the fracture energy results calculated using Equation 7. The results show that BMS has similar fracture energy values compared to RAS, with the biggest difference occurring at 24 hours. However, after PAV aging, a significant difference was observed in fracture energy results between RAS and BMS. The fracture energy of the aged BMS was nearly double that of the aged RAS after 48 hours of isothermal conditioning, indicating that the RAS samples were more susceptible to physical hardening than the BMS. It has been documented that materials with higher fracture energy values tend to have improved low-temperature performance (Hill et al., 2013).

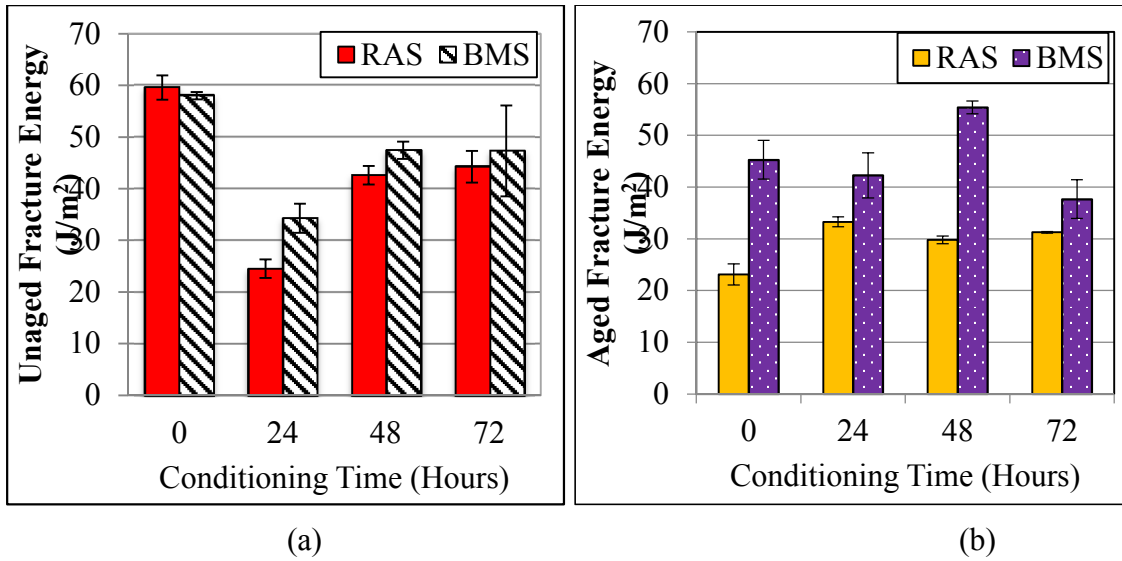


Figure 2-17 Fracture Energy for 40% BMS and 40% RAS Samples at -18°C: (a) Unaged, (b) Aged

2.4 Conclusions

To facilitate the increased use of Recycled Asphalt Shingles (RAS) in pavement construction, this paper examines how RAS properties can be improved through bio-modification by creating bio-modified shingles (BMS). Accordingly, the thermo-mechanical properties of BMS were studied both after oxidation and extended sub-zero conditioning to study the efficacy of bio-modification. It was found that BMS had a lower viscosity compared to RAS both before and after oxidative aging with higher differences being observed at higher Bio-binder to shingle ratios. Also, the shear susceptibility and activation energy of BMS were found to be lower than that of RAS

samples indicating a plausible reduction of intermolecular interactions in oxidized asphalt in presence of Bio-binder.

The complex modulus curves of BMS were found to be consistently below those of RAS both before and after aging and was more evident at low shingle percentages. Comparing values of $G^* \sin(\delta)$ as indicators of fatigue cracking, it was shown that BMS fatigue resistance is higher than that of RAS. BMS crossover modulus and crossover frequency values were found to be higher than those of RAS indicating possible deagglomeration of nanoaggregates of oxidized asphaltenes which are known to increase in size due to aging.

The low temperature stiffness of BMS samples was consistently lower than that of RAS both before and after aging. In addition, Delta T_c values of BMS were significantly lower than those of RAS. Specially, a significant improvement was observed at 30% shingle concentration where Delta T_c was reduced from 4.73 to 1.36 after bio-modification. The latter could lead to enhanced fatigue cracking performance due to bio-modification. The failure strain of BMS was 258% and 300% higher than that of RAS at the unaged status, and 114% and 839% higher than RAS after aging indicating BMS remains more ductile than RAS even after aging. The enhancement effect was also observed after extended sub-zero conditioning.

Studying the performance of BMS after extended sub-zero conditioning showed bio-modification could delay physical hardening as evidenced by a higher fracture energy and failure strain in BMS compared to RAS even after 72hr conditioning at -18°C . The latter can be attributed to bio-modifier's delaying molecular packing and structuring of alkane

chains in oxidized asphalt. The outcome of this study contributes to the body of knowledge by showing that the durability and performance of recycled asphalt shingles can be improved via bio-modification to facilitate its application as a sustainable construction practice.

2.5 Acknowledgments

This research is sponsored by the National Science Foundation (Award No: 1640517). The authors also want to acknowledge the valuable help of Angelina Zimmer of Bob Jones University. The contents of this paper reflect the view of the authors, who are responsible for the facts and the accuracy of the data presented.

2.6 References

- AASHTO-M320-05. (2002). Standard Specification for Performance Graded Asphalt Binder. *American Association of State Highway and Transportation Officials, Washington, D.C.*
- Abbas, A. R., Mannan, U. A., & Dessouky, S. (2013). Effect of recycled asphalt shingles on physical and chemical properties of virgin asphalt binders. *Construction and building materials, 45*, 162-172.
- Al-Mansoori, T., Norambuena-Contreras, J., Micaelo, R., & Garcia, A. (2018). Self-healing of asphalt mastic by the action of polymeric capsules containing rejuvenators. *Construction and building materials, 161*, 330-339.
- Anderson, D. A., Christensen, D. W., Bahia, H. U., Dongre, R., Sharma, M. G., Antle, C. E., & Button, J. (1994). Binder characterization and evaluation, volume 3: Physical characterization. *Strategic Highway Research Program, National Research Council, Report No. SHRP-A-369.*
- Anderson, M. (2017). Delta Tc: Concept and Use. *Transportation Research Board Annual Meeting, Washington, DC, January 2017.*
- ASTMD2872-12e1. (2012). Standard Test Method for Effect of Heat and Air on a Moving Film of Asphalt (Rolling Thin-Film Oven Test). *ASTM International, West Conshohocken, PA, 2012, www.astm.org.*
- ASTMD4402. (2015). *Standard test method for viscosity determination of asphalt at elevated temperatures using a rotational viscometer.* Paper presented at the American Society for Testing and Materials.
- ASTMD6373-13. (2013). Standard Specification for Performance Graded Asphalt Binder. *ASTM International, West Conshohocken, PA, 2013, www.astm.org.*
- ASTMD6521-13. (2013). Standard Practice for Accelerated Aging of Asphalt Binder Using a Pressurized Aging Vessel (PAV). *ASTM International, West Conshohocken, PA.*
- ASTMD6648-08. (2016). Standard Test Method for Determining the Flexural Creep Stiffness of Asphalt Binder Using the Bending Beam Rheometer (BBR). *ASTM International, West Conshohocken, PA, 2016, www.astm.org.*
- ASTMD6723. (2012). Standard Test Method for Determining the Fracture Properties of Asphalt Binder in Direct Tension (DT). *West Conshohocken, PA; ASTM International, 2012. doi:https://doi.org/10.1520/D6723-12*
- ASTMD7175-15. (2015). Standard Test Method for Determining the Rheological Properties of Asphalt Binder Using a Dynamic Shear Rheometer. *ASTM International, West Conshohocken, PA, 2015, www.astm.org.*

- Bahia, H. U. M. (1992). Low-temperature isothermal physical hardening of asphalt cements.
- Elkashef, M., Podolsky, J., Williams, R. C., & Cochran, E. W. (2018). Introducing a soybean oil-derived material as a potential rejuvenator of asphalt through rheology, mix characterisation and Fourier Transform Infrared analysis. *Road Materials and Pavement Design*, 19(8), 1750-1770.
- Elseifi, M. A., Salari, S., Mohammad, L. N., Hassan, M., Daly, W. H., & Dessouky, S. (2012). New approach to recycling asphalt shingles in hot-mix asphalt. *Journal of Materials in Civil Engineering*, 24(11), 1403-1411.
- Fini, E. H., Kalberer, E. W., Shahbazi, A., Basti, M., You, Z., Ozer, H., & Aurangzeb, Q. (2011). Chemical characterization of biobinder from swine manure: Sustainable modifier for asphalt binder. *J. Mater. Civ. Eng.*, 23(11), 1506.
- Hansen, K. R., & Newcomb, D. E. (2011). Asphalt pavement mix production survey on reclaimed asphalt pavement, reclaimed asphalt shingles, and warm-mix asphalt usage: 2009-2010. *Information Series*, 138, 21.
- Hesp, S. A. M., & Subramani, S. (2009). *Another look at the bending beam rheometer for specification grading of asphalt cements*.
- Hill, B., Oldham, D., Behnia, B., Fini, E., Buttlar, W., & Reis, H. (2013). Low-temperature performance characterization of biomodified asphalt mixtures that contain reclaimed asphalt pavement. *Transportation Research Record: Journal of the Transportation Research Board*(2371), 49-57 %@ 0361-1981.
- Hill, B., Oldham, D., Behnia, B., Fini, E. H., Buttlar, W. G., & Reis, H. (2013). Low-temperature performance characterization of biomodified asphalt mixtures that contain reclaimed asphalt pavement. *Transp. Res. Rec.*, 2371(1), 49.
- Hung, A. M., Mousavi, M., Pahlavan, F., & Fini, E. H. (2017). Intermolecular Interactions of Isolated Bio-Oil Compounds and Their Effect on Bitumen Interfaces. *ACS Sustainable Chemistry & Engineering*, 5(9), 7920-7931.
- Ji, J., Yao, H., Suo, Z., You, Z., Li, H., Xu, S., & Sun, L. (2017). Effectiveness of vegetable oils as rejuvenators for aged asphalt binders. *Journal of Materials in Civil Engineering*, 29(3), D4016003.
- Marasteanu, M., Austin, J., & Moon, K. H. (2012). Recycling Asphalt Roofing Shingles in Asphalt Pavements. *CURA Reporter*, 42(1).
- Marasteanu, M., Buttlar, W., Bahia, H., Williams, C., Moon, K. H., Teshale, E. Z., . . . Paulino, G. (2012). Investigation of low temperature cracking in asphalt pavements national pooled fund study–phase II.
- Maupin, G. W. (2010). Investigation of the use of tear-off shingles in asphalt concrete (No. VTRC 10-R23). Virginia Transportation Research Council.

- Mogawer, W., Bennert, T., Daniel, J. S., Bonaquist, R., Austerman, A., & Booshehrian, A. (2012). Performance characteristics of plant produced high RAP mixtures. *Road Materials and Pavement Design*, 13(sup1), 183-208.
- Mogawer, W. S., Booshehrian, A., Vahidi, S., & Austerman, A. J. (2013). Evaluating the effect of rejuvenators on the degree of blending and performance of high RAP, RAS, and RAP/RAS mixtures. *Road Materials and Pavement Design*, 14(sup2), 193-213.
- Mousavi, M., Pahlavan, F., Oldham, D., Hosseinneshad, S., & Fini, E. H. (2016). Multiscale investigation of oxidative aging in biomodified asphalt binder. *J. Phys. Chem. C*, 120(31), 17224.
- NAPA. (2016). Recycled Materials and Warm-Mix Asphalt Usage. *National Asphalt Pavement Association*.
- NCDOT. (2018). Monthly Terminal Asphalt Binder & Fuel FOB Prices. *North Carolina Department of Transportation Business Partner Resources*.
- Oldham, D. J., Fini, E. H., & Chailleux, E. (2015). Application of a bio-binder as a rejuvenator for wet processed asphalt shingles in pavement construction. *Construction and building materials*, 86, 75-84.
- Ongel, A., & Hugener, M. (2015). Impact of rejuvenators on aging properties of bitumen. *Construction and building materials*, 94, 467-474.
- Pahlavan, F., Hung, A. M., Zadshir, M., Hosseinneshad, S., & Fini, E. H. (2018). Alteration of π -Electron Distribution To Induce Deagglomeration in Oxidized Polar Aromatics and Asphaltenes in an Aged Asphalt Binder. *ACS Sustainable Chem. Eng.*, 6(5), 6554.
- Pahlavan, F., Mousavi, M., Hung, A. M., & Fini, E. H. (2018). Characterization of oxidized asphaltenes and the restorative effect of a bio-modifier. *Fuel*, 212, 593.
- Romero, P., Youtcheff, J., & Stuart, K. (1999). Low-temperature physical hardening of hot-mix asphalt. *Transportation Research Record: Journal of the Transportation Research Board*(1661), 22-26 %@ 0361-1981.
- Samieadel, A., Høgsaa, B., & Fini, E. H. (2019). Examining the Implications of Wax-Based Additives on the Sustainability of Construction Practices: Multiscale Characterization of Wax-Doped Aged Asphalt Binder. *ACS Sustainable Chem. Eng.*, 7(3), 2943.
- Su, J.-F., Schlangen, E., & Wang, Y.-Y. (2015). Investigation the self-healing mechanism of aged bitumen using microcapsules containing rejuvenator. *Construction and building materials*, 85, 49-56.

- Wang, D., Wang, L., Gu, X., & Zhou, G. (2013). Effect of basalt fiber on the asphalt binder and mastic at low temperature. *Journal of materials in civil engineering*, 25(3), 355-364 %@ 0899-1561.
- West, R. C., & Willis, J. R. (2014). *Case Studies on Successful Utilization of Reclaimed Asphalt Pavement and Recycled Asphalt Shingles in Asphalt Pavements*. Retrieved from
- Williams, B. A., Copeland, A., & Ross, T. C. Asphalt Pavement Industry Survey on Recycled Materials and Warm-Mix Asphalt Usage: 2017; National Asphalt Pavement Association: Lanham, MD, USA, 2018; No. Information Series, 138.
- Williams, R. C., Cascione, A. A., Yu, J., Haugen, D., Marasteanu, M., & McGraw, J. (2013). Performance of recycled asphalt shingles in hot mix asphalt.
- You, Z., Mills-Beale, J., Fini, E., Goh, S. W., & Colbert, B. (2011). Evaluation of low-temperature binder properties of warm-mix asphalt, extracted and recovered RAP and RAS, and bioasphalt. *Journal of Materials in Civil Engineering*, 23(11), 1569-1574.
- Zadshir, M., Hosseini-zhad, S., Ortega, R., Chen, F., Hochstein, D., Xie, J., . . . Fini, E. H. (2018). Application of a Biomodifier as Fog Sealants to Delay Ultraviolet Aging of Bituminous Materials. *J. Mater. Civ. Eng.*, 30(12), 04018310.
- Zaumanis, M., Mallick, R. B., & Frank, R. (2015). Evaluation of different recycling agents for restoring aged asphalt binder and performance of 100% recycled asphalt. *Mater. Struct.*, 48(8), 2475.
- Zeng, M., Li, J., Zhu, W., & Xia, Y. (2018). Laboratory evaluation on residue in castor oil production as rejuvenator for aged paving asphalt binder. *Construction and building materials*, 193, 276-285.
- Zhang, R., You, Z., Wang, H., Ye, M., Yap, Y. K., & Si, C. (2019). The impact of bio-oil as rejuvenator for aged asphalt binder. *Construction and building materials*, 196, 134-143.
- Zhao, S., Nahar, S. N., Schmets, A. J., Huang, B., Shu, X., & Scarpas, T. (2015). Investigation on the microstructure of recycled asphalt shingle binder and its blending with virgin bitumen. *Road Materials and Pavement Design*, 16(sup1), 21-38.
- Zhou, F. (2013). Balanced RAP/RAS mix design and performance evaluation for project-specific service conditions.

CHAPTER 3 THE EFFECT OF CHEMICAL COMPOSITION OF RECYCLING AGENTS ON REVITALIZING OXIDIZED ASPHALT

A version of this paper submitted in Journal of Materials of Civil Engineering
Fini, E. H., Rajib, A. I., Oldham, D., Samieadel, A., & Hosseinnezhad, S. (2020). The Role of Chemical Composition of Recycling Agents in Their Interactions with Oxidized Asphaltene Molecules. Journal of Materials in Civil Engineering, Forthcoming.

3.1 Abstract

The utilization of reclaimed asphalt pavement (RAP) in neat asphalt mixture has received significant attention because of its economic and environmental advantages. However, bitumen contained in RAP is severely aged and when blended with neat asphalt at high percentages, it can negatively affect properties of the resulting blend. Recycling Agents (RA) have been utilized to improve certain properties of aged asphalt and subsequently the performance of the mixture. This paper studies the effectiveness of four different RAs on enhancing properties of aged bitumen while examining mechanical, chemical, and surface properties of aged bitumen doped with each RA. Accordingly, the dynamic shear rheometer (DSR) was used to examine the rheological properties of several blends containing aged asphalt and RA. In addition, FT-IR, TLC-FID, and GPC were employed to track changes in chemical composition, polarity, and solubility of bitumen constituents, as well as molecular size distribution. The surface properties were evaluated

using contact angles measurements in dry and wet condition. The latter analysis was also used to investigate the moisture susceptibility of each blend. Study results showed that the performance of aged bitumen was significantly improved after adding RA as evidenced in the reduction of stiffness and increase of phase angle and colloidal stability index of aged bitumen. In addition, the most effective RA found to be the one leading to the highest increase in crossover modulus of aged bitumen. Some of the studied RAs found to be effective in reducing moisture susceptibility of the aged bitumen as evidenced in reducing the difference between wet and dry contact angle of aged bitumen.

Keywords: asphalt binder, aged asphalt, reclaimed asphalt, complex modulus, moisture, adhesion, contact angle

3.2 Introduction

Recycling of Reclaimed Asphalt Pavement (RAP) and Recycled Asphalt Shingle (RAS) in new pavement constructions is a common practice, which leads to a significant environmental and economic advantages (Mohammadafzali et al., 2018). Studies have revealed that the reuse of RAP annually saves approximately \$2.5 billion while it restores vast landfill spaces as well as preserves natural resources (Hajj et al., 2009; Moghadas Nejad et al., 2014; NAPA, 2016). Despite the benefits of RAP, state departments of transportation have posed limits on how much RAP can be used in a ton of asphalt

mixture due to the potential negative effect of RAP on pavement performance (West et al., 2013).

Studies found that physicochemical properties of aged bitumen found in RAP are adversely affected by oxidation and ultraviolet (UV) radiation during pavement's service life. In addition, during aging, bitumen loses some of the light components of maltenes, which changes the balance between asphaltene and maltene portion (Tran et al., 2012). Several researchers have shown that content of asphaltene in bitumen increases during aging and that aged bitumen in RAP has higher asphaltene content than unaged bitumen. Accordingly, replacing some of the bitumen in new pavement construction with RAP bitumen can disturb the colloidal balance of the overall blend (Mogawer et al., 2013; Shen et al., 2007). It has been also documented that aged bitumen has higher stiffness and lower workability than unaged bitumen; low workability prevents achieving proper compaction in the field giving rise to premature failure (Mogawer et al., 2012). Furthermore, aging increases the content of carbonyl and sulfoxide of bitumen and gives rise to the formation of aromatic conjugates (Yang et al., 2018). To enhance the properties of aged bitumen in RAP and facilitate the use of high percentages of RAP, many researchers utilize recycling agent, which in some cases mentioned as a rejuvenator.

Studies have successfully applied various rejuvenators to restore both the rheological and mechanical properties of aged bitumen. For instance, the low temperature cracking resistance of aged bitumen was improved by the addition of bio-oil which was derived

from biodiesel residue (Gong et al., 2016). The viscosities, stiffness, shear susceptibilities, and crossover temperatures of recycled asphalt shingle (RAS) were reduced due to the addition of bio-binder produced from biomass (Oldham et al., 2019). Moreover, the enhanced durability of the biomodified RAS was observed compared to the unmodified RAS (Oldham et al., 2019). The stiffness and glass transition temperature of the aged binder was found to be lower while m-value and fracture energy were higher after the addition of bio-based and refined waste oil to the aged binder (Lei et al., 2015). The complex modulus and phase angle of RAP binder found to become closer to the value that of the neat binder when either of natural seed oil, cashew shell oil, and tall oil was added to the aged bitumen (Cavalli et al., 2018). Other study showed sulfoxide index and the large molecule size (LMS) content of aged bitumen decreased by the addition of vegetable oil to aged bitumen (Cao et al., 2018). Crack healing performance of RAP binder was enhanced by the addition of cooking oil and steel wool fibers (Dinh et al., 2018). Rutting and fatigue performances of aged asphalt were upgraded with the addition of soybean-derived rejuvenator (Elkashef et al., 2018). The low temperature cracking performance of aged asphalt and polymer modified aged asphalt was improved by the addition of Polyphosphoric acid (PPA) (Liu et al., 2018). Addition of date seed oil to aged asphalt reduced the viscosity, increased the fatigue behavior of the aged asphalt (Mirhosseini et al., 2018). In a case study, low saturate aromatic extract oil functioned as a recycling agent in restoring aged bitumen engineering and chemical properties (Chen et al., 2018).

In addition to the rejuvenator effect on the aged binder physicochemical study, the study of the effect of rejuvenator on surface properties and adhesion of aged asphalt binder is also essential to evaluate the overall durability and bond strength between binder and aggregate. Moreover, the plausible susceptibility of the interface to moisture damage should be considered. As such, previous studies have shown that when water is introduced to the surface of the aggregate covered by the binder, the binder may strip off and cause a failure in asphalt pavement (Apeageyi et al., 2014; Hasan et al., 2015). Hung et al. (2017), studied the contact angle measurement of asphalt binder on a glass slide to qualitatively measure how binder adhesion to glass changes in presence of water and found that the extent of change in contact angle values highly depend on the binder composition and environmental condition (Hung et al., 2017). Considering the correlation between contact angle, wettability, and adhesion, the study indicated that asphalt binder's resistance to moisture damage can be altered by changing the surface properties of binder using dopants (Hung et al., 2017).

Accordingly, the objective of this study was to investigate the effect of recycling agents to change the physicochemical and surface properties of the aged asphalt. These were studied using rheological characterization, chemical functional group analysis, deagglomeration capability of asphaltene molecule, and measurement of the molecular size distribution of aged asphalt in the presence of several recycling agents. Qualitative assessment of adhesion of the aged asphalt binder doped with recycling agents was further examined in wet and dry condition to evaluate the moisture susceptibility of each

specimen. Furthermore, the efficiency of recycling agents on oxidized asphaltene molecules deagglomeration through molecular dynamic simulation was studied to support the results of the experimental part.

3.3 Materials and Method

3.3.1 Materials

The neat asphalt binder used in this project was a Superpave PG 64-22, which is one of the most commonly used grades of asphalt binders across the US. Four different recycling agents were collected from Nebraska and Maryland where three of them were organic bio-based and one petroleum-based recycling agent. The recycling agents (RA) were specifically chosen based on their sources and structures to cover a wide array of molecular structures and sources. This in turn helped the study results be generalizable and cover variety of products in the market. Table 3-1 shows the chemistry and source of RA. In this study, the four RA are labeled as RA-A, RA-B, RA-C, and RA-D.

Table 3-1 Chemistry and Source of RA

Recycling Agent	Organic/Petroleum
A	Plant Extract based
B	Vegetable oil-based
C	Plant-based

D	Aromatic Extract
---	------------------

3.3.2 Asphalt Binder Aging

Neat asphalt binder was aged in a two-step aging process including short-term aging and long-term aging. Short-term aging was performed via a Rolling Thin Film Oven (RTFO) which was done according to (ASTMD2872-12e1, 2012). After the short-term aging, the sample was placed in a pressure aging vessel (PAV) for long-term aging following (ASTMD6521-13, 2013). 50 g of each RTFO aged samples were placed onto a steel plate and subjected to a pressure of 2.10 MPa at 100° C for 40h. The extended aging was selected based on previous research which found that 40h aging would represent the aging level of asphalt pavement at the end of its service life representative of RAP asphalt binder (Bowers et al., 2014). In this paper, the acronym used for the samples aged as described above is 2PAV.

To prepare blended samples, 10% (by weight of asphalt binder) of each RA was mixed into 2PAV sample. To do so, the aged binder was heated to 135°C for 30 min, then the RA was added to the binder and mixed for 5 minutes by hand using a spatula. The four RA added samples were labeled as A, B, C, and D, respectively.

3.3.3 Dynamic Shear Rheometer (DSR)

According to (ASTMD7175-15, 2015), the elastic and viscous behavior of all samples were measured using Thermo Scientific HAAKE rheometer at 17 frequency intervals

between 0.1 to 46.42 Hz and at a temperature range of 22°C to 70°C at the 6-degree interval. For this study, a 20 mm spindle was utilized. Complex shear modulus (G^*) and phase angle (δ) were calculated from the measured data following Equation 3-1. The complex shear modulus (G^*) is a measure of material resistance to deformation when repeatedly sheared, and δ , the time lag between stress and strain, is used to evaluate pavement rutting and fatigue cracking resistance (AASHTOT315, 2012).

$$G^* = \frac{\tau_{\max}}{\gamma_{\max}} \quad (3-1)$$

In which $\gamma_{\max} = \left(\frac{\theta r}{h} \right)$ and $\tau_{\max} = \frac{2T}{\pi r^3}$

Where:

γ_{\max} = maximum strain

τ_{\max} = maximum stress

T = maximum applied torque

r = radius of the sample

θ = deflection (rotational) angle

h = height of the sample

The results were then evaluated based on the performance grade specifications (ASTMD6373-13, 2013) in which $G^*/\sin(\delta)$ is used as a measure of rutting resistance,

and $G^* \sin(\delta)$ is used as a measure of susceptibility to fatigue. In addition, master curves at 52°C were generated for all samples using Time-Temperature Superposition (TTS) shifting of complex modulus and phase angle data to the reference temperature of 52°C. Additionally, using the corresponding elastic (G') and viscous (G'') moduli results, the crossover frequency and moduli were determined (Huang et al., 2014).

3.3.4 Fourier Transform Infrared (FTIR) Spectroscopy

Thermo Scientific Nicolet iS10 FT-IR spectrometer has been used to characterize the functional groups of RAs blended with aged asphalt binder. FTIR analysis helps to understand the chemical changes during the interactions between the RA and binder. Before testing each sample, the FTIR diamond crystal surface was cleaned with acetone and the background spectra were collected and subtracted from the sample spectra. Each FTIR spectrum was collected from a 400 to 4000 cm^{-1} wavenumbers with a resolution of 4 cm^{-1} with 16 number of scans. To analyze the peaks and estimate the area under the peaks, the OMNIC software was used. Three (3) replicates of each sample were tested for the statistical significance.

3.3.5 Thin-layer Chromatography with Flame Ionization Detection (TLC-FID)

To study the effect of the recycling agents on the fractional composition of the aged binder, an Iatroscan MK-6s model TLC-FID analyzer was utilized. The hydrogen and the

airflow rate was set to 160 mL/min and 2 L/min, respectively. n-Heptane insoluble part separated following the (ASTM, 2007) standard, the asphaltene content was determined. After that, 20 µg of n-Heptane soluble (maltene), was spotted on the chromrods; Pentane, Toluene, and Chloroform solutions from Sigma Aldrich were used for solvent development. Dried chromrods were developed in pentane tank for 35-40 minutes and dried in the air for 2-5 minutes, then chromrods were transferred into the second developing chamber filled with 9:1 ratio of Toluene to Chloroform solution for 9 minutes. Then, the rods dried in the oven at 85°C, the prepared specimen was scanned for 30s utilizing an Iatroscan with FID detector.

3.3.6 *Gel Permeation Chromatography (GPC)*

To understand the effect of recycling agents on the molecular size of the aged binder, the size exclusion chromatography analysis was used. A Waters 2414 RI detector with Styragel HR1 SEC column (7.8mm × 300mm) was utilized and Waters 600-MS System controller was connected to a 600-multi-solvent delivery system, and 717-plus auto-sampler was connected to a Dionex U120 Universal Interface. 0.12 gram of each sample was prepared in 3.6 ml Tetrahydrofuran (THF) (samples of 3% w/w) and filtered using 0.45 µm Millipore PTFE to remove suspended particulates. A pump flow rate of 1.0 mL/min with THF as the carrier solvent and injection volumes of 50 µL were used.

3.3.7 *Moisture Conditioned Contact Angle Measurement*

To examine the contact angle in wet condition, glass slides were cut into 0.5”x0.5” squares and cleaned very carefully by sequential ultrasonication in acetone, isopropanol, and deionized (DI) water for 10 min each. The slides were then dried under a stream of N₂ gas followed by ultraviolet cleaning for 15 min. 15 mg of the asphalt binder samples were then put onto the glass slides. The samples were then annealed at 150°C for 30 min and then allowed to cool to room temperature for one hour. Later, the samples were taken to measure the dry contact angle. Afterward, they were conditioned in an aqueous solution at 80°C for 2h as shown in Figure 3-1.

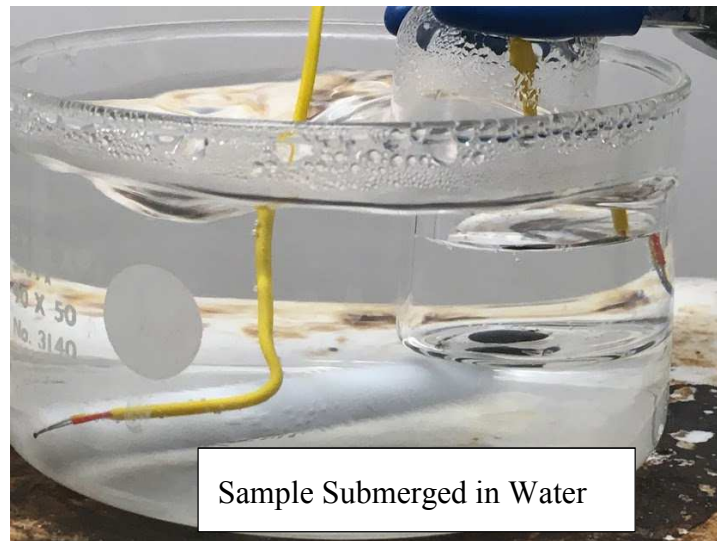


Figure 3-1 Moisture Conditioning Apparatus for Contact Angle Measurement

The resulting wet contact angle was measured and compared with the dry results following the work by (Hung et al., 2017). From these results, the contact angle moisture susceptibility index (CAMSI) was calculated using Equation 3-2.

$$\text{Contact Angle Moisture Susceptibility Index} = \frac{(\text{Contact Angle Wet} - \text{Contact Angle Dry})}{\text{Contact Angle Dry}} \quad (3-2)$$

3.3.8 *Molecular Dynamics Simulation*

Molecular dynamics simulation was performed on a system of oxidized asphaltene molecules at equilibrium state and heptane solvent was used as a medium. Using Large-scale Atomic and Molecular Massively Parallel (LAMMPS) source code deployed in MedeA® software version 2.2, a simulation box was composed to study the effect of molecules found in RA A and C on self-interaction of oxidized asphaltene molecules. For this purpose, RAs' molecules were introduced to the system of oxidized asphaltene after the formation of nanoaggregates to simulate the situation in aged bitumen. The model was built using the MedeA® environment and by using the molecular builder, which allows an interactive, step-by-step construction of polyaromatic units with attached aliphatic chains and pyrrole rings. This tool is helpful in constructing of asphaltene molecules. In this study, PCFF+ force field, which is an extension of the PCFF force field is used. Force field refers to the functional form of parameters used to calculate the potential and kinetic energy of the system of atoms and molecules. PCFF+ is an all-atom forcefield designed to provide excellent accuracy on hydrocarbon and liquid modeling

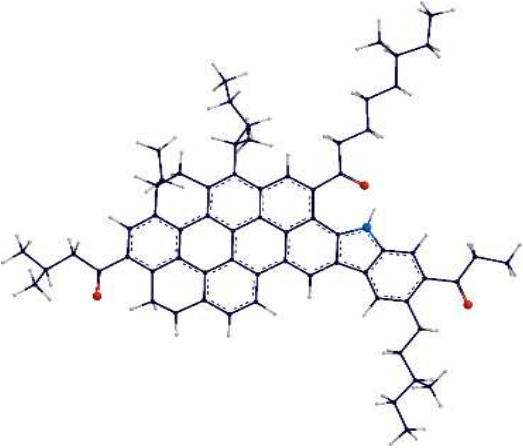
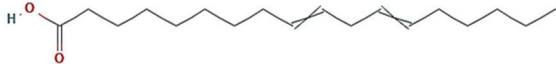
from ab initio simulations (Sun et al., 1994; Ungerer et al., 2014; Waldman & Hagler, 1993). This forcefield includes a Lenard-Jones 9-6 potential for intermolecular and intramolecular interactions and specific stretching, bending, and torsion terms to involve 1-2, 1-3, and 1-4 interactions (Samieadel et al., 2017; Ungerer et al., 2014).

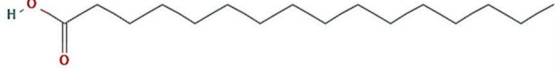
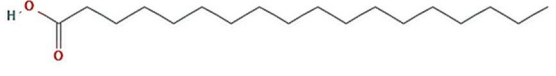
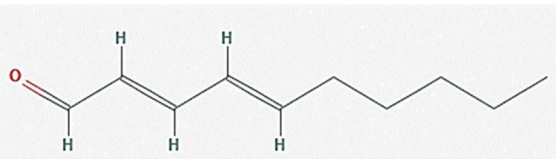
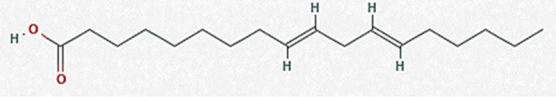
3.3.9 *Structure of Oxidized Asphaltene and selected rejuvenator's molecules*

The oxidized asphaltene molecule used in this study was a continental structure asphaltene (Samieadel et al., 2018) containing a core of poly-aromatic ring (Li & Greenfield, 2014; Morgan et al., 2010; Wiehe, 2008). The selected oxidized asphaltene-pyrrole contains 3 carbonyl groups. The analysis of where the functional groups should be added was based on previous studies on hetero atoms and molecular weight of asphaltene conducted in SHRP accounting for the mechanism of formation of carbonyl groups during oxidation (Jennings et al., 1992; Lesueur, 2009).

The selection of molecules for representing RA A and C was based on GC-MS results which the molecules with higher concentration and score were selected. The molecules with higher concentration have a higher number in simulation to better correlate with the effect of RAs at the macro scale. The selected molecules, their chemical formula, chemical structure, and the number of each used in the study are presented in Table 3-2. The total molecular mass of RAs added to asphaltene ensembles are equal to 10% of the mass of oxidized asphaltene molecules.

Table 3-2 Selected Molecules for Molecular Simulation to Study the Effect of RA A and C on Self-Interaction of Oxidized Asphaltene Molecules

Molecular formula	Chemical structure	Number of molecules in the simulation	Concentration in GC-MS
Oxidized asphaltene pyrrole; C ₆₆ N ₃ H ₇₅		18	NA
RA A selected molecules			
9,12-Octadecadieno		4	57.4%

ic acid (Z,Z)-; C18H32O2			
n- Hexadecanoic acid; C16H32O2		1	4.7%
Octadecanoic acid; C18H36O2		1	2.2%
RA C selected molecules			
2,4- Decadienal; C10H16O		4	9.6%
Linoelaidic acid; C18H32O2		4	7.8%

3.3.10 Simulation Method

The simulation comprised of two subsequent LAMMPS stages starting with energy minimization using conjugate gradients method at a constant volume with a low average density to avoid molecular overlaps. The first stage started with an NVT (constant number of atoms, volume, and temperature) at a high temperature (800K) for 100ps followed by an NPT (constant number of atoms, pressure, and temperature) at pressure of 200 atm and temperature of 800 K for 500 ps to shake the system and prevent its trapping at a local minimum energy state. The second stage of the two-stage LAMMPS was started with an NVT ensemble with a temperature of 350 K (76.85°C) for 2ns to reach an equilibrium and correcting any possible overlaps of molecules with no pressure on the system followed by an NPT ensemble with a temperature of 350 K (76.85°C) and a pressure of 1atm for 20ns. During all the stages of simulation a Nose-Hoover thermostat and barostat (Plimpton, 1995) were utilized and the time step was set to 1 fs (10-15 s). The short-range interactions were calculated directly while long-range interactions were measured with the particle-particle-particle-mesh (PPPM) method. Non-bonded terms were calculated with a simple cutoff of 9.5 Å. The average temperature and pressure during NPT simulations were checked to ensure the system was in equilibrium. During final NPT stage, the coordinates of the center of masses of asphaltene molecules were dumped in an output file for postprocessing of aggregation studies.

After equilibration of oxidized asphaltenes in heptane, RAs' molecules were added to the system and the simulation was continued for another 20ns to investigate the effect of RAs

on self-assembled stacks of oxidized asphaltenes. The average pressure and temperature were monitored during the simulation to ensure the system was in equilibrium. During the simulation, the coordinates for the center of mass of asphaltene molecules were recorded for aggregation study, and the radial distribution function results were calculated for the most centered carbon atom of oxidized asphaltene molecules. Figure 3-2 shows the snapshot of the first step of simulation after addition of RA A's molecules to an equilibrated oxidized asphaltene molecules. The heptane molecules are not shown for clarity.

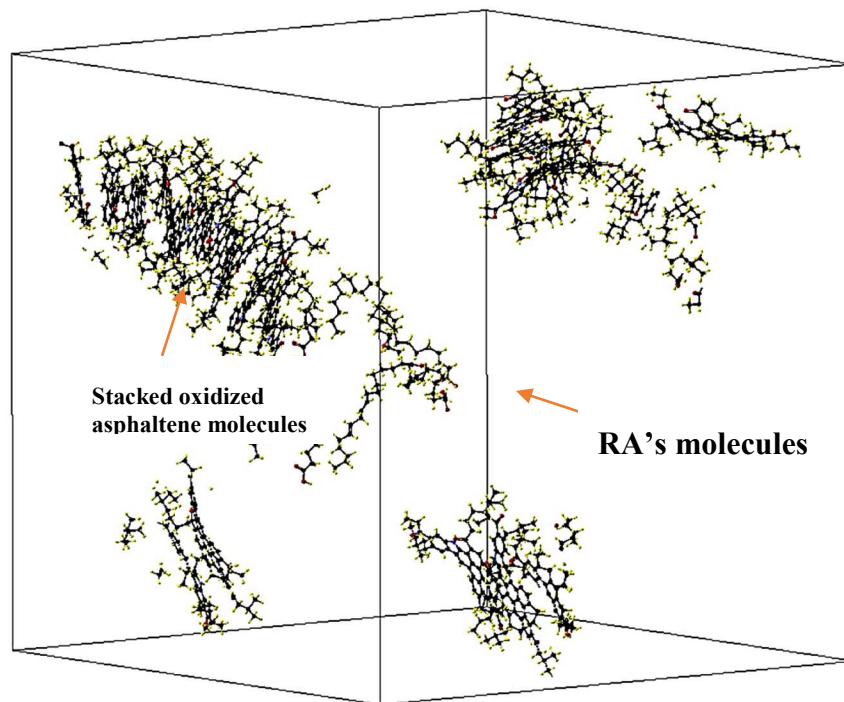


Figure 3-2 The Initial Simulation Box after Addition of RA A's Molecules

3.3.11 Methods of Analysis

To investigate the effect of RAs' molecules on the self-assembled oxidized asphaltene molecules, the average aggregation number of oxidized asphaltene molecules in the presence of dopant was calculated. The average aggregation number (g_z) was determined using Equation 3 (Samieadel et al., 2018).

$$g_z = \frac{\sum_i n_i g_i^3}{\sum_i n_i g_i^2} \quad (3-3)$$

Where n_i is the number of aggregates containing g_i monomers.

The radial distribution function ($g(r)$) was calculated for oxidized asphaltene molecules before and after RAs were introduced. The results of the radial distribution function illustrate the most probable separation distance of oxidized asphaltene molecules.

Increase in RDF peaks is directly correlated with higher interaction between oxidized asphaltene molecules and reduction in peaks shows disturbing in self-interaction of oxidized asphaltene molecules. RDF allows visualizing the degree of separation between a group of atoms, which in this study is a subset comprised of a most centered atom of each oxidized asphaltene molecule. $g(r)$ is calculated using Equation 3-4:

$$g(r) = \lim_{dr \rightarrow 0} \frac{V}{N(N-1)4\pi r^2 dr} \sum_i^N \sum_{j \neq i}^N \delta(r - r_{ij}) \quad (3-4)$$

Where V is the volume, N is the number of atoms included in the calculation, δ is the Kronecker delta function and r_{ij} is the distance between the two atoms (Levine et al., 2011; Lowry et al., 2017).

3.4 Results and Discussion

3.4.1 Dynamic Shear Rheometer (DSR)

In Figure 3-3, the $G^*/\sin(\delta)$, which is an indicator of rutting resistance of the neat, aged, and blended samples at 64°C are shown. The 2PAV aged sample showed the highest $G^*/\sin(\delta)$ among all samples since the 2PAV sample was exposed to aging which increased stiffness. On the other hand, the RA blended samples showed significantly decreased $G^*/\sin(\delta)$ which indicated the ability of RA in stiffness reduction of the aged sample. Among four RA blended samples the highest stiffness reduction was achieved by A and B. A, and B decreased the parameter by 97% and 100%, where C and D decreased $G^*/\sin(\delta)$ by 85% and 84%, respectively.

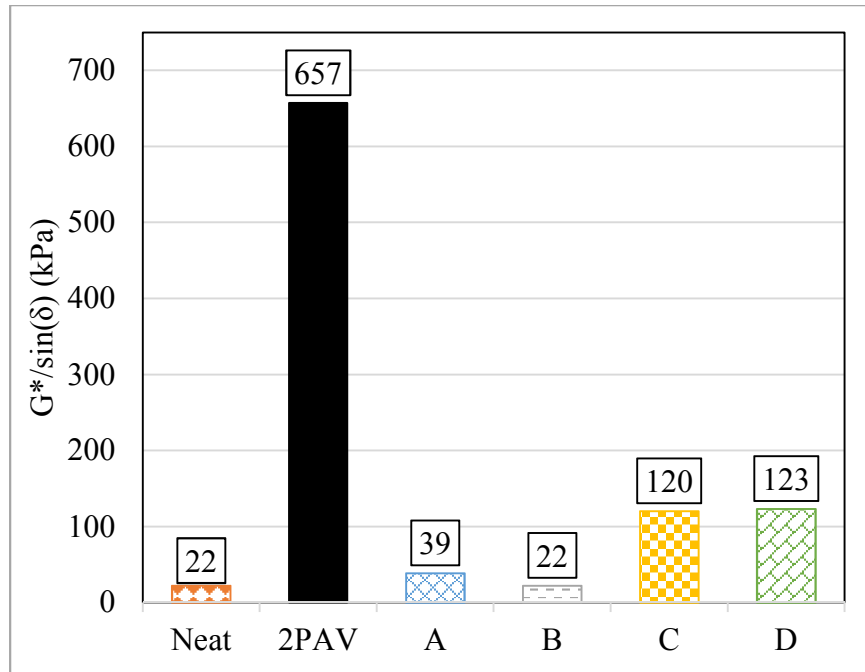


Figure 3-3 $G^*/\sin(\delta)$ Value for All Samples at 64° C

Figure 3-4 showed the $G^*\sin(\delta)$, which is an indicator of fatigue susceptibility, at the intermediate temperature of 46°C for all samples. Similar to the $G^*/\sin(\delta)$ value the aged sample had the highest $G^*\sin(\delta)$ value as well. All blended samples had a reduced value of $G^*\sin(\delta)$ than the aged asphalt. B reduced the highest $G^*\sin(\delta)$ which is over 100% and below that of the neat asphalt. A, C, and D decreased the fatigue parameter by 99%, 85%, and 75%, respectively. In both $G^*/\sin(\delta)$, and $G^*\sin(\delta)$ the organic-based RA reduced the parameters more than that of the petroleum-based RA. A similar result was found by (Zaumanis et al., 2015) where the organic additives required less amount compared to the petroleum additives to achieve similar level rheology of asphalt binder.

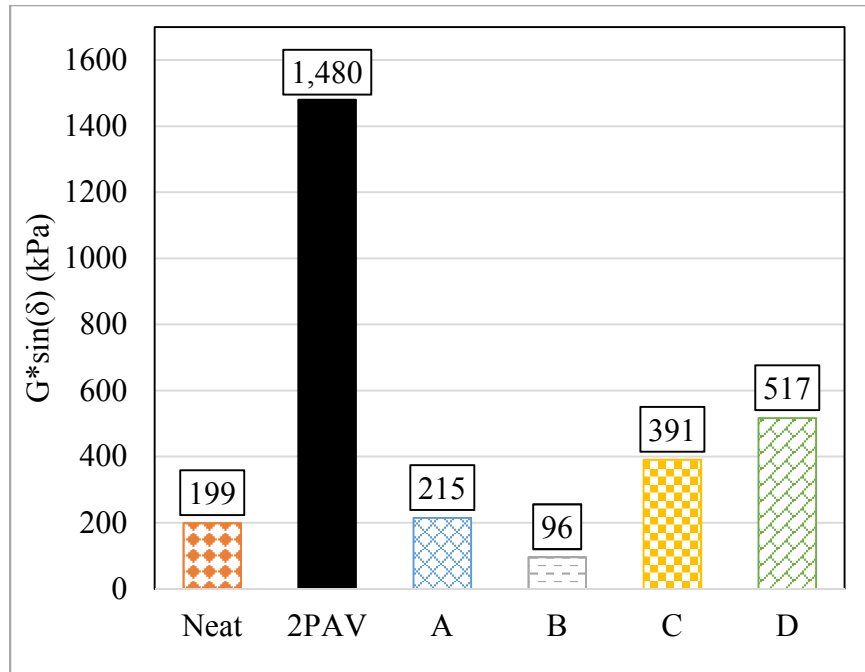


Figure 3-4 $G^* \sin(\delta)$ Value for All Samples at 46° C

The master curves of the neat, 2PAV and blended binders are shown in Figure 3-5. It can be depicted that the complex modulus of aged asphalt was significantly higher than that of the neat binder. RA was effective in reducing the modulus with A and B being the most effective followed by D and C. The effect of D and C found to be very close to each other. In addition, the slope of the aged binder is significantly lower than that of the neat binder which indicates aging reduced frequency (temperature) dependency of the asphalt binder. The slope of the curve among blended samples varies depending on their source and composition. D and C appear to be less effective in changing the slope of the curve, while A and B could change the slope more significantly. Which indicated C, and D reduced the stiffness while A, and B not only reduced the stiffness but also changed the

slope (similar to the neat binder). Addition of A to aged asphalt led to the closest slope (Table 3-3) and modules to that of the neat binder. This may indicate A is more effective to restore overall viscoelastic behavior of the aged binder.

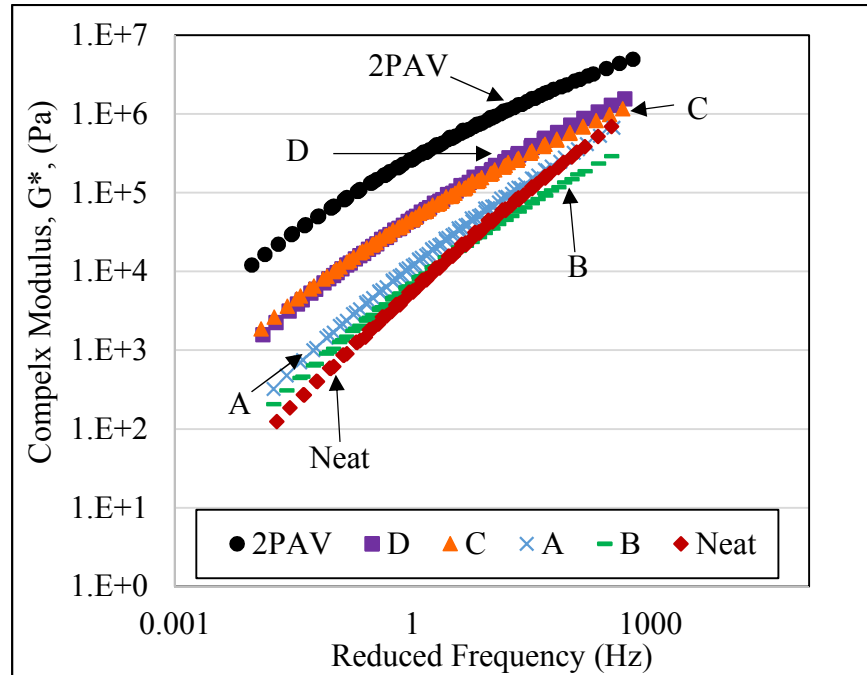


Figure 3-5 Complex Shear Modulus (G^*) Master Curves for All Samples

Table 3-3 Slope Value Calculated Using Power Fit for All Samples

Sample	2PAV	D	C	A	B	Neat
Slope	0.53	0.64	0.60	0.76	0.72	0.89

Figure 3-6 depicted the phase angle values for all samples. From Figure 6, the 2PAV sample showed the lowest phase angle value. All blended samples showed a higher phase angle compared to the aged one. Phase angle results were consistent with the complex modulus results as the sample A, and B found to be most effective to restore phase angle compared to the other RA.

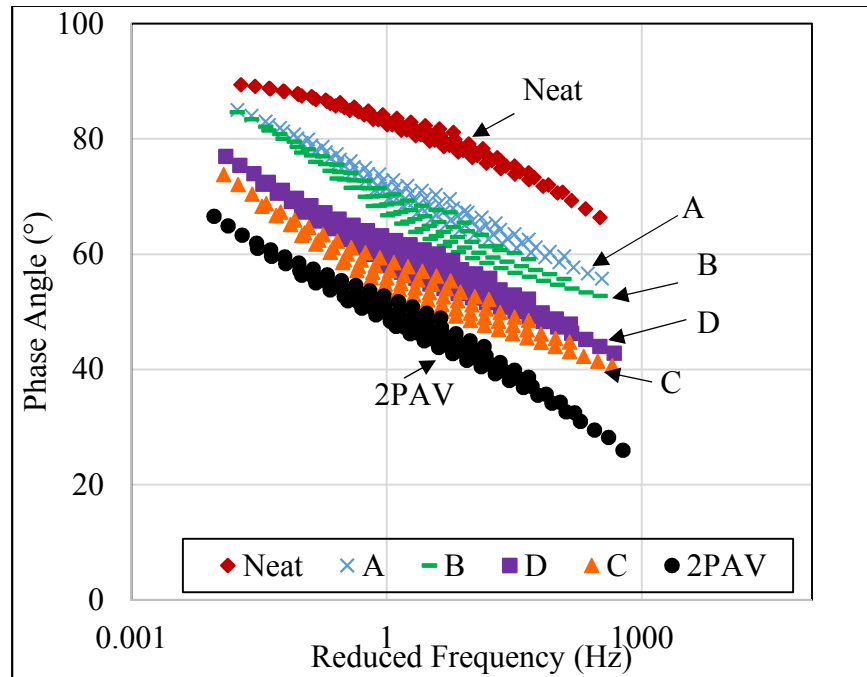


Figure 3-6 Phase Angle Plot for All Samples

Figure 3-7 depicted an estimate for sample C showing the demonstration of how crossover modulus and crossover frequency value were estimated. It is the value where the G' and G'' crosses and corresponding crossover modulus and crossover frequency was calculated. It has been reported that increased crossover values indicate increased viscous component of the materials. Furthermore, the crossover modulus is inversely

related to polydispersity (Oldham et al., 2020). Polydispersity is defined as the ratio of weight average molecular weight by number average molecular weight. With aging, the polydispersity value increases (Cao et al., 2018). It was shown that rejuvenation helps reduce the polydispersity, which in turn increases the crossover modulus.

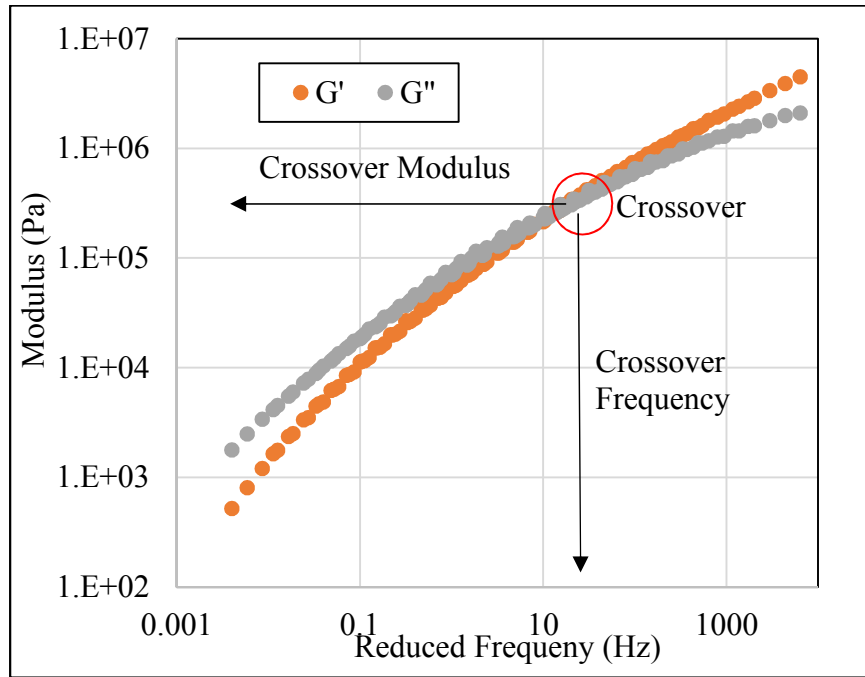


Figure 3-7 Crossover Modulus Values Estimation for Sample C

Figure 3-8 represents the change in 2PAV crossover modulus for each of the four RA. The crossover modulus is the modulus at $\tan\delta=1$ where viscous and elastic modulus intersect. The crossover modulus of 2PAV was significantly lower than that of the neat binder. Here, the Δ crossover modulus refers to the difference of the crossover moduli of the four blended samples relevant to the 2PAV sample. Considering that, A, B, and D were able to increase the crossover modulus by 243%, 92%, and 29% respectively.

However, C showed a nearly 50% decrease in crossover modulus compared to 2PAV. The observed differences in the extent of change in crossover modulus among the four RA (Δ crossover modulus) indicate the chemistry of RA dependency of rejuvenation mechanisms. While some RA mainly impacts the viscous component of asphalt playing as a softener, others restore both the viscous and elastic properties of aged asphalt.

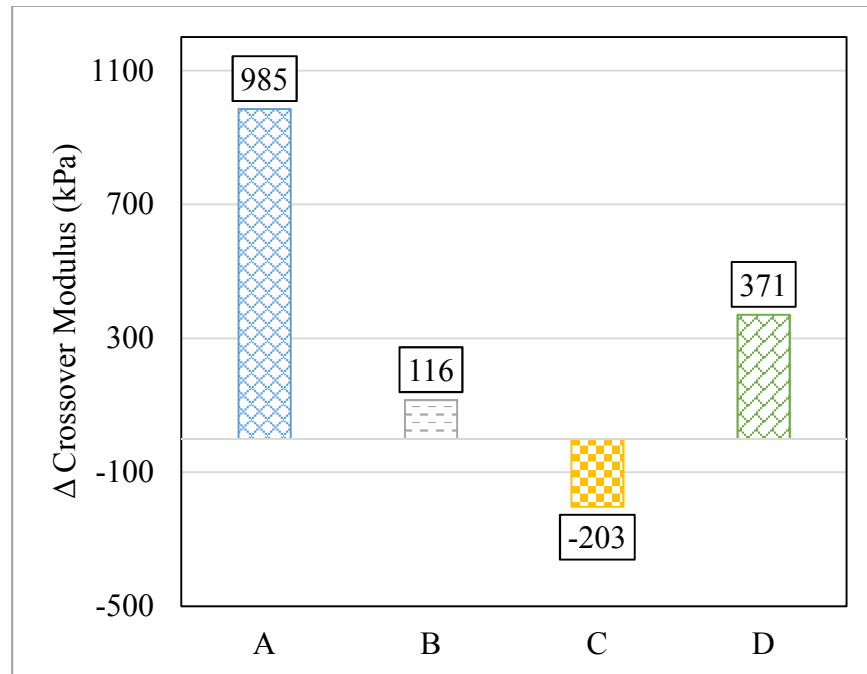


Figure 3-8 Crossover Modulus Values for All Samples

In addition to the crossover modulus values, the crossover frequency values were calculated and plotted in Figure 3-9. Samples with improved relaxation properties have increased crossover frequencies. As it can be seen both A and B significantly increased the crossover frequency followed by D, while C was not effective in changing the

crossover frequency. Overall, the crossover frequency of the blended samples was improved compared to 2PAV.

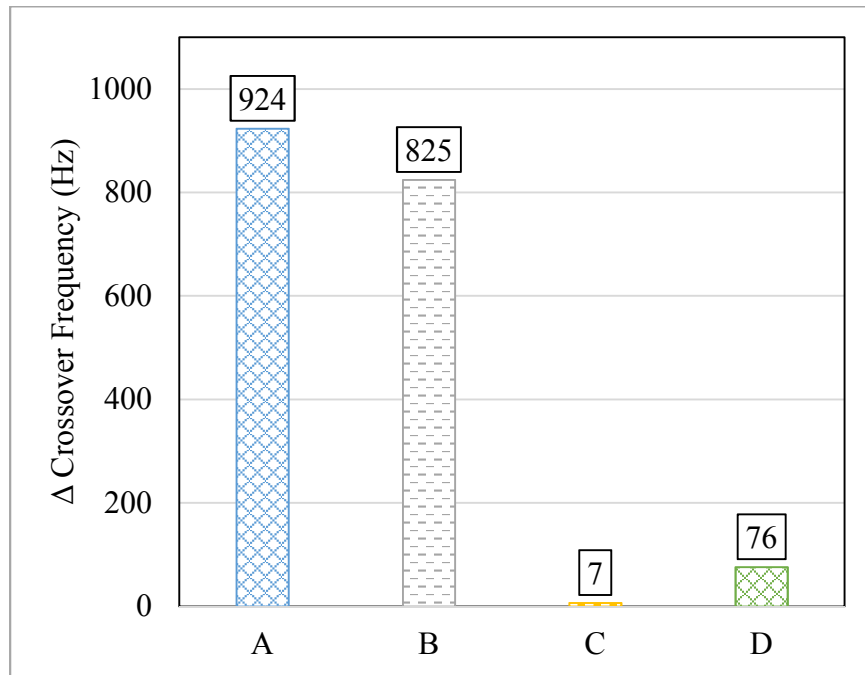
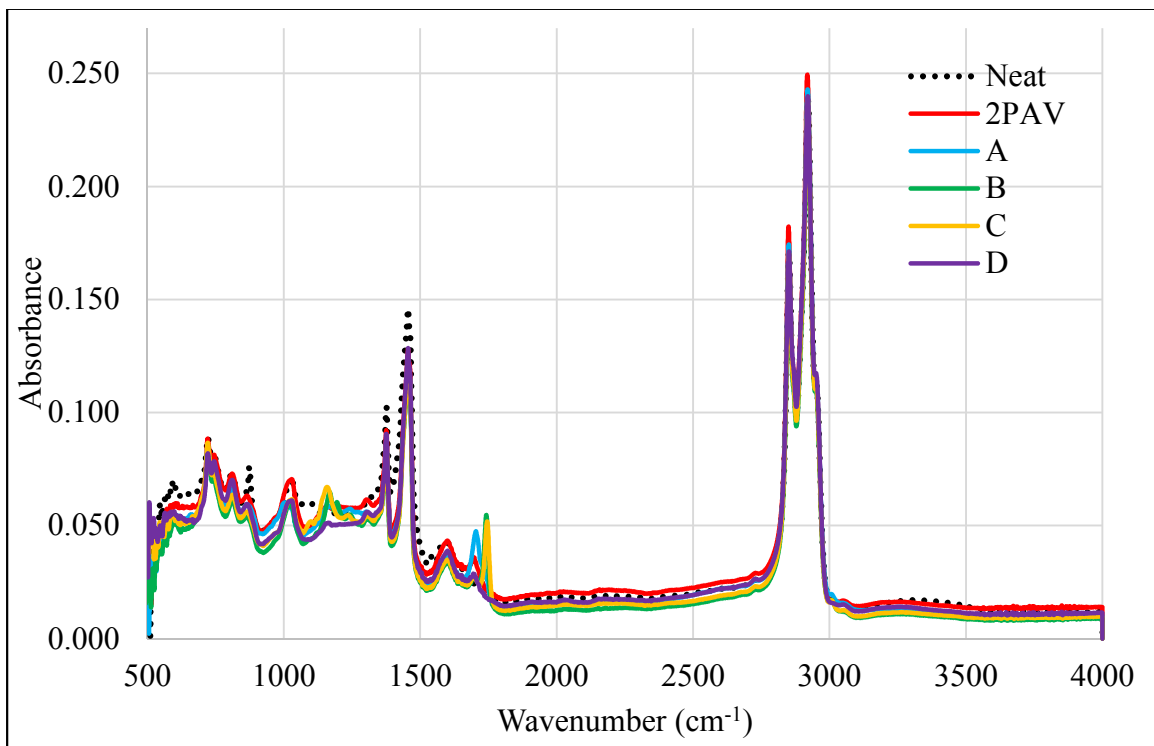


Figure 3-9 Crossover Frequency Value for All Samples

3.4.2 FTIR Test

Figure 3-10-a represents the FTIR spectra of neat, 2PAV aged, and modified samples. To better differentiate the effect of RA on the chemical structure of modified binders the area under 680 to 1850 cm^{-1} was zoomed-in in Figure 3-10-b. In Figure 3-10-b, the presence of a peak at 1700 cm^{-1} which is an index for the aging of the binder is more obvious. This peak was not detected for the neat binder but after aging and even after the addition of RA the peak was observed. This peak is related to the creation of ketone (carbonyl group). As the binder oxidize, this carbonyl peak appears. There is another peak near

1700 cm^{-1} around 1747 cm^{-1} , which is related to compounds with carbonyl groups from esters, ketones, or acids. This peak mostly associated with the presence of five and seven-membered cyclic ketones (Kupareva et al., 2012). The peak around 1030 cm^{-1} is related to the sulfoxide group and it is another indicator of aging of the binder. The peak around 1076-1105 cm^{-1} is attributed to the C-O vibration of the ester group. This peak was disappeared after aging, but due to the different chemical structure of RA, after addition of the C as recycling agent, this functional group by the distinct peak in this area appeared. The results of FTIR indicates the interaction between recycling agent and aged binder causing a change in the chemical structure and consequently a change in the physical performance of binder.



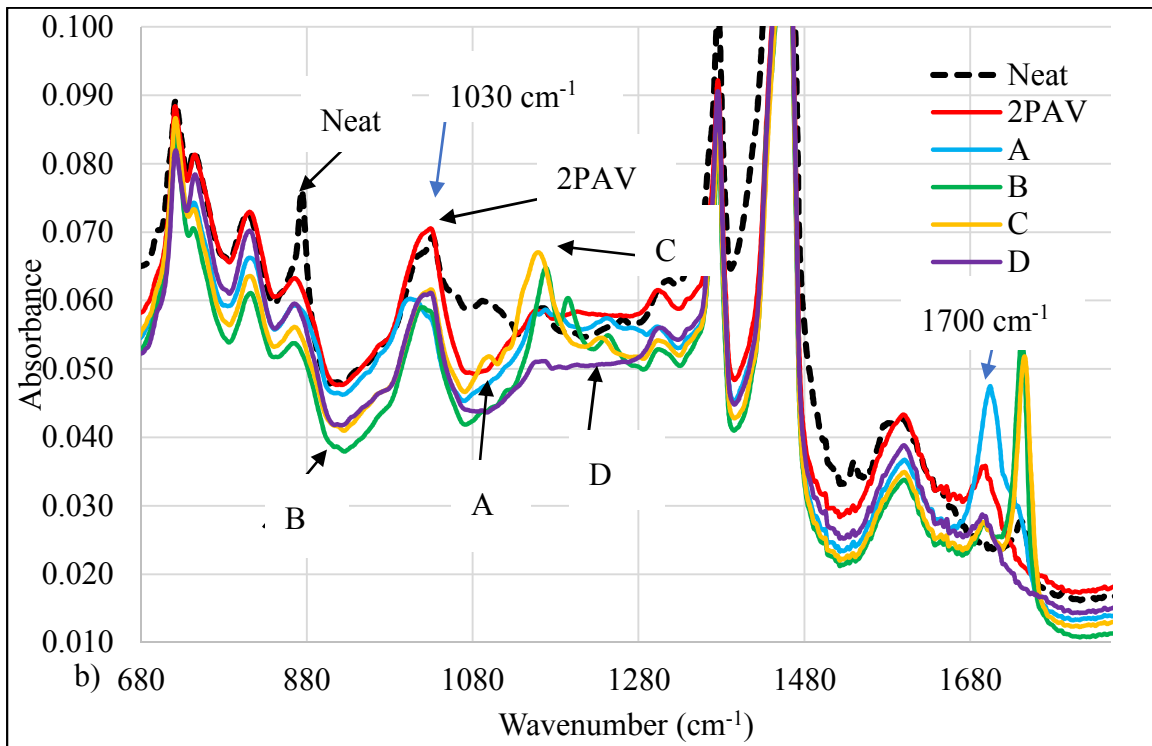


Figure 3-10 (a, b) FTIR Spectra of All Samples

3.4.3 TLC-FID Studies

Asphalt binder is divided into two parts based on solubility in n-heptane, the soluble part is called asphaltene, and the other non-soluble part is called maltene. After that, the maltene was fractionated in three parts including saturates, aromatics, and resins. All the fractions together are called SARA fractions (saturates, aromatics, resins, and asphaltene). In Figure 3-11, SARA fractions of the neat binder and 2PAV aged binders, are compared with those of modified samples with RA. Here, to better understand the effect of RA in aged binder pure RA have also been analyzed and added to the results.

Comparing 2PAV and unaged binder, it was observed that after 2PAV aging, a significant increase of 76.24% in the asphaltene fraction happened and there was a decrease in all other fractions, especially the aromatics occurred. The increasing asphaltene fraction after 2PAV is consistent with previous studies (Puello et al., 2013). All modified samples showed a reduction in asphaltene fractions and A showed the most reduction from 28.41 to 23.76.

In comparing pure RA, C as the recycling agent was excepted by having a high aromatic fraction of 89.16% would compensate for the lost aromatic in the aged binder while the increase was up to 30% and it increased the resins content 2.45% even more elevated than 2PAV aged one. B showed the highest increment in the aromatic fraction by rising 88.5% for the modified binder, and A by having the lowest aromatic content increased the aromatic fraction by 74%. From the results, RA not necessarily compensates for the fractions that lost during the aging process. Previous studies showed that the molecular structure of RA play the most important role in the modification of aged binder and the interaction between RA can result in molecular conformation change and consequently changing the SARA fractions (Pahlavan et al., 2018).

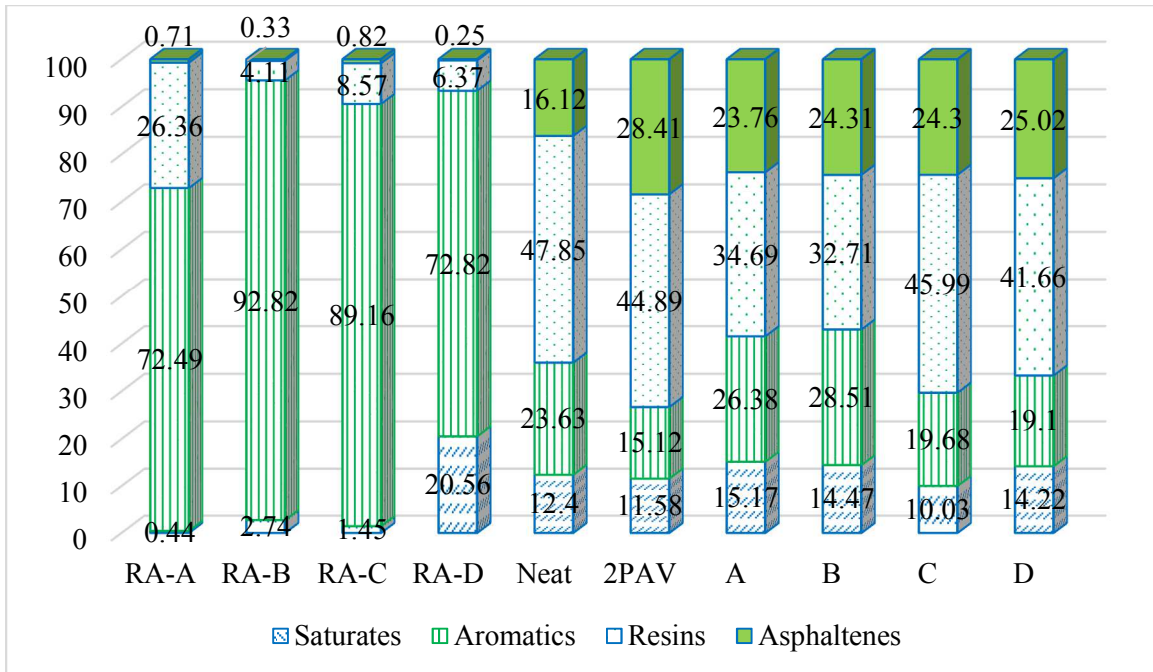


Figure 3-11 SARA Fractions of Pure RA and All Other Samples

Asphaltene molecules by having the highest polarity and molecular weight are dispersed inside the maltene fraction, and interaction between asphaltene and maltene molecules is responsible for the physical performance of a colloidal system of asphalt binder (Loeber et al., 1998). In the maltene fraction, resins are the most polar molecules, aromatics polarity is lower than resins, and saturates are the non-polar component of maltene fraction. Different concentration of asphaltene molecules results in different mechanical properties. To evaluate the stability of the colloidal system of asphalt, colloidal stability index was used as below Equation 3-5 (Loeber et al., 1998):

$$CI = \frac{(resins + aromatics)}{(asphaltenes + saturates)} \quad (3-5)$$

Figure 3-12 shows the colloidal stability for the neat binder, 2PAV aged binder and modified binders with RA. A higher index indicates better peptizing asphaltene molecules by resins and aromatics. After aging by converting aromatics to resins and resins to asphaltene this effect reduced, and the index decreased 40% from 2.5 for the neat binder to 1.5 for the 2PAV aged binder. Addition of RA resulted in the enhancement of CI for all the modified samples, and the highest index was observed for sample C.

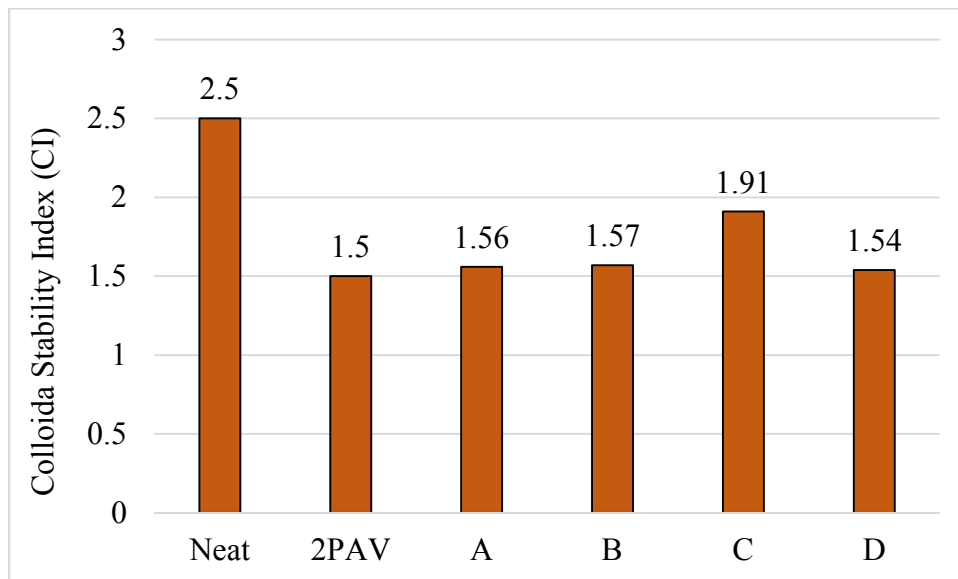


Figure 3-12 Colloidal Stability Index for All Samples

3.4.4 Gel permeation chromatography (GPC) Analysis

Figure 3-13 shows the molecular size distribution of neat binder, aged binder, and modified binder with recycling agents. Gel permeation chromatography (GPC) results showed a variation in the molecular size distribution of the samples. In this analysis the

molecular size separates into three portions, being the large molecular size (LMS), medium molecular size (MMS), and small molecular size (SMS) (Shen et al., 2007). It was observed, after aging the LMS increased 23.25% for 2PAV. This increment can be attributed to the aging process when due to the oxidation the polarity of asphalt molecules increases and consequently the aggregation of asphaltene molecules happens and confirms the belief to the assumption of nano-agglomerates behavior of oxidized asphaltene molecules of asphalt binder. The decreasing the MMS from 0.49 for the neat binder to 0.45 in 2PAV is another evidence for converting the molecules to more polar due to the oxidizing (Noureldin & Wood, 1989). Reducing the SMS of neat binder after aging can be related to volatilization of the lighter molecules during the aging process due to heating.

After the addition of recycling agents, the LMS was decreased for all the modified binders while A had the highest effect on reducing the LMS up to 11.33%. Previous studies showed the properties of the binders are strongly related to the LMS. In the study by Shen et al., they showed the decrease in LMS through the addition of the rejuvenating agents in the aged binders decreases the viscosity of the binders (Shen et al., 2007).

Hence, any change in the molecular size distribution close to the neat binder can result in restoring the properties of the aged binder to that of the neat binder.

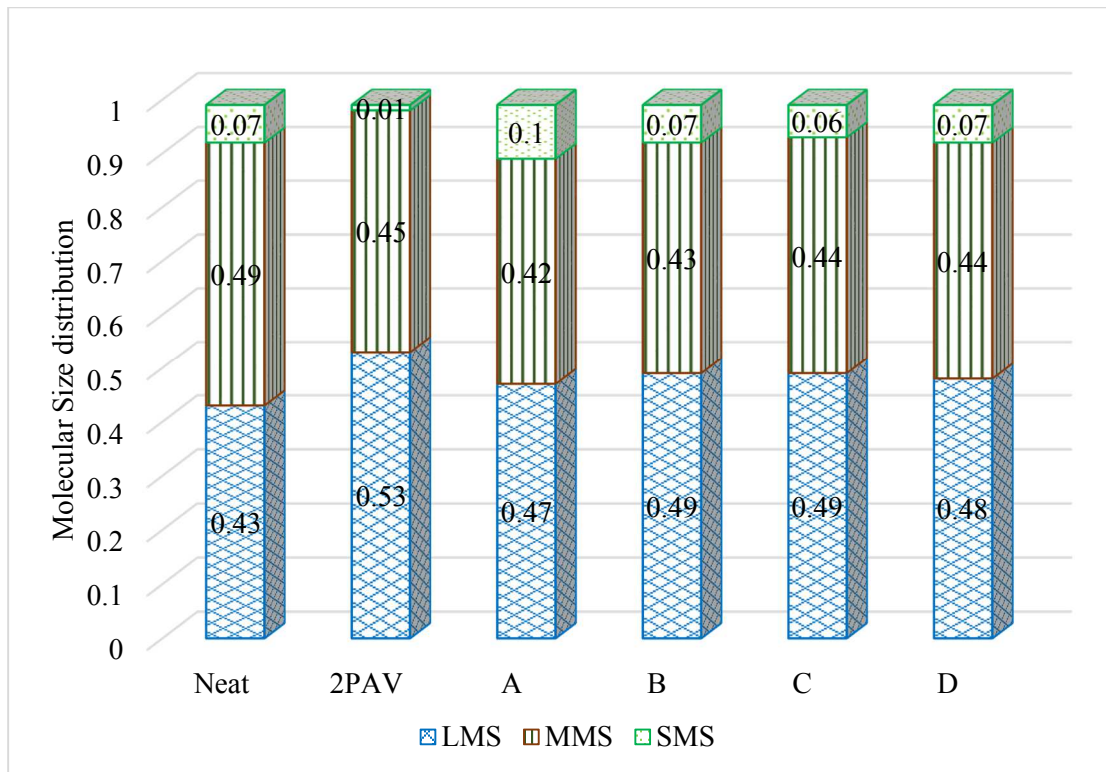


Figure 3-13 Molecular Size Distribution

3.4.5 Contact Angle Measurements

Figure 3-14 depicted the contact angle value of neat binder for dry and wet conditioned. It was observed that the contact angle increased after water conditioning of the sample. This phenomenon was observed for all other samples as well.

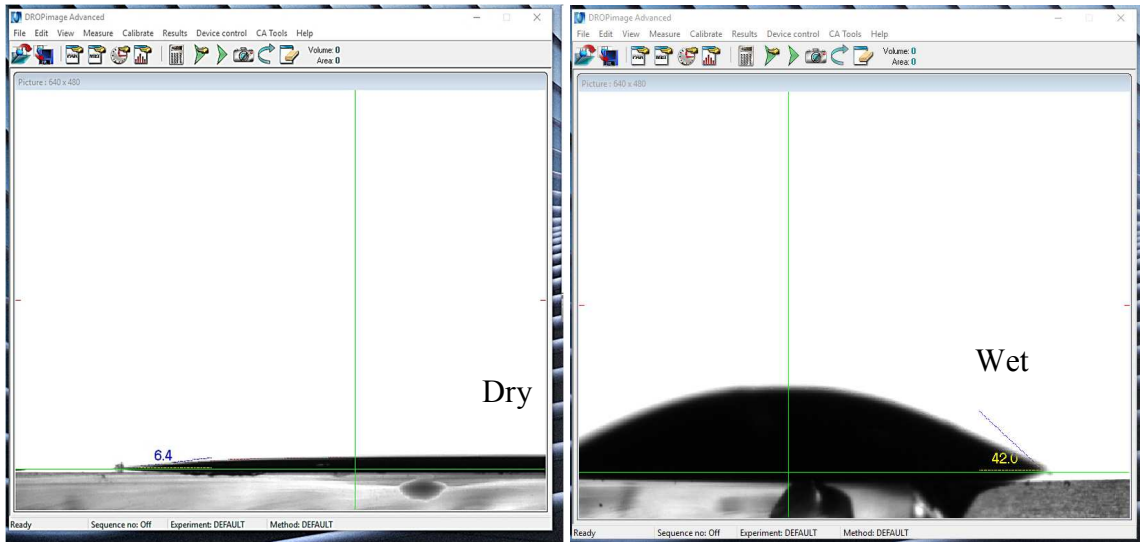


Figure 3-14 Dry and Wet Contact Angle for Neat Binder

The contact angle values measured for dry and wet samples (unconditioned and conditioned) is shown in Figure 3-15. From the observed moisture damage, it was found that the sample B and sample D were significantly affected by the water conditioning and it was reported that the samples were not suitable for moisture susceptibility study. Hence, the results for Neat, 2PAV, A, and C are shown in Figure 3-15. For unconditioned samples, as it can be seen the inclusion of RA increased the 2PAV contact angle where C increased 8% and A increased 65%. As the same glass slides were used as a substrate the change in contact angles were dominated by the effect of chemical interactions between the aged binder and the RA. For conditioned samples, the inclusion of A showed to decrease the conditioned contact angle by 38% which signifies the improved wettability of sample A. However, the inclusion of C rather increased the conditioned contact angle by 63%.

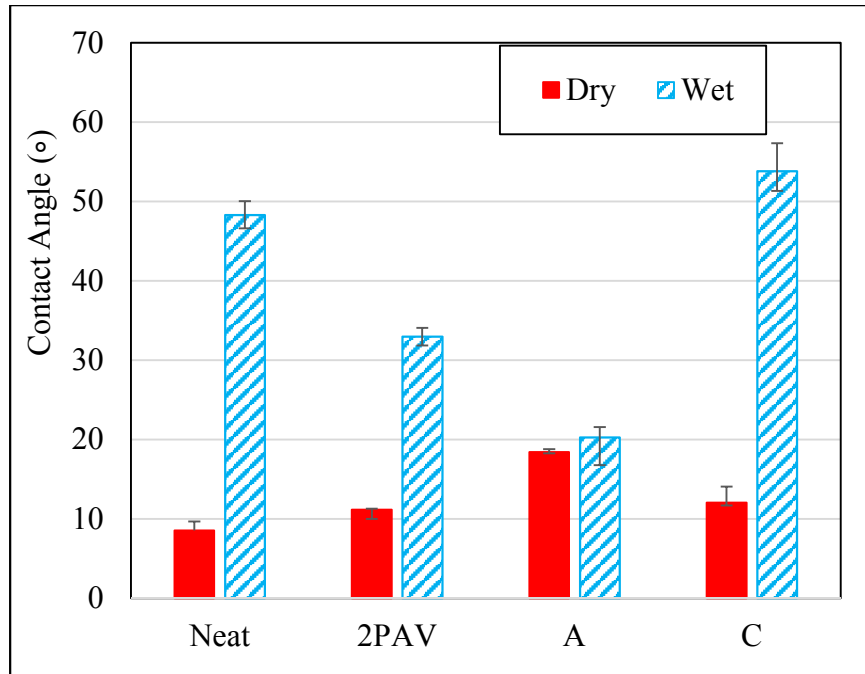


Figure 3-15 Unconditioned and Conditioned Contact Angle Measurements at 23° C

To further examine the effect of water on changing contact angle, the contact angle moisture susceptibility index (CAMSI) values of all specimens were determined by calculating the difference between values for dry and wet samples and the values are shown in Figure 16. CAMSI was used as a measure of moisture susceptibility; the lower the index indicates higher resistance to moisture damage. Among the four samples, A has the lowest CAMSI (9%) and therefore possibly the highest resistance to moisture damage. C showed results in between the Neat and aged sample. It can be concluded that A is more effective in improving the moisture resistance of aged asphalt.

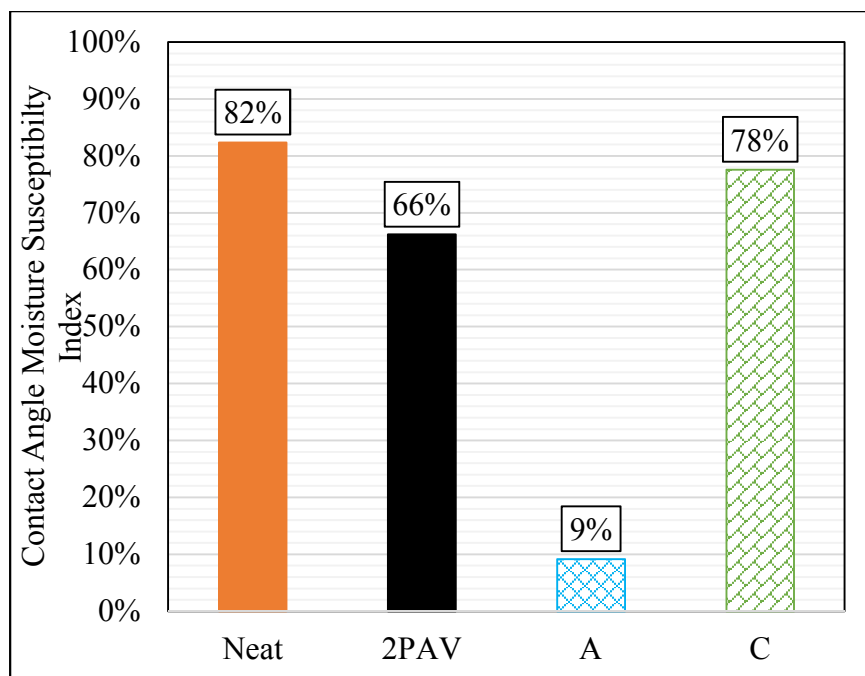


Figure 3-16 Contact Angle Moisture Susceptibility Index Values at 23° C

3.4.6 Molecular Dynamics Simulation Results

3.4.6.1 Average Aggregation Number

The results for average aggregation number of oxidized asphaltene molecules with and without the presence of RAs' molecules calculated using Equation 3-3 are presented in Figure 3-17. The stacking criteria was set to distance equal or less than 8.5 Å to include all possible forms of known stacking. This includes parallel stacking, offset stacking and T-shaped stacking (Pahlavan et al., 2018; Samieadel et al., 2018). The initial section of data points (from 0 to 20ns) are aggregation number of isolated oxidized asphaltene molecules. At 20 ns, two scenarios (one with and one without RAs' molecules) start. It can be observed that the addition of RA A molecules caused prevention of average

aggregation number for oxidized asphaltene molecules to increase. This shows that RA A molecules have the potential of preventing the oxidized asphaltene molecules from stacking. At the final part of the simulation (after 35ns), there is a reduction in nanoaggregates' size more than isolated oxidized asphaltene molecules showing that selected molecules from RA A have the potential of peptizing oxidized asphaltene and reduce the nano-aggregates size further isolated asphaltenes. On the other hand, RA C promotes aggregation and prevents asphaltene molecules from deagglomeration. It can be observed that in the majority of timesteps after addition of RA C, the aggregation number is at its maximum opposite to that of RA A.

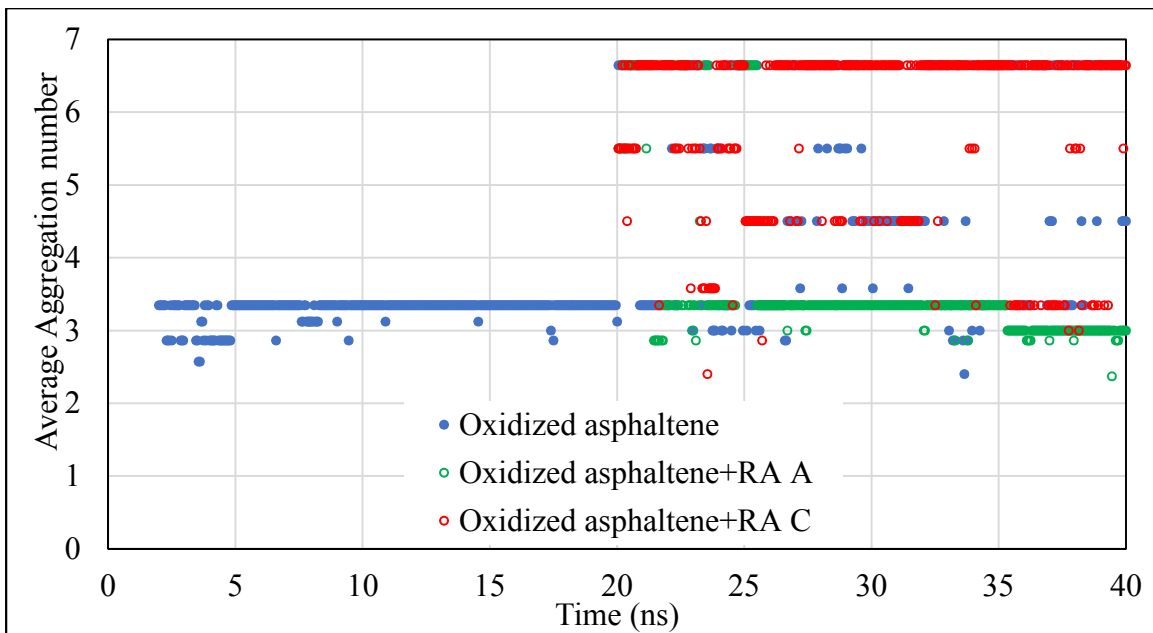


Figure 3-17 Aggregation Study of Oxidized Asphaltene Molecules with and Without the Presence of RAs' A and C Molecules

3.3.6.2 Radial distribution function

The average radial distribution function for the last 5 ns of the simulation was calculated for the most centered carbon atom of oxidized asphaltene molecules and the results are presented in Figure 3-18. Radial distribution function as a measure of separation of oxidized asphaltene molecules helps to understand the effect of RAs' molecules on deagglomeration of asphaltenes. The results show that after the addition of RA A's molecules, the intensity of RDF peaks decreased as a result of the interplay of RA molecules and oxidized asphaltene molecules. The first peak at a distance range of 4-5 Å is reported to be associated with parallel stacking (π - π interaction) while the peak at 7-8 Å is attributed to displaced and T-shaped stacking (π - σ interaction) (Mousavi et al., 2016; Yaseen & Mansoori, 2018). This decreasing effect shows that RA A's molecules were able to reduce the self-assembly of oxidized asphaltenes which can lead to a reduction of viscosity at the macro scale. Conversely, RA C increased the radial distribution function intensity at the range of parallel stacking distance showing RA C's potential to promote lower parallel stacking of asphaltene molecules which is an indicator of higher interaction between oxidized asphaltene molecules.

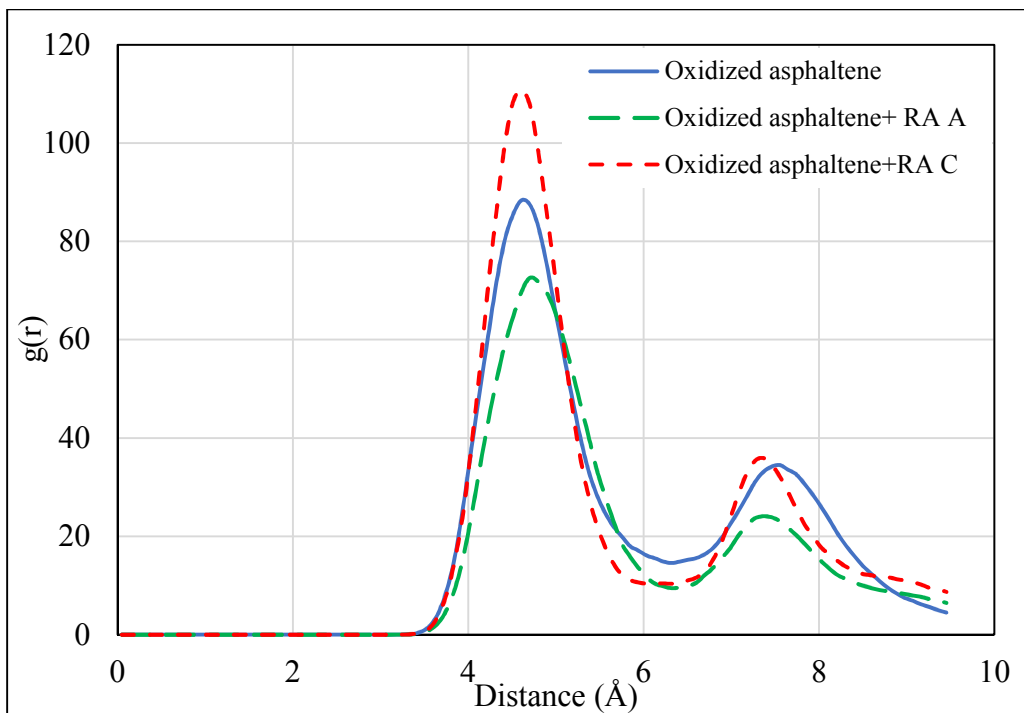


Figure 3-18 Radial Distribution Function Plot for the Last Five Seconds of the Simulation

Shown in Figure 3-17

For better comprehension of the sequence of events in the rejuvenation process Figure 3-19 shows snapshots of both RAs. Figure 3-19-top shows deagglomeration process of RA A molecules comprising of three steps of attraction of RAs to nano-aggregate of asphaltene, penetration of molecules and deagglomeration of asphaltenes. Contrary, the RA C molecules caused the forming of a large nano-aggregate of oxidized asphaltene molecule (Figure 3-19-bottom).

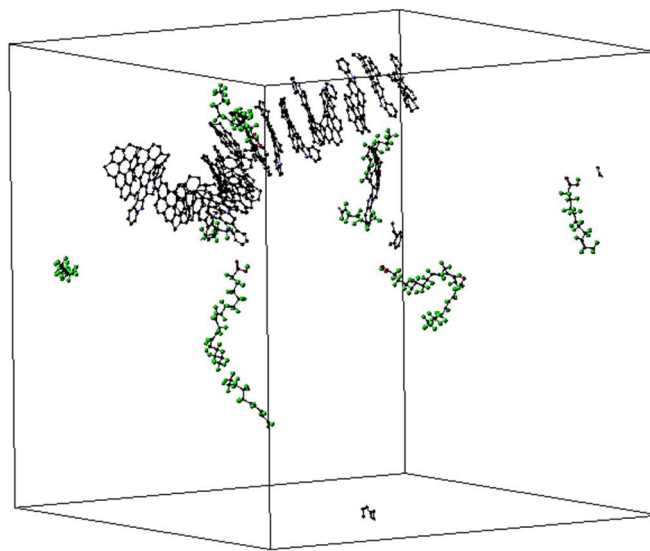
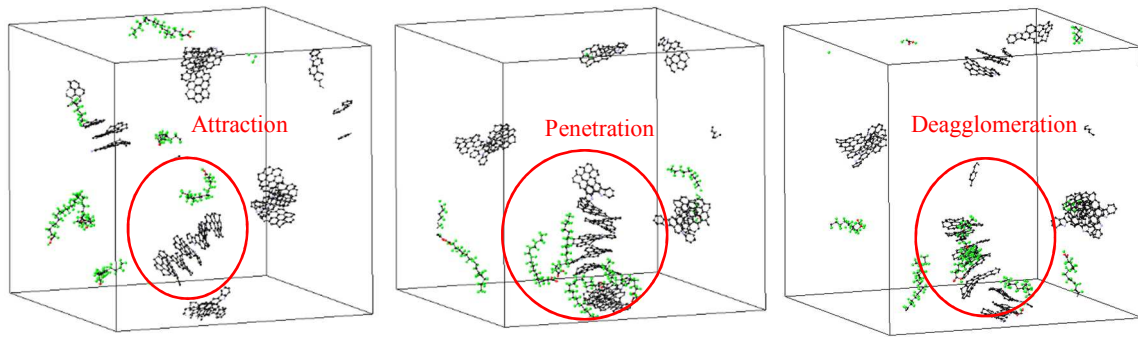


Figure 3-19 Snapshots of Simulation: Top- Subsequent Snapshots Showing Deagglomeration Process of Oxidized Asphaltene Molecules with the Presence of RA A; Bottom- Formation of a Large Agglomerate of Oxidized Asphaltenes After Supplying RA C's Molecules

3.5 Conclusion

This study investigated the effect of recycling agents to the laboratory prepared aged asphalt to its physicochemical properties. Accordingly, rheological characterization, chemical functional group, deagglomeration of asphaltene molecule, and moisture damage resistance of aged asphalt modified with recycling agents were studied. The $G^*/\sin(\delta)$, and $G^*\sin(\delta)$ which were the indicator of rutting and fatigue cracking, all the recycling agents reduced these values and found that the organic-based recycling agents reduced the value more than that of the petroleum-based recycling agent. This observation may indicate the efficacy of recycling agents in rutting and fatigue depends on their source and chemical composition. From complex modulus results, it was found that some of the studied recycling agents only lowered the stiffness while some others not only lowered the stiffness but also changed the slope of the aged asphalt master curves. This phenomenon was found to be appropriate as the A, and B samples showed a similar slope in complex modulus that of neat binder and this action can be attributed as the recycling agent's rejuvenation efficiency.

Crossover modulus, which is the modulus where the storage modulus and loss modulus intersects. Increase of crossover modulus and crossover frequency value may indicate the possible deagglomeration of nanoaggregates of oxidized asphaltenes which agglomerate during the aging process. It was found RA A increased both the crossover modulus and crossover frequency largely while other recycling agent increased either the crossover modulus or crossover frequency indicating A performed better than others.

FTIR analysis showed the change in chemical functional groups after aging and after addition of recycling agents. The results of FTIR indicated the interaction between recycling agents and aged binder causing a change in the chemical structure which consequently changed the mechanical performance of the binder. TLF-FID results showed that recycling agents not necessarily compensate for the fractions that lost during the aging process and the most important effect of recycling agents is to alter the molecular conformation. After aging, the asphaltene fraction increased up to 76% while other fractions, maltene, decreased. In accordance with rheology study, A showed the most reduction of asphaltene fraction of aged asphalt compared to other recycling agents. From GPC study, it was observed, after aging the large molecular size (LMS) increased 23.25% for 2PAV. GPC results confirmed the successful effect of recycling agents in resorting the molecular size distribution close to that of the neat binder, especially A performed best in the reduction of LMS of aged binder among all other recycling agents. Contact angle measurements showed all recycling agents has an effect on contact angle which signifies the effect of chemical interactions between the aged binder and the recycling agents. Moisture susceptibility index (CAMSI) calculated based on the changes in contact angle values of each specimen in dry and wet conditions showed sample A had the lowest index. This, in turn, may indicate A was not only effective in restoring bulk properties of the aged binder as reflected in the rheological properties but also enhanced moisture susceptibility of the aged asphalt binder.

Furthermore, the results of molecular dynamics show that the molecules presented in RA A are effective on asphaltene molecules deagglomeration which can result in restoring of rheological properties of aged asphalt binder. However, RA C promoted aggregation which is well-correlated with experimental results. Radial distribution function results are also in line with aggregation study as RA A was able to reduce the intensity of RDF and RA C caused an increase in intensity.

3.6 Acknowledgments

This research is sponsored by the National Science Foundation (Awards No: 1640517) and University Transportation Center: Center for Highway Pavement Preservation. The authors would like to acknowledge the invaluable assistance provided by Dr. Albert Hung with Sustainable Infrastructure Materials Lab. The contents of this paper reflect the view of the authors, who are responsible for the facts and the accuracy of the data presented. This paper does not constitute a standard, specification, or regulation.

3.7 References

- AASHTOT315, T. (2012). 315 (2012).“ . *Standard Method of Test for Determining the Rheological Properties of Asphalt Binder Using a Dynamic Shear Rheometer (DSR).*” *American Association of State Highway and Transportation Officials, Washington, DC.*
- Apeageyi, A. K., Grenfell, J. R., & Airey, G. D. (2014). Moisture-induced strength degradation of aggregate–asphalt mastic bonds. *Road Materials and Pavement Design, 15*(sup1), 239-262.
- ASTM, D. (2007). 3279 Standard Test Method for n□Heptane Insolubles. *Annual Book of Standards.*
- ASTMD2872-12e1. (2012). Standard Test Method for Effect of Heat and Air on a Moving Film of Asphalt (Rolling Thin-Film Oven Test). *ASTM International, West Conshohocken, PA, 2012, www.astm.org.*
- ASTMD6373-13. (2013). Standard Specification for Performance Graded Asphalt Binder. *ASTM International, West Conshohocken, PA, 2013, www.astm.org.*
- ASTMD6521-13. (2013). Standard Practice for Accelerated Aging of Asphalt Binder Using a Pressurized Aging Vessel (PAV). *ASTM International, West Conshohocken, PA.*
- ASTMD7175-15. (2015). Standard Test Method for Determining the Rheological Properties of Asphalt Binder Using a Dynamic Shear Rheometer. *ASTM International, West Conshohocken, PA, 2015, www.astm.org.*
- Bowers, B. F., Huang, B., & Shu, X. (2014). Refining laboratory procedure for artificial RAP: A comparative study. *Construction and building materials, 52*, 385-390.
- Cao, X., Wang, H., Cao, X., Sun, W., Zhu, H., & Tang, B. (2018). Investigation of rheological and chemical properties asphalt binder rejuvenated with waste vegetable oil. *Construction and building materials, 180*, 455-463.
- Cavalli, M. C., Zaumanis, M., Mazza, E., Partl, M. N., & Poulidakos, L. D. (2018). Effect of ageing on the mechanical and chemical properties of binder from RAP treated with bio-based rejuvenators. *Composites Part B: Engineering, 141*, 174-181.
- Chen, J.-S., Lee, C.-T., & Lin, Y.-Y. (2018). Characterization of a Recycling Agent for Restoring Aged Bitumen. *Journal of Materials in Civil Engineering, 30*(8), 05018003.
- Dinh, B. H., Park, D.-W., & Le, T. H. M. (2018). Effect of rejuvenators on the crack healing performance of recycled asphalt pavement by induction heating. *Construction and building materials, 164*, 246-254.

- Elkashaf, M., Williams, R. C., & Cochran, E. (2018). Effect of Asphalt Binder Grade and Source on the Extent of Rheological Changes in Rejuvenated Binders. *Journal of Materials in Civil Engineering*, 30(12), 04018319.
- Gong, M., Yang, J., Zhang, J., Zhu, H., & Tong, T. (2016). Physical–chemical properties of aged asphalt rejuvenated by bio-oil derived from biodiesel residue. *Construction and building materials*, 105, 35-45.
- Hajj, E. Y., Sebaaly, P. E., & Shrestha, R. (2009). Laboratory evaluation of mixes containing recycled asphalt pavement (RAP). *Road Materials and Pavement Design*, 10(3), 495-517.
- Hasan, M. R. M., You, Z., Porter, D., & Goh, S. W. (2015). Laboratory moisture susceptibility evaluation of WMA under possible field conditions. *Construction and building materials*, 101, 57-64.
- Huang, S.-C., Qin, Q., Grimes, W. R., Pauli, A. T., & Glaser, R. (2014). Influence of rejuvenators on the physical properties of RAP binders. *Journal of Testing and Evaluation*, 43(3), 594-603.
- Hung, A. M., Mousavi, M., Pahlavan, F., & Fini, E. H. (2017). Intermolecular Interactions of Isolated Bio-Oil Compounds and Their Effect on Bitumen Interfaces. *ACS Sustainable Chemistry & Engineering*, 5(9), 7920-7931.
- Jennings, P., Desando, M., Raub, M., Moats, R., Mendez, T., Stewart, F., . . . Smith, J. (1992). NMR spectroscopy in the characterization of eight selected asphalts. *Fuel science & technology international*, 10(4-6), 887-907.
- Kupareva, A., Mäki-Arvela, P. i., Grénman, H., Eränen, K., Sjöholm, R., Reunanen, M., & Murzin, D. Y. (2012). Chemical characterization of lube oils. *Energy & Fuels*, 27(1), 27-34.
- Lei, Z., Bahia, H., & Yi-qiu, T. (2015). Effect of bio-based and refined waste oil modifiers on low temperature performance of asphalt binders. *Construction and building materials*, 86, 95-100.
- Lesueur, D. (2009). The colloidal structure of bitumen: Consequences on the rheology and on the mechanisms of bitumen modification. *Advances in colloid and interface science*, 145(1-2), 42-82.
- Levine, B. G., Stone, J. E., & Kohlmeyer, A. (2011). Fast analysis of molecular dynamics trajectories with graphics processing units—Radial distribution function histogramming. *Journal of computational physics*, 230(9), 3556-3569.
- Li, D. D., & Greenfield, M. L. (2014). Chemical compositions of improved model asphalt systems for molecular simulations. *Fuel*, 115, 347-356.

- Liu, X., Cao, F., Xiao, F., & Amirkhanian, S. (2018). BBR and DSR Testing of Aging Properties of Polymer and Polyphosphoric Acid–Modified Asphalt Binders. *Journal of Materials in Civil Engineering*, 30(10), 04018249.
- Loeber, L., Muller, G., Morel, J., & Sutton, O. (1998). Bitumen in colloid science: a chemical, structural and rheological approach. *Fuel*, 77(13), 1443-1450.
- Lowry, E., Sedghi, M., & Goual, L. (2017). Polymers for asphaltene dispersion: Interaction mechanisms and molecular design considerations. *Journal of Molecular Liquids*, 230, 589-599.
- Mirhosseini, A. F., Kavussi, A., Tahami, S. A., & Dessouky, S. (2018). Characterizing temperature performance of bio-modified binders containing RAP binder. *Journal of Materials in Civil Engineering*, 30(8), 04018176.
- Mogawer, W., Bennert, T., Daniel, J. S., Bonaquist, R., Austerman, A., & Booshehrian, A. (2012). Performance characteristics of plant produced high RAP mixtures. *Road Materials and Pavement Design*, 13(sup1), 183-208.
- Mogawer, W. S., Booshehrian, A., Vahidi, S., & Austerman, A. J. (2013). Evaluating the effect of rejuvenators on the degree of blending and performance of high RAP, RAS, and RAP/RAS mixtures. *Road Materials and Pavement Design*, 14(sup2), 193-213.
- Moghadas Nejad, F., Azarhoosh, A., Hamed, G. H., & Roshani, H. (2014). Rutting performance prediction of warm mix asphalt containing reclaimed asphalt pavements. *Road Materials and Pavement Design*, 15(1), 207-219.
- Mohammadafzali, M., Ali, H., Sholar, G. A., Rilko, W. A., & Baqersad, M. (2018). Effects of Rejuvenation and Aging on Binder Homogeneity of Recycled Asphalt Mixtures. *Journal of Transportation Engineering, Part B: Pavements*, 145(1), 04018066.
- Morgan, T., Alvarez-Rodriguez, P., George, A., Herod, A., & Kandiyoti, R. (2010). Characterization of Maya crude oil maltenes and asphaltenes in terms of structural parameters calculated from nuclear magnetic resonance (NMR) spectroscopy and laser desorption– mass spectroscopy (LD– MS). *Energy & Fuels*, 24(7), 3977-3989.
- Mousavi, M., Pahlavan, F., Oldham, D., Hosseinneshad, S., & Fini, E. H. (2016). Multiscale investigation of oxidative aging in biomodified asphalt binder. *The Journal of Physical Chemistry C*, 120(31), 17224-17233.
- NAPA. (2016). Recycled Materials and Warm-Mix Asphalt Usage. *National Asphalt Pavement Association*.

- Noureldin, A. S., & Wood, L. E. (1989). Variations in molecular size distribution of virgin and recycled asphalt binders associated with aging. *Transportation Research Record*(1228).
- Oldham, D. J., Rajib, A. I., Onochie, A., & Fini, E. H. (2019). Durability of bio-modified recycled asphalt shingles exposed to oxidation aging and extended sub-zero conditioning. *Construction and building materials*, *208*, 543-553.
doi:<https://doi.org/10.1016/j.conbuildmat.2019.03.017>
- Oldham, D., Qu, X. Q., Wang, H., & Fini, E. H. (2020). Investigating Change of Polydispersity and Rheology of Crude Oil and Bitumen Due to Asphaltene Oxidation. *Energy & Fuels*. <https://doi.org/10.1021/acs.energyfuels.0c01344>
- Pahlavan, F., Hung, A., & Fini, E. H. (2018). Evolution of molecular packing and rheology in asphalt binder during rejuvenation. *Fuel*, *222*, 457-464.
- Pahlavan, F., Mousavi, M., Hung, A. M., & Fini, E. H. (2018). Characterization of oxidized asphaltenes and the restorative effect of a bio-modifier. *Fuel*, *212*, 593-604.
- Plimpton, S. (1995). Fast parallel algorithms for short-range molecular dynamics. *Journal of computational physics*, *117*(1), 1-19.
- Puello, J., Afanasjeva, N., & Alvarez, M. (2013). Thermal properties and chemical composition of bituminous materials exposed to accelerated ageing. *Road Materials and Pavement Design*, *14*(2), 278-288.
- Samieadel, A., Høgsaa, B., & Fini, E. H. (2018). Examining the Implications of Wax-Based Additives on the Sustainability of Construction Practices: Multiscale Characterization of Wax-Doped Aged Asphalt Binder. *ACS Sustainable Chemistry & Engineering*, *7*(3), 2943-2954.
- Samieadel, A., Oldham, D., & Fini, E. H. (2017). Multi-scale characterization of the effect of wax on intermolecular interactions in asphalt binder. *Construction and building materials*, *157*, 1163-1172.
- Shen, J., Amirhanian, S., & Tang, B. (2007). Effects of rejuvenator on performance-based properties of rejuvenated asphalt binder and mixtures. *Construction and building materials*, *21*(5), 958-964.
- Shen, J., Amirhanian, S. N., & Lee, S.-J. (2007). HP-GPC characterization of rejuvenated aged CRM binders. *Journal of Materials in Civil Engineering*, *19*(6), 515-522.
- Sun, H., Mumby, S. J., Maple, J. R., & Hagler, A. T. (1994). An ab initio CFF93 all-atom force field for polycarbonates. *Journal of the American Chemical society*, *116*(7), 2978-2987.

- Tran, N. H., Taylor, A., & Willis, R. (2012). Effect of rejuvenator on performance properties of HMA mixtures with high RAP and RAS contents. *NCAT Report*, 12-05.
- Ungerer, P., Rigby, D., Leblanc, B., & Yiannourakou, M. (2014). Sensitivity of the aggregation behaviour of asphaltenes to molecular weight and structure using molecular dynamics. *Molecular Simulation*, 40(1-3), 115-122.
- Waldman, M., & Hagler, A. T. (1993). New combining rules for rare gas van der Waals parameters. *Journal of Computational Chemistry*, 14(9), 1077-1084.
- West, R. C., Willis, J. R., & Marasteanu, M. O. (2013). *Improved mix design, evaluation, and materials management practices for hot mix asphalt with high reclaimed asphalt pavement content* (Vol. 752): Transportation Research Board.
- Wiehe, I. A. (2008). *Process chemistry of petroleum macromolecules*: CRC press.
- Yang, Z., Zhang, X., Zhang, Z., Zou, B., Zhu, Z., Lu, G., . . . Yu, H. (2018). Effect of Aging on Chemical and Rheological Properties of Bitumen. *Polymers*, 10(12).
- Yaseen, S., & Mansoori, G. A. (2018). Asphaltene aggregation due to waterflooding (A molecular dynamics study). *Journal of Petroleum Science and Engineering*, 170, 177-183.
- Zaumanis, M., Mallick, R. B., & Frank, R. (2015). Evaluation of different recycling agents for restoring aged asphalt binder and performance of 100% recycled asphalt. *Materials and Structures*, 48(8), 2475-2488.

CHAPTER 4 EVALUATING SOURCE DEPENDENCY OF REJUVENATORS

A version of this paper submitted in Journal of Road Materials and Pavement Design

Rajib, A. I., Samieadel, A., Zalghout, A., Kaloush, K., Sharma, B., Fini, E. H., (2020).
Evaluating Efficacy of Asphalt Rejuvenators via a Multi-scale Characterization. Journal
of Road Materials and Pavement Design

4.1 Abstract

Reclaimed asphalt pavement (RAP) and recycled asphalt shingles (RAS) contain various amounts of aged asphalt binder and their application in new constructions have been promoted as a sustainable practice in the pavement industry. However, this effort has faced challenges such as aged binder's inferior properties compared to the virgin binder and its unknown contribution to new pavements. To address latter issue, liquid additives were used under a general title of rejuvenators. That poses an additional challenge associated with the lack of clear metrics to differentiate between softeners and comprehensive rejuvenators. While revitalizing aged asphalt binder to regain its desirable properties would be an ideal solution, progress in this area has been limited by a lack of understanding of rejuvenation mechanisms at the molecular level and the absence of representative test parameter(s) to evaluate plausible revitalizations. In this study, both laboratory experiments and computer modeling were combined to compare and justify the efficacy of several rejuvenators. It was found that all studied rejuvenators have a softening effect on aged asphalt, but only a few of them can revitalize aged asphalts'

physicochemical and rheological properties. Lower number of gyratory compaction and reduced rate of crack propagation were observed after the addition of rejuvenator to the asphalt mixtures containing a certain percentage of recycled asphalt pavement. The reduction in crack propagation rate could be attributed to both enhanced blending between aged and virgin binder and the revitalization of aged binder properties. Latter phenomenon was explained at the molecular level based on rejuvenator's ability to interact with aged asphaltene molecules intercalating into and separating asphaltene nanoaggregates. Accordingly, this molecular-level phenomenon is reflected in two ways: an increase in crossover modulus and crossover frequency at the binder level, and a reduced crack propagation rate at the mixture level.

Keywords: Rejuvenator, molecular conformation, aged asphalt, crossover modulus, nanoaggregates, asphaltene, crack propagation rate, rheology

4.2 Introduction

Recycling of RAP and RAS can be considered as an efficient method to lessen the cost of new pavement construction, with both economic and environmental benefits. However, their incorporation in new pavement encounters challenges because their properties are inferior to those of neat binder. Aged asphalts such as RAP and RAS are highly oxidized during their service life; oxidation causes aged asphalt's poor properties. Asphalt undergoes oxidation during their service life, which causes pavement embrittlement and leads to premature pavement failure (Lu & Isacsson, 2002; Qin et al., 2014). Studies have

found that mixing recycled aged asphalt with neat binder causes increased mixture stiffness and decreased pavement cracking resistance (Al-Qadi et al., 2012; West et al., 2013; Zaumanis & Mallick, 2015). Oxidative aging alters the chemical balance of the asphalt by changing some chemical functional groups (such as carbonyl (C=O) and sulfoxide (S=O)) of the asphalt (Dony et al., 2016). Moreover, during aging, bitumen loses its chemical balance between the asphaltene and maltene portions (Tran et al., 2012). Aged asphalts such as RAP and RAS have an increased asphaltene content compared to unaged bitumen; adding RAP with unaged bitumen causes the overall blend to suffer colloidal instability (Shen et al., 2007). Aging also causes the glass transition temperature to shift to a relatively higher temperature. It means that aging changes the glass transition phenomenon (hard and brittle glassy state from viscous state) to occur at a relatively higher (less negative) temperature (Kriz et al., 2008), which in turns lead to cracking of aged asphalt at a higher (less negative) temperature. In order to revitalize aged asphalt to its desirable properties, many studies have used recycling agents or proposed rejuvenators from various sources with varying success rates (Cao et al., 2018; Cavalli et al., 2018; Oldham et al., 2019). For example, the addition of waste cooking oil derived bio-oil resulted in softer asphalt binders with increased phase angles (Cao et al., 2019). The waste wood-based bio-oil caused an increase in viscous components and a decrease in stiffness of aged asphalt (Zhang et al., 2018). An increased temperature susceptibility and decreased viscosity of aged asphalt were obtained by the addition of a bio-rejuvenator produced from sawdust (Zhang et al., 2019). The addition of rejuvenators

derived from soybean oil shifted the glass transition temperature of asphalt toward a low temperature (Elkashef et al., 2019). The addition of 10% paraffin wax to aged asphalt reduced temperature of glass transition up to 9 degrees (Samieadel et al., 2019).

Several studies found that the efficiency of rejuvenators in revitalizing the properties of aged asphalt mostly depends on their sources of origin. For example, organic-sourced rejuvenators outperformed a petroleum-sourced rejuvenator in revitalizing the properties of aged asphalt (Zaumanis & Mallick, 2015). A plasticizer-based bio-rejuvenator made from cotton-oil by-products in combination with dibutylephthalate (DBP) restored the viscosity of a laboratory-based Pressure Aging Vessel (PAV)-aged asphalt to its original level (Zhu et al., 2017). Two rejuvenators sourced from non-edible oil showed different efficiency in reducing the carbonyl index of aged asphalt (Nayak & Sahoo, 2017).

Rejuvenators from four different sources (petroleum sourced, green technology sourced, agriculture sourced, and amine-based) performed differently in revitalizing the properties of aged asphalt, which shows that a rejuvenator's efficiency depends on the source from which it originates (Haghshenas et al., 2016).

Similarly, many other studies used various source-dependent recycling agents or rejuvenators to help revitalize the properties of aged asphalt. Most studies track the effectiveness of their rejuvenator by using selected properties while ignoring other properties. This, in turn, may lead to erroneous conclusions promoting products that can improve some properties but make other performance characteristics worse. Table 4-1

shows the specific performance characteristic measures used by selected studies as measures of rejuvenation.

Table 4-1 Literature Review of Indicators Used to Measure Rejuvenator Performance

Measures	Target	Studied by
Crossover modulus	Increase	(Pahlavan et al., 2019; Pahlavan et al., 2018)
De-agglomeration of oxidized asphaltenes	Increase	(Samieadel et al., 2018b; Zadshir et al., 2019)
Intercalation and separation	Increase	(Pahlavan et al., 2019)
Polydispersity (molecule weight avg./number avg.)	Decrease	(Cao et al., 2018)
Large Molecular Size (LMS)/ Small Molecular Size (SMS) index	Decrease	(Cao et al., 2018; Chen et al., 2014)
Complex-modulus-based Aging Index, Crossover temperature	Decrease	(Cavalli et al., 2018)

Chemical aging index	Decrease	(Cao et al., 2018; Cavalli et al., 2018; Chen et al., 2014; Mirhosseini et al., 2018)
“Bee” length	Decrease	(Oldham et al., 2018)
Colloidal stability index	Increase	(Cavalli et al., 2018)
Rheological aging index	Decrease	(Mousavi et al., 2016a)

Consequently, a comprehensive rejuvenation mechanism is needed to thoroughly evaluate the effectiveness of rejuvenators. In this study, combined laboratory experiments and modeling was used to compare the efficacy of several rejuvenators while determining the effect of composition on the success rate of rejuvenators.

4.3 Materials and Methods

The unaged asphalt binder was chosen from a Superpave PG 64-22 grade. Table 4-2 shows some properties of the selected asphalt binder. Eight rejuvenators were collected: seven are organic bio-based, and one is petroleum-based. Table 4-3 shows the sources of rejuvenators.

Table 4-2 Selected Binder Properties (PG 64-22)

Specific Gravity at 15.6 °C	1.039
Flash Point, Cleveland Open Cup, °C	335
Change in Mass RTFO	-0.0129
Absolute Viscosity at 60 °C, Pa.s	202
Stiffness (MPa) at -12°C @ 60s	112.5

Table 4-3 Sources of Rejuvenators

Rejuvenators	Source
A	plant extract (rosin, fatty acid, vegetable oil)
B	vegetable oil
C	soy-based oil
D	petroleum-based
W	waste vegetable oil

R	rubberwood oil
S	swine manure
L	algae

4.3.1 Preparation of Laboratory-Aged Asphalt

A two-step aging process (short-term and long-term) was conducted to age the unaged binder in the laboratory. Short-term aging was conducted using a rolling thin film oven (RTFO) (ASTMD2872-12e1, 2012). The RTFO-aged sample was subjected to long-term aging using a pressure aging vessel (PAV) (ASTMD6521-13, 2013). The PAV was conducted at 2.10 MPa pressure and at 100 °C temperature for 40h. The extended aging of 40h would represent the end of service life aging of asphalt pavement representative of RAP asphalt binder (Bowers et al., 2014).

To prepare each blended sample, 10% (by weight of aged binder) rejuvenator was added into the aged sample. The rejuvenator was mixed into the heated aged sample (135°C) and hand-blended for 5 minutes. The binders modified with each of the eight rejuvenators were labeled as A, B, C, D, W, R, S, and L (Table 3).

4.3.2 Preparation of RAP Mixtures

To quantify the rejuvenator effect on the cracking of asphalt mixtures containing RAP, two mixtures sample were made. The first mixture (Control) is a RAP mixture produced

by a City of Phoenix (Arizona) plant, with a nominal maximum aggregate size of $\frac{3}{4}$ in. The mix is 25% RAP and 75% PG 64-16 virgin binder. The second mixture was prepared by spraying a selected rejuvenator (rejuvenator A) at 5% by weight of total asphalt binder on the first mixture. The two mixture scenarios were labeled as without rejuvenator (Control), and with rejuvenator (Control + 5% Rej. A), respectively.

4.3.3 Compaction Procedure

A Servopac Superpave Gyrotory (SSG) compactor with 600 kPa pressure, 1.16° gyration angle, and 30 gyrations per minute gyration speed was utilized to compact all the mixture specimens. Following ASTM D6925, all the samples were compacted to 180 mm height with 150 mm diameter (ASTMD6925-15, 2015).

4.3.4 Preparation of Specimens for C Fracture Test*

After compaction, two samples were cut having 150 mm diameter and 50 mm thickness from each gyrotory specimen. After that, a right-angle wedge was made in each specimen, including a notch to serve as a crack propagation point, following the method developed by Stempihar & Kaloush (Stempihar & Kaloush, 2017).

4.3.5 Preparation of Field-Aged Binder Sample

The extraction and recovery of field-aged asphalt binder was from the RAP recovered from the field. The extracted RAP (100% RAP binder) was then mixed with 5% rejuvenator (by weight of RAP). The dosage of rejuvenator for 100% RAP was $(5/100 = 5\%)$. Two samples were prepared and labeled as Extracted RAP and Extracted RAP + 5% Rej. A.

In addition, binder was extracted from mixture samples from each fractured specimen (prepared with and without rejuvenator) that was used for the C* test (explained in a later section), according to (ASTMD5404, 2017). The samples were labeled as without rejuvenator (Control) and with rejuvenator (Control + 5 % Rej. A). The dosage of rejuvenator only for RAP belongs to the control sample (25%RAP+75% virgin binder) was $(5/25=20\%)$.

4.3.6 Thin-layer Chromatography with Flame Ionization Detection (TLC-FID)

The fractional composition of each rejuvenator, as well as rejuvenated asphalt binder specimens, was investigated using an Iatroscan MK-6s model TLC-FID analyzer. 160 mL/min hydrogen flow rate and 2 L/min airflow rate were supplied. The n-heptane-insoluble part, the asphaltene content, was separated and determined following (ASTMD3279, 2007). Later, 20 µg of maltene (n-heptane soluble part) was spotted on the chromrods; solvent was developed using pentane, toluene, and chloroform solutions. In a pentane tank, the chromrods were developed for 35-40 minutes and dried in the air for 2-5 minutes. A second developing chamber filled with a 9:1 ratio of toluene to chloroform solution was used to keep the dried chromrods for 9 minutes. Finally, the rods were dried in the oven at 85 °C, and the prepared specimen was scanned for 30s using an Iatroscan with FID detector.

4.3.7 Gel Permeation Chromatography (GPC)

A size-exclusion chromatography analysis was performed to examine the efficacy of rejuvenators. 3.6 mL tetrahydrofuran (THF) was used to prepare 0.12 gram of each

sample. To remove suspended particulates, a PTFE filter with 0.45 μm Millipore was used. THF as a carrier solvent with a pump flow rate of 1.0 mL/min with 50 μL injection volumes were used. The system contains a Waters 2414 RI detector with Styragel HR1 SEC column (7.8mm \times 300mm). A Waters 600-MS System controller was connected to a 600-multi-solvent delivery system, and a 717-plus auto-sampler was connected to a Dionex U120 Universal Interface. Based on the retention time, the resulting chromatogram was divided into small, medium, and large molecular sizes.

4.3.8 Differential Scanning Calorimeter (DSC)

The glass transition temperature, T_g , was determined using a TA Instruments Discovery DSC 2500 instrument. Approximately 10-20 mg of asphalt samples were put into a Tzero aluminum hermetic pans covered by a hermetic lid and sealed without further drying process. The following thermal cycles were conducted for all samples where 15 minutes isothermal conditioning was adopted after each cycle: (i) initial fast cooling from 160°C to -80°C with a rate of 20°C/min (ii) 1st heating cycle from -80°C to 160°C at 20°C/min (iii) cooling from 160°C to -80°C at 20°C/min (iv) 2nd heating cycle from -80°C to 160°C at 20°C/min. 2nd heating cycle data was considered to calculate the glass transition temperature.

4.3.9 Dynamic Shear Rheometer (DSR)

An Anton Paar Modular Compact Rheometer MCR 302 was used to measure the elastic behavior and viscous behavior of each sample following (ASTMD7175-15, 2015). Tests were conducted at 10 °C with frequencies of 0.1 to 100 rad/s and at a strain rate of 0.1 %.

For this study, an 8 mm parallel plate spindle was used. Using the corresponding elastic (G') and viscous (G'') moduli results, the crossover frequency and crossover modulus (at which G' is equal to G'') were determined. Additionally, the complex shear modulus (G^*) which is the material deformation resistance with repeated share, and phase angle (δ), the time lag between stress and strain were calculated from the measured stress and strain data, using Equation 4-1 (AASHTO-T315, 2012).

$$G^* = \frac{\tau_{\max}}{\gamma_{\max}} \quad (4-1)$$

in which $\gamma_{\max} = \left(\frac{\theta r}{h}\right)$ and $\tau_{\max} = \frac{2T}{\pi r^3}$

where:

γ_{\max} = maximum strain

τ_{\max} = maximum stress

T = maximum applied torque

r = radius of the sample

θ = deflection (rotational) angle

h = height of the sample

4.3.10 Binder Bond Strength (BBS) Test

The Pneumatic Adhesion Tensile Testing Instrument, commonly known as PATTI, was used to measure the binder adhesion according to (AASHTO-TP91, 2015). The substrate used for this test was a glass substrate with 3.175 mm thickness and cut into a 3”x 3” square. The glass was cleaned with acetone and then with an ultrasonic cleaner with distilled water at 60 °C for 60 min (Fini et al., 2011). After ultrasonic cleaning, the glass slide was placed in an oven at 60 °C for a minimum of 30 minutes to dry the surface. The pull-out stub was degreased with acetone and then put in an oven at 60 °C for 30 minutes to eliminate any water absorbed on the stub surface. The asphalt binder sample was prepared in a silicone mold having a diameter of 8 mm and 2mm depth, approximately 0.4 g ±0.05 g. 3 replicates of each rejuvenated sample were prepared and tested. Before testing, dry samples were kept at room temperature for 2 hr. For water conditioned samples, the samples were kept at a water bath at 50 °C for 2 hr. The duration and temperature are selected to observe the effect of water damage to the samples. For higher time and temperature conditioning, some samples ripped off completely from the glass, and it is impossible to measure the tensile strength of those samples. After water conditioning, samples were kept at room temperature for 30 minutes.

The moisture susceptibility index (MSI) based on dry and wet peak tensile strength was developed based on Equation 4-2.

$$MSI = \frac{\text{Peak Tensile Strength (Dry)} - \text{Peak Tensile Strength (Wet)}}{\text{Peak Tensile Strength (Dry)}} \times 100 \quad (4-2)$$

4.3.11 Fracture Test

From the mixture specimen fracture test, the power or energy rate difference between two specimens, under the same loading defined as C^* can be measured experimentally from J-integral and the C^* parameter. J can be defined as the energy difference between two specimens subjected to the same load yet have different crack length (Begley & Landes, 1972; Rice, 1968), as expressed in Equation 4-3. And C^* relation is shown in Equation 4-4.

$$J = -\frac{dU}{da} \quad (4-3)$$

Where

U = potential energy

a = crack length

$$C^* = \frac{dU^*}{da^*} \quad (4-4)$$

Where

U^* = power or energy rate for a given load P

a^* = crack growth rate

The rate of work done (U^*) is defined as the area under the P vs. displacement curve. It is calculated using Equation 4-5.

$$U^* = \int_0^u P du \quad (4-5)$$

The test was conducted at 10°C by applying a load at a constant displacement rate, and the crack length over time was measured for each disk. The test was performed at 3 different displacement rates (0.3, 0.38, and 0.42 mm/min); each disk was tested at one displacement rate.

The load versus displacement rate plot was plotted for different crack lengths, and the area under the curve (power or energy rate (U^*)) was calculated. Next, U^* as a function of crack length was plotted for various displacement rates. The slope of the curve is the C^* -integral, which was plotted later for crack growth rate.

4.3.12 Computational Modeling via Molecular Dynamics (MD)

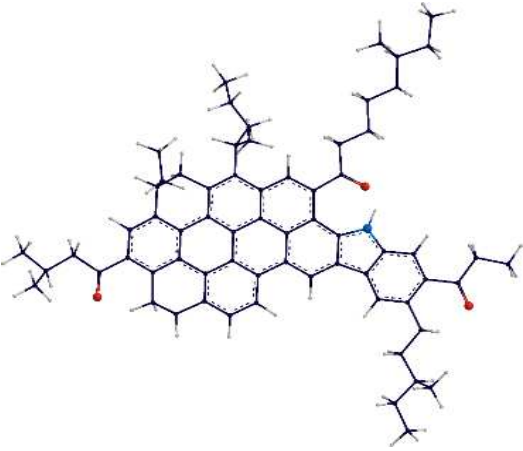
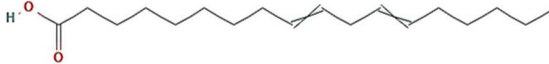
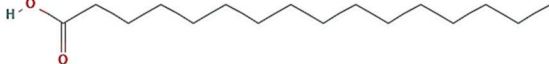
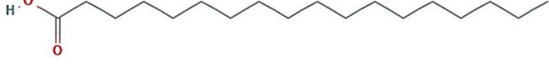
MD simulations were performed on a system of oxidized asphaltene molecules at equilibrium state; heptane solvent was used as a medium. By utilizing Large-scale Atomic/Molecular Massively Parallel Simulator (LAMMPS) source code deployed in Medea® software version 2.2, a simulation box was composed to study the effect of molecules found in rejuvenator A on interactions of oxidized asphaltene molecules. For this purpose, after the nanoaggregates formation, rejuvenator molecules were supplied into the oxidized asphaltene system to simulate the situation in aged bitumen. In this study the extended PCFF force field, PCFF+ was used (Sun et al., 1994; Ungerer et al., 2014; Waldman & Hagler, 1993).

4.3.13 Structure of Oxidized Asphaltene and Rejuvenator Molecules

In this study, the oxidized asphaltene molecule used has a continental structure asphaltene (Samieadel et al., 2018) comprising a core of a poly-aromatic ring and a number of side chains (Li & Greenfield, 2014; Morgan et al., 2010; Wiehe, 2008). The selected oxidized asphaltene comprises 3 carbonyl groups. The selection of molecules to represent rejuvenator A was based on GC-MS results. The three molecules with the highest concentration were selected. The molecules with a higher concentration have a higher number in the simulation, to better correlate with the effect of rejuvenator A at a macro scale. The selected molecules, their chemical formula, chemical structure, and the number of each used are presented in Table 4-4. The total molecular mass of rejuvenator molecules is equal to 10% of that of the oxidized asphaltene molecules.

Table 4-4 Molecules Selected for Molecular Dynamics Simulation

Molecular formula	Chemical structure	Number of molecules in simulation	Concentration in GC-MS
-------------------	--------------------	-----------------------------------	------------------------

<p>Oxidized asphaltene pyrrole; C₆₆NO₃H₇₅</p>		18	NA
<p>9,12-Octadecadienoic acid (Z, Z)-; C₁₈H₃₂O₂</p>		4	57.4%
<p>n-Hexadecanoic acid; C₁₆H₃₂O₂</p>		1	4.7%
<p>Octadecanoic acid; C₁₈H₃₆O₂</p>		1	2.2%

4.3.14 Method of Simulation

The simulation consisted of two consecutive LAMMPS stages. The simulation started with a low average density and underwent the energy minimization using the conjugate gradients method at a constant volume, in order to prevent molecular overlaps. The first stage of simulation was an NVT ensemble (constant number of atoms, volume, and temperature) starting at a high temperature of 800 K for 100 ps, followed by an NPT ensemble (constant number of atoms, pressure, and temperature) at a pressure of 200 atm and temperature of 800 K for 500 ps, to shake the system. This will prevent the simulation from trapping at a local minimum energy state. The second stage began with an NVT ensemble with a temperature of 350 K for 2ns, to reach an equilibrium and to correct any probable overlaps of molecules, considering there is no pressure on the system. Following by an NPT ensemble, the simulation continued for 20ns with a temperature of 350 K and a pressure of 1atm. A Nose-Hoover thermostat and barostat were used during all the stages, and the time step of 1 fs (10⁻¹⁵ s) was selected. After equilibration of oxidized asphaltenes in heptane, the rejuvenator molecules were added to the system, and the simulation was resumed for another 20ns. The average pressure and temperature were checked during the simulation to ensure the system energy is at equilibrium state. During the simulation, the coordinates for the center of mass of asphaltene molecules were dumped in an output file to study the aggregation behavior of oxidized asphaltenes. Furthermore, the radial distribution function outcomes were analyzed for the most centered carbon atom of oxidized asphaltene molecules. Figure 4-1

shows the first step of simulation after addition of rejuvenator A's molecules to equilibrated oxidized asphaltene molecules. The heptane molecules are not shown for clarity.

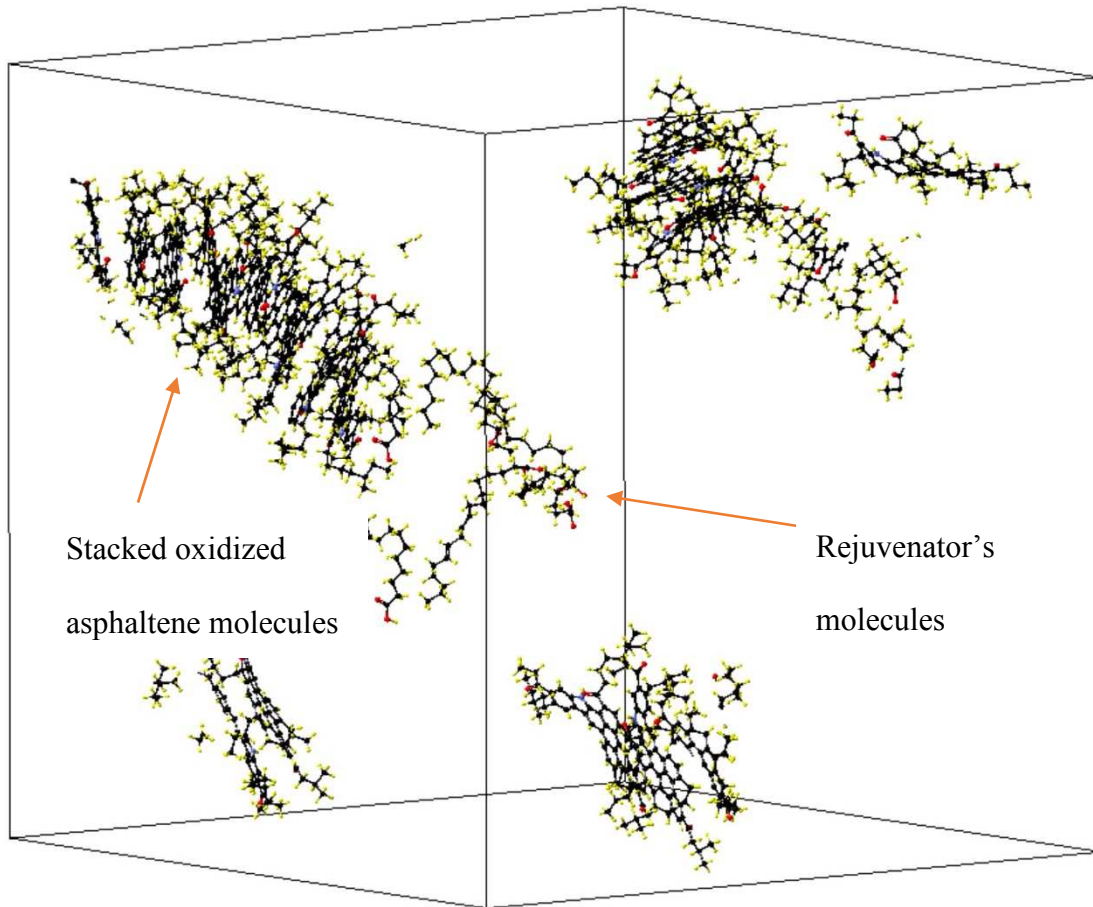


Figure 4-1 The Initial Simulation Box After Addition of Rejuvenator's Molecules

4.4 Results and Discussion

4.4.1 Binder Study

4.4.1.1 Dynamic Shear Rheometer (DSR) Results

The complex modulus (G^*) vs. phase angle plot is shown in Figure 4-2. The results showed that after aging, the complex modulus value increased, and the phase angle value decreased for the aged sample. All rejuvenators decreased the modulus value and increased the phase angle value. Rejuvenators A, S, and L showed top performance in reducing the complex modulus value and in increasing the phase angle value, indicating their rejuvenation efficacy.

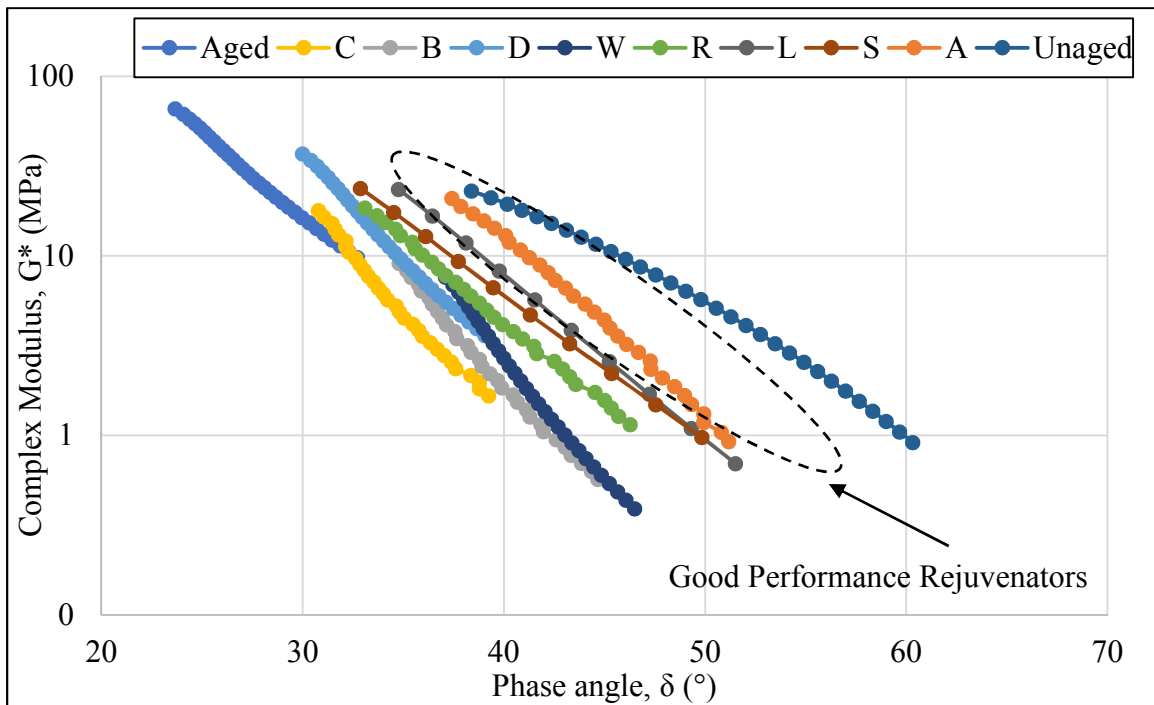


Figure 4-2 Complex Modulus (G^*) vs. Phase Angle Data

The crossover modulus is the modulus at $\tan \delta = 1$, where the viscous modulus and elastic modulus intersect. Aging reduced both the crossover modulus and crossover frequency compared to the unaged sample. All the rejuvenators were able to restore the crossover modulus value closer to that of the unaged binder. The maximum value was achieved by sample A, which restored the crossover modulus approximately 84%, followed by samples L, D, and S. Sample B had the lowest performance in improving the crossover modulus value. In contrast, some rejuvenators were able to change the crossover frequency value, but others did not change the crossover frequency significantly compared to the aged binder. The highest change in crossover frequency value was found for sample A, followed by samples L and S. Table 4-5 shows the value for crossover modulus and frequency.

Table 4-5 Crossover Modulus and Frequency Values

Crossover	Unaged Binder	Aged Binder	Aged Binder + 10% Rejuvenator							
			A	B	C	D	W	R	S	L
Modulus (MPa)	3.3	0.50	2.81	0.40	1.17	2.53	0.55	1.12	2.49	2.63
Frequency (Hz)	1.59	0.016	0.40	0.016	0.016	0.016	0.04	0.03	0.34	0.34

The observed crossover modulus and frequency results indicate the rejuvenators' performance dependency on their chemical sources. While some rejuvenators mainly

impact the viscous component of asphalt, acting as a softener, other rejuvenators restore both the viscous and elastic performance of aged asphalt.

4.4.1.2 Binder Bond Strength (BBS)

Table 4-6 shows the dry and wet-conditioned peak tensile strengths and the moisture susceptibility index.

Table 4-6 Dry and Wet Peak Tensile Strength, and Moisture Susceptibility Index

Peak Tensile Strength (kPa)	Unaged Binder	Aged Binder	Aged Binder + 10% Rejuvenator							
			A	B	C	D	W	R	S	L
Dry	1379	510	1310	1434	1372	1365	1282	1172	896	1165
Wet	986	365	1220	1275	1179	1227	1110	303	786	1069
Moisture Susceptibility Index (MSI)	28.50	28.43	6.87	11.08	14.06	10.11	13.41	74.14	12.27	8.24

Table 4-6 shows that different rejuvenators performed differently in reducing the effect of water conditioning. Water conditioning reduced the peak tensile strength, and for some

samples, it changed the failure mode from cohesive to adhesive; similar results were observed by (Figueroa et al., 2013). The moisture susceptibility index (MSI) was developed based on Equation 4-2. Sample A had the lowest moisture susceptibility index, followed by L and S. Sample R showed the lowest performance in preventing water damage, with the highest MSI value. This sample pulled off completely from the glass surface after 2 hr water conditioning at this temperature (50 °C), making it adhesive (detachment) failure (Figueroa et al., 2013). The dry and wet-conditioned BBS test photos are shown in Figure 4-3.



Figure 4-3 Binder Residue From Bitumen Sample R (Left) Adhering to the Glass Surface in Dry Condition; (Right) after Adhesive Failure Following 2 hr Water Conditioning

4.4.1.3 Differential Scanning Calorimeter (DSC)

The temperature for glass transition for each sample was analyzed through “Trios” software based on the tangent transition type. The Tg was chosen as a midpoint of half-height of the curve changed or the inflection point. Figure 4-4 shows a plot of Tg for all samples. Sample B has two Tg values, which suggests that this sample had phase separation with the aged sample and thus gave two different transition temperatures.

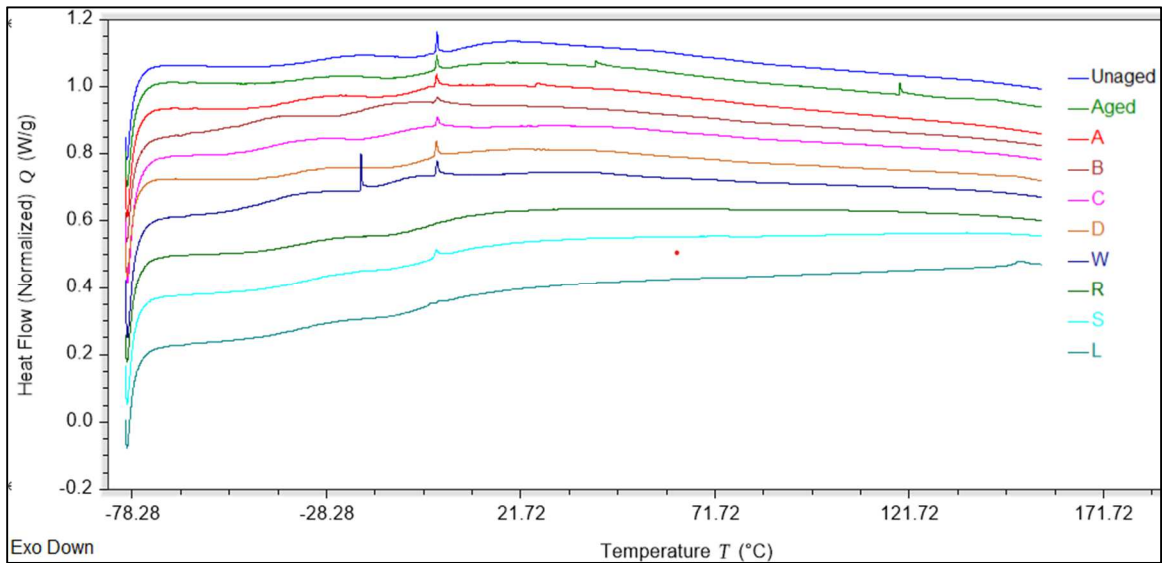


Figure 4-4 Measurement of Glass Transition Temperature at the Second Heating Cycle with Exothermic Down Positive

Table 4-7 shows the Tg values found for the samples. It shows that aging increases the Tg values, which agrees with the literature. The addition of rejuvenators lowered the Tg value; the highest reduction was found for waste vegetable oil (W), followed by samples

L and A. Only sample B did not perform well in lowering the T_g value since it had phase separation with the aged sample. All other rejuvenators lowered the T_g value of the aged binder, even to the T_g value (or lower) of the unaged sample.

Table 4-7 Glass Transition Temperature (T_g) for All Samples

Sample	Unaged Binder	Aged Binder	Aged Binder + 10% Rejuvenator							
			A	B	C	D	W	R	S	L
T _g (°C)	-31.9	-19.2	-36.2	-16.3	-33.4	-36.7	-39.5	-31.7	-33.7	-36.4

4.4.1.4 TLC-FID Results

Table 4-8 (upper portion) displays the combination of SARA (saturates, aromatics, resins, and asphaltene) of unaged binder, aged binder, and aged binder modified with each rejuvenator. The SARA fractions of the pure rejuvenators were also analyzed and are shown in Table 4-8 (lower portion). Comparing aged and unaged binder, Table 4-8 shows that the asphaltene fraction increased up to 76.24% after aging while other fractions decreased. This increase in the asphaltene portion is consistent with the previous studies (Puello et al., 2013). Some rejuvenators showed a reduction in asphaltene content, while others showed an increase; this is an example of how the effectiveness of a rejuvenator

depends on its source. Table 4-8 (lower portion) shows that some rejuvenators are rich in aromatic components, while others are mostly dominated by resins.

Table 4-8 SARA Fractions of Blended Samples and Pure Rejuvenators

Binder	Unaged Binder	Aged Binder	Aged Binder + 10% Rejuvenator							
			A	B	C	D	W	R	S	L
Saturates	12.40	11.58	15.17	14.47	10.03	14.22	6.07	10.20	9.35	12.09
Aromatics	23.63	15.12	26.38	28.51	19.68	19.10	27.20	17.09	12.77	12.19
Resins	47.85	44.89	34.69	32.71	45.99	41.66	42.03	42.80	48.38	48.39
Asphaltenes	16.12	28.41	23.76	24.31	24.30	25.02	24.69	29.91	29.51	26.60
Rejuvenator	-	-	Pure Rejuvenator Without Binder							
			A	B	C	D	W	R	S	L
Saturates	-	-	0.44	2.74	20.56	1.45	0.00	20.95	1.93	0.00
Aromatics	-	-	72.49	92.82	72.82	89.16	87.19	0.00	3.06	15.37
Resins	-	-	26.36	4.11	6.37	8.57	12.80	78.17	71.24	83.48
Asphaltenes	-	-	0.71	0.33	0.25	0.82	0.00	0.87	23.76	1.13

The colloidal stability index (CI) was calculated to estimate the stability of the asphalt colloidal system using Equation 4-6 (Loeber et al., 1998).

$$CI = \frac{(\text{resins} + \text{aromatics})}{(\text{asphaltenes} + \text{saturates})} \quad (4-6)$$

Table 4-9 shows the colloidal stability index for the unaged, aged, and rejuvenated binders. A higher index indicates better peptizing of asphaltene molecules by resins and aromatics. After aging by converting aromatics to resins and resins to asphaltene, this effect is reduced, and the index decreased to 1.50 from 2.51, with a 40% reduction from unaged to the aged binder. The rejuvenator addition resulted in the enhancement of the CI for all the rejuvenated samples except R; the highest index was observed for the sample modified with waste vegetable oil.

Table 4-9 Colloidal Stability Index for All Samples

	Unaged Binder	Aged Binder	Aged Binder + 10% Rejuvenator							
			A	B	C	D	W	R	L	S
Colloidal Stability Index	2.51	1.50	1.57	1.58	1.91	1.55	2.25	1.49	1.57	1.57

4.4.1.5 Gel Permeation Chromatography (GPC) Analysis

Figure 4-5 shows the GPC results with molecular size distribution. The molecular size was differentiated into three categories: large molecular size (LMS), medium molecular

size (MMS), and small molecular size (SMS) (Shen et al., 2007). Aging increased the percentage of large molecular size: the LMS of the aged sample was about 32% larger than the LMS of the unaged sample. On the other hand, aging reduced the percentage of medium and small molecular size. An explanation for the increase in large molecular size is that during the aging process, the polarity of asphaltene molecules increased due to oxidation; this led to the formation of the nano-agglomerates of asphaltene molecules (Noureldin & Wood, 1989). After the addition of rejuvenators, the value of LMS decreased for all rejuvenated samples compared to aged samples. The largest reduction was found for sample R, followed by sample W; both samples' LMS was even lower than the LMS of the unaged sample. In contrast, all rejuvenated samples increased both the MMS and SMS closer to that of the unaged sample. A study found that the GPC analysis of molecular size distribution has a linkage to the performance prediction in binder rheological properties (Shen et al., 2007).

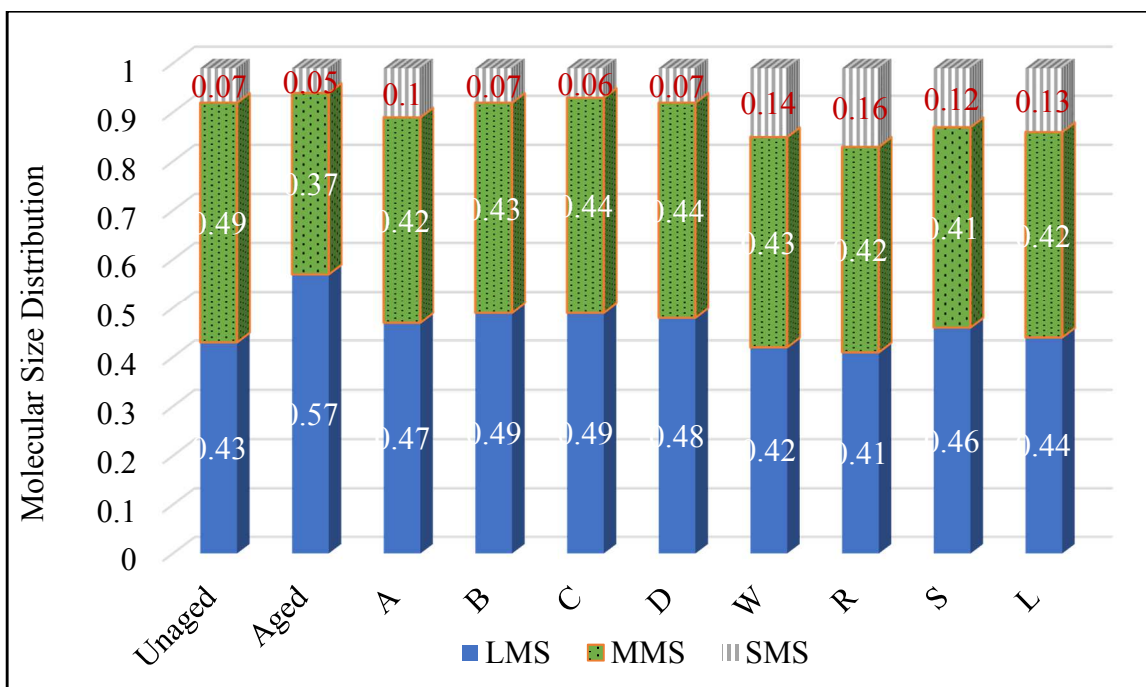


Figure 4-5 The Molecular Size Distribution of All Samples

4.4.2 Molecular Simulation Results

4.4.2.1 Average Aggregation Number

Figure 4-6 (a) shows the oxidized asphaltene and oxidized asphaltene plus rejuvenator A molecules average aggregation number. The initial data points (from 0 to 20ns) are the aggregation number of isolated oxidized asphaltene molecules. At 20 ns, two scenarios (with and without rejuvenator A molecules) start. As Figure 4-6 (a) shows, the addition of rejuvenator A molecules prevented an increase in the oxidized asphaltene molecules average aggregation number. This shows that rejuvenator A molecules have the ability to prevent the oxidized asphaltene molecules from stacking. At the final part of the simulation (after 35 ns), there is a reduction in nanoaggregates' size to a level lower than

that of isolated oxidized asphaltene molecules. This phenomenon shows that selected molecules from rejuvenator A have the potential of peptizing oxidized asphaltene and reducing the nanoaggregates' size, which was shown in Figure 4-6 (b).

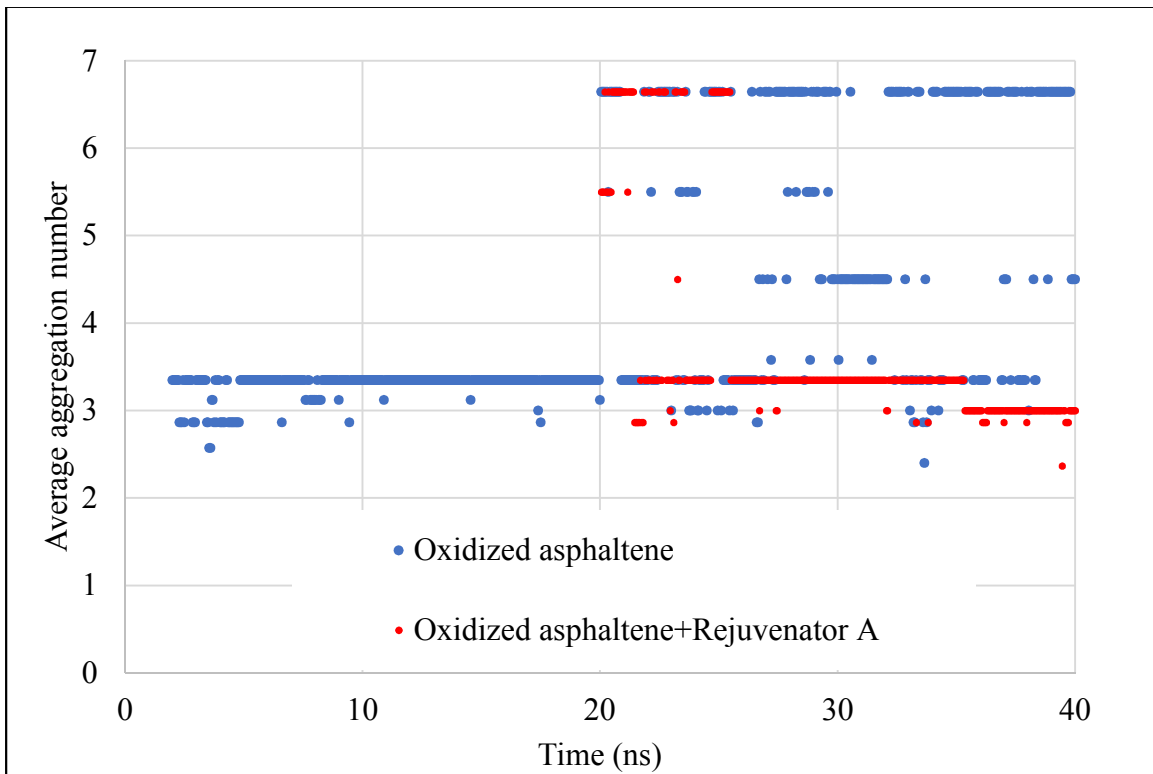


Figure 4-6 (a) Oxidized Asphaltene and Oxidized Asphaltene Plus Rejuvenator A Molecules Average Aggregation Number Plot

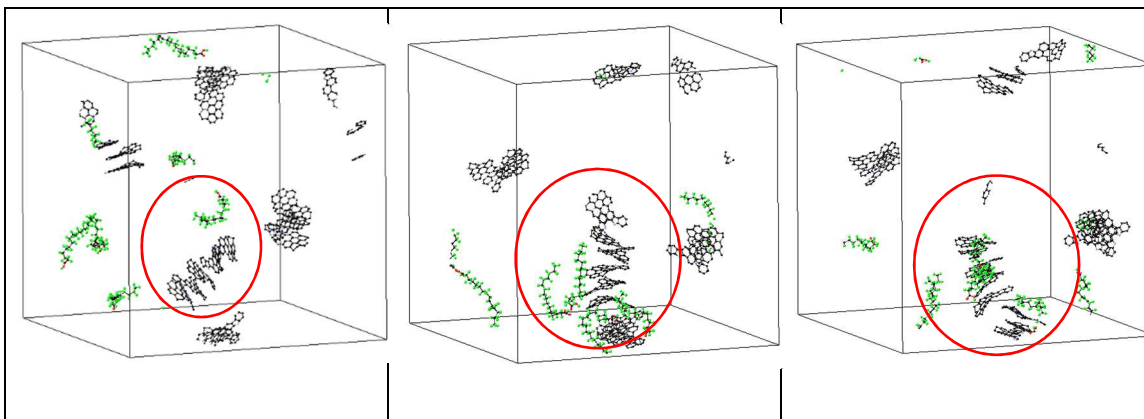


Figure 4-6 (b). Subsequent Snapshots Showing the Deagglomeration Process of Oxidized Asphaltene Molecules

4.4.2.2 Radial Distribution Function (RDF)

The average radial distribution function for the last 5 ns of the simulation was measured for the oxidized asphaltene molecules most-centered carbon atom; the results are presented in Figure 4-7. The RDF is a measure of separation of oxidized asphaltene molecules helps to comprehend the consequence of dopant molecules on the deagglomeration of asphaltenes. The results show that after the addition of rejuvenator A molecules, the intensity of RDF peaks decreased as a result of the interplay of rejuvenator A molecules and oxidized asphaltene molecules. The first peak at a distance range of 4-5 Å is reported to be associated with parallel stacking, while the peak at 7-8 Å is attributed to displaced and T-shaped stacking (Mousavi et al., 2016; Yaseen & Mansoori, 2018). This decreasing effect shows that rejuvenator A's molecules were able to reduce the self-assembly of oxidized asphaltenes, which can lead to a reduction of viscosity at a macro scale.

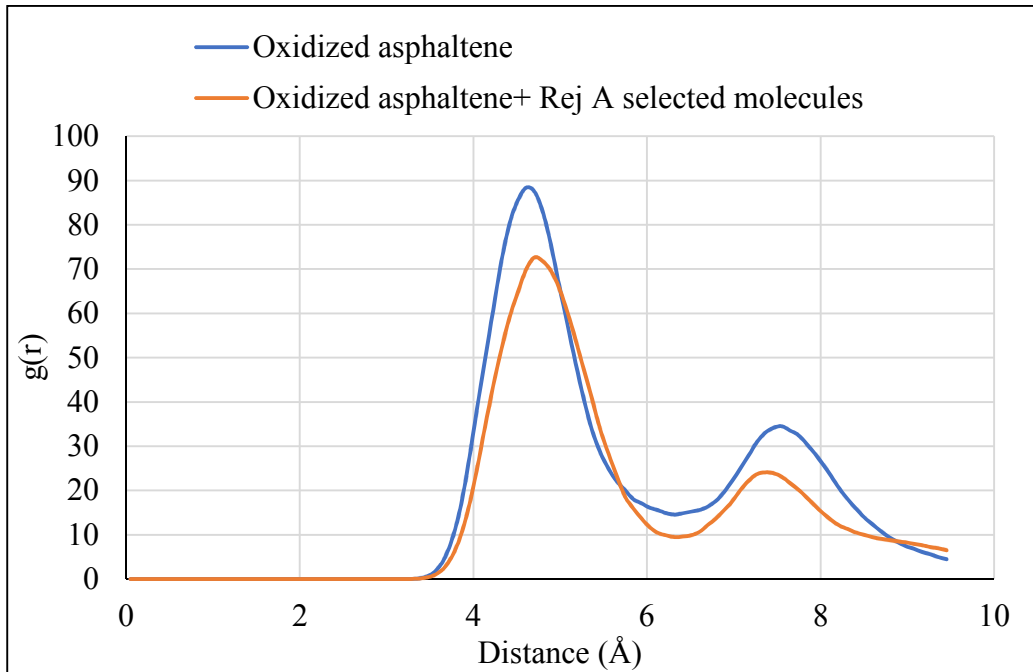


Figure 4-7 RDF Plot For the Last Five Seconds of the Simulation Shown in Figure 6 (a)

4.4.3 Mixture Test Results

4.4.3.1 Compaction Data Analysis

The measured number of gyrations, N , for compacting at 6.5% air void content needed to attain at the required gyratory height (180 mm) was recorded and shown in Table 4-10.

The control sample (without rejuvenator) required 25 gyrations, whereas the control +5% rejuvenator (rejuvenator A) samples required 18 gyrations to reach 180 mm. The rejuvenator was able to revitalize the binder in the mix, which is reflected by the smaller number of gyrations (for the same material weight) required to achieve the same compaction level. It showed that with the addition of 5% rejuvenator (by weight of total

binder), a 28% reduction in gyratory could be achieved to reach the same height of the specimen.

Table 4-10 Measured Number of Gyration for Mixture Samples

Sample	Height (mm)	Compaction number	% Reduction in compaction number
Control	180	25	-
Control + 5% Rej.	180	18	28%

4.4.3.2 Crack Propagation Rate Analysis Based on C* Fracture Test

Figure 4-8 shows a graph of C* versus the crack growth rate (a*). The higher the slope, the more energy needed for crack propagation. Figure 4-8 shows, the addition of the rejuvenator A yielded a higher slope (from 0.0019 to 0.0035), which indicates that more energy was needed to propagate the crack in the mix with rejuvenator.

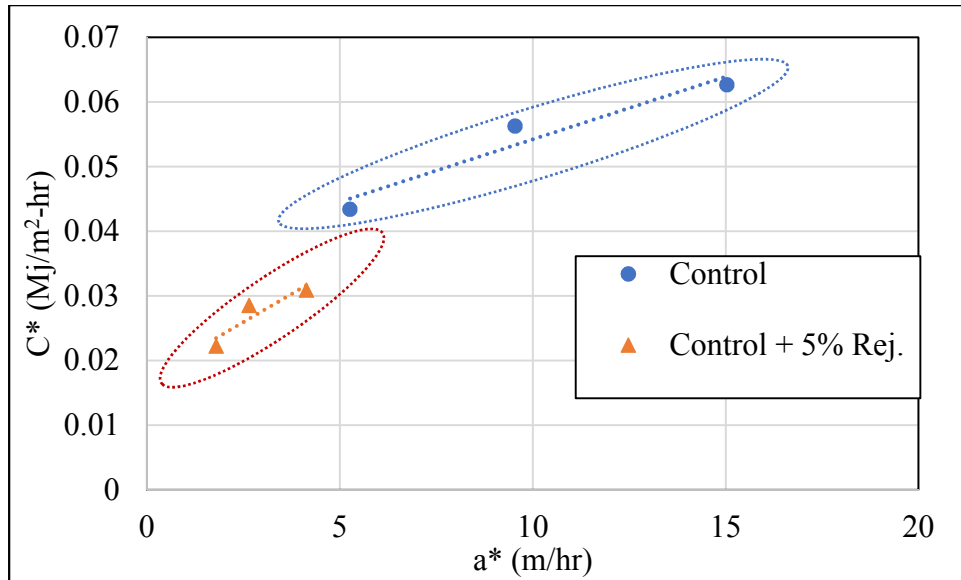


Figure 4-8 C* vs. Crack Growth Rate (a^*) Plot for Control and Control +5%Rej. Samples

4.4.3.3 Dynamic Shear Rheometer Results for RAP

The crossover modulus and frequency were determined for the extracted binder. It was found that with the addition of 5% rejuvenator A, the rejuvenated sample showed increased crossover modulus and frequency values, as shown in Table 4-11. The rejuvenator revitalized in both the control (25% RAP+75% PG 64-16) scenario and the extracted RAP (100% RAP) scenario. Since the dosages of rejuvenator were different for control (which has 20% rejuvenator only for RAP) and extracted RAP (5% rejuvenator), the increases in crossover modulus and frequency value for rejuvenated samples were different, which reflects the effectiveness of rejuvenator dosages. While a 5% dosage increased the crossover modulus about 40%, a 20% dosage increased it about 70%. It was

found that the rejuvenation efficiency in changing crossover modulus and frequency values was non-linear with the dosage of rejuvenator.

Table 4-11 Crossover Modulus and Frequency Values for Field Aged Samples

Crossover values	Control	Control +5% Rej. A	Extracted RAP	Extracted RAP +5% Rej. A
Modulus (kPa)	3,536	6,009	2,300	3,207
Frequency (Hz)	1.165	11.16	0.738	3.42
% Change				
Modulus (kPa)	-	69.91	-	39.44
Frequency (Hz)	-	900	-	363

4.5 Conclusion

This research explored the efficacy of various rejuvenators via laboratory experiments and modeling. The rheological characterization results, such as crossover modulus and frequency, indicated the source dependency of the effectiveness of the rejuvenator. While

some rejuvenators only softened the binder, others revitalized both the viscous and elastic components of the aged binder, which was shown with increased crossover modulus and crossover frequency values. The binder bond strength test results showed that the peak tensile strength of all specimens was reduced after water exposure; however, some rejuvenated binder samples showed more moisture susceptibility than others. The glass transition temperature (T_g) shifts to a higher value (less negative) after aging.

Rejuvenators were able to reduce T_g to be closer to that of the unaged binder. The SARA fraction and colloidal stability index results showed that some rejuvenators were able to restore the chemical balances of the aged asphalt closer to the levels of unaged asphalt.

The GPC results showed that aging of asphalt binder led to an increase in its large molecular size and that all rejuvenators successfully reduced the percentage of large molecular size. The percent reduction varied among rejuvenators, based on their compositions. Molecular simulation results indicated the selected molecules from rejuvenator A have the potential to peptize oxidized asphaltene and reduce the nano-aggregates' size. The effect of rejuvenators on mixture properties was reflected in a reduction of the number of gyratory compaction and a reduction in the crack propagation rate. The C^* fracture test indicated that samples containing rejuvenator have a lower crack propagation rate compared to their counterparts containing no rejuvenator. In conclusion, rejuvenator A met comprehensive rejuvenation measures by showing its interaction with aged asphaltene molecules leads to intercalation and separation of asphaltene nanoaggregates. Moreover, this molecular-level phenomenon of rejuvenator A

is reflected in two ways: an increase in crossover modulus and crossover frequency at the binder level, and a reduced crack propagation rate at the mixture level.

4.6 Acknowledgments

The authors acknowledge the support of the National Science Foundation (Award Numbers 1935723, and 1928795), which enabled the research. The authors would like to acknowledge the valuable help from Dr. Ramadan Salim, Daniel Oldham, Sk Faisal Kabir, and Samuel Brockman with ASU and Dr. Shahrzad Hosseinezhad with NC A&T State University.

4.7 References

- AASHTO-T315. (2012). Standard Method of Test for Determining the Rheological Properties of Asphalt Binder Using a Dynamic Shear Rheometer (DSR). *American Association of State Highway and Transportation Officials, Washington, DC.*
- AASHTO-TP91. (2015). Standard Method of Test for Determining Asphalt Binder Bond Strength by Means of the Binder Bond Strength (BBS) Test. *American Association of State Highway and Transportation Officials, Washington, DC.*
- Al-Qadi, I. L., Aurangzeb, Q., Carpenter, S. H., Pine, W. J., & Trepanier, J. (2012). *Impact of high RAP contents on structural and performance properties of asphalt mixtures* (0197-9191). Retrieved from
- ASTMD2872-12e1. (2012). Standard Test Method for Effect of Heat and Air on a Moving Film of Asphalt (Rolling Thin-Film Oven Test). *ASTM International, West Conshohocken, PA, 2012, www.astm.org.*
- ASTMD3279. (2007). Standard Test Method for n-Heptane Insolubles. *Annual Book of Standards.*
- ASTMD5404. (2017). Standard Practice for Recovery of Asphalt from Solution Using the Rotary Evaporator. *ASTM International, West Conshohocken, PA, 2017, www.astm.org.*
- ASTMD6521-13. (2013). Standard Practice for Accelerated Aging of Asphalt Binder Using a Pressurized Aging Vessel (PAV). *ASTM International, West Conshohocken, PA.*
- ASTMD6925-15. (2015). Standard Test Method for Preparation and Determination of the Relative Density of Asphalt Mix Specimens by Means of the Superpave Gyratory Compactor. *ASTM International, West Conshohocken, PA, 2015, www.astm.org.*
- ASTMD7175-15. (2015). Standard Test Method for Determining the Rheological Properties of Asphalt Binder Using a Dynamic Shear Rheometer. *ASTM International, West Conshohocken, PA, 2015, www.astm.org.*
- Begley, J., & Landes, J. (1972). The J integral as a fracture criterion *Fracture Toughness: Part II*: ASTM International.
- Bowers, B. F., Huang, B., & Shu, X. (2014). Refining laboratory procedure for artificial RAP: A comparative study. *Construction and building materials, 52*, 385-390.
- Cao, W., Wang, Y., & Wang, C. (2019). Fatigue characterization of bio-modified asphalt binders under various laboratory aging conditions. *Construction and building materials, 208*, 686-696.

- Cao, X., Wang, H., Cao, X., Sun, W., Zhu, H., & Tang, B. (2018). Investigation of rheological and chemical properties asphalt binder rejuvenated with waste vegetable oil. *Construction and building materials*, *180*, 455-463.
- Cavalli, M. C., Zaumanis, M., Mazza, E., Partl, M. N., & Poulidakos, L. D. (2018). Effect of ageing on the mechanical and chemical properties of binder from RAP treated with bio-based rejuvenators. *Composites Part B: Engineering*, *141*, 174-181.
- Dony, A., Ziyani, L., Drouadaine, I., Pouget, S., Faucon-Dumont, S., Simard, D., . . . Boulange, L. (2016). *MURE National Project: FTIR spectroscopy study to assess ageing of asphalt mixtures*. Paper presented at the Proceedings of the E&E congress.
- Elkashaf, M., Jones, D., Jiao, L., Williams, R. C., & Harvey, J. (2019). Using thermal analytical techniques to study rejuvenators and rejuvenated reclaimed asphalt pavement (RAP) binders. *Energy & Fuels*.
- Figuroa, A. S., Velasquez, R., Reyes, F. A., & Bahia, H. (2013). Effect of water conditioning for extended periods on the properties of asphalt binders. *Transportation Research Record*, *2372*(1), 34-45.
- Fini, E. H., Al-Qadi, I. L., Abu-Lebdeh, T., & Masson, J.-F. (2011). Use of surface energy to evaluate adhesion of bituminous crack sealants to aggregates. *American Journal of Engineering and Applied Sciences*, *4*(2).
- Haghshenas, H., Nabizadeh, H., Kim, Y.-R., & Santosh, K. (2016). Research on high-rap asphalt mixtures with rejuvenators and WMA additives.
- Kriz, P., Stastna, J., & Zanzotto, L. (2008). Glass transition and phase stability in asphalt binders. *Road Materials and Pavement Design*, *9*(sup1), 37-65.
- Li, D. D., & Greenfield, M. L. (2014). Chemical compositions of improved model asphalt systems for molecular simulations. *Fuel*, *115*, 347-356.
- Loeber, L., Muller, G., Morel, J., & Sutton, O. (1998). Bitumen in colloid science: a chemical, structural and rheological approach. *Fuel*, *77*(13), 1443-1450.
- Lu, X., & Isacson, U. (2002). Effect of ageing on bitumen chemistry and rheology. *Construction and building materials*, *16*(1), 15-22.
- Morgan, T., Alvarez-Rodriguez, P., George, A., Herod, A., & Kandiyoti, R. (2010). Characterization of Maya crude oil maltenes and asphaltenes in terms of structural parameters calculated from nuclear magnetic resonance (NMR) spectroscopy and laser desorption– mass spectroscopy (LD– MS). *Energy & Fuels*, *24*(7), 3977-3989.
- Mousavi, M., Pahlavan, F., Oldham, D., Hosseinneshad, S., & Fini, E. H. (2016). Multiscale investigation of oxidative aging in biomodified asphalt binder. *The Journal of Physical Chemistry C*, *120*(31), 17224-17233.

- Nayak, P., & Sahoo, U. C. (2017). Rheological, chemical and thermal investigations on an aged binder rejuvenated with two non-edible oils. *Road Materials and Pavement Design*, 18(3), 612-629.
- Noureldin, A. S., & Wood, L. E. (1989). Variations in molecular size distribution of virgin and recycled asphalt binders associated with aging. *Transportation Research Record*(1228).
- Oldham, D. J., Rajib, A. I., Onochie, A., & Fini, E. H. (2019). Durability of bio-modified recycled asphalt shingles exposed to oxidation aging and extended sub-zero conditioning. *Construction and building materials*, 208, 543-553.
doi:<https://doi.org/10.1016/j.conbuildmat.2019.03.017>
- Puello, J., Afanasjeva, N., & Alvarez, M. (2013). Thermal properties and chemical composition of bituminous materials exposed to accelerated ageing. *Road Materials and Pavement Design*, 14(2), 278-288.
- Qin, Q., Schabron, J. F., Boysen, R. B., & Farrar, M. J. (2014). Field aging effect on chemistry and rheology of asphalt binders and rheological predictions for field aging. *Fuel*, 121, 86-94.
- Rice, J. R. (1968). A path independent integral and the approximate analysis of strain concentration by notches and cracks. *Journal of applied mechanics*, 35(2), 379-386.
- Samieadel, A., Høgsaa, B., & Fini, E. H. (2018). Examining the Implications of Wax-Based Additives on the Sustainability of Construction Practices: Multiscale Characterization of Wax-Doped Aged Asphalt Binder. *ACS Sustainable Chemistry & Engineering*, 7(3), 2943-2954.
- Samieadel, A., Høgsaa, B., & Fini, E. H. (2019). *Investigation of Thermo-Mechanical Characteristics of Wax-doped Aged Asphalt Binder*. Retrieved from
- Shen, J., Amirhanian, S., & Tang, B. (2007). Effects of rejuvenator on performance-based properties of rejuvenated asphalt binder and mixtures. *Construction and building materials*, 21(5), 958-964.
- Shen, J., Amirhanian, S. N., & Lee, S.-J. (2007). HP-GPC characterization of rejuvenated aged CRM binders. *Journal of Materials in Civil Engineering*, 19(6), 515-522.
- Stempihar, J., & Kaloush, K. (2017). A Notched Disk Crack Propagation Test for Asphalt Concrete. *MOJ Civil Eng*, 3(5), 00084.
- Sun, H., Mumby, S. J., Maple, J. R., & Hagler, A. T. (1994). An ab initio CFF93 all-atom force field for polycarbonates. *Journal of the American Chemical society*, 116(7), 2978-2987.

- Tran, N. H., Taylor, A., & Willis, R. (2012). Effect of rejuvenator on performance properties of HMA mixtures with high RAP and RAS contents. *NCAT Report*, 12-05.
- Ungerer, P., Rigby, D., Leblanc, B., & Yiannourakou, M. (2014). Sensitivity of the aggregation behaviour of asphaltenes to molecular weight and structure using molecular dynamics. *Molecular Simulation*, 40(1-3), 115-122.
- Waldman, M., & Hagler, A. T. (1993). New combining rules for rare gas van der Waals parameters. *Journal of Computational Chemistry*, 14(9), 1077-1084.
- West, R. C., Willis, J. R., & Marasteanu, M. O. (2013). *Improved mix design, evaluation, and materials management practices for hot mix asphalt with high reclaimed asphalt pavement content* (Vol. 752): Transportation Research Board.
- Wiehe, I. A. (2008). *Process chemistry of petroleum macromolecules*: CRC press.
- Yaseen, S., & Mansoori, G. A. (2018). Asphaltene aggregation due to waterflooding (A molecular dynamics study). *Journal of Petroleum Science and Engineering*, 170, 177-183.
- Zaumanis, M., & Mallick, R. B. (2015). Review of very high-content reclaimed asphalt use in plant-produced pavements: state of the art. *International Journal of Pavement Engineering*, 16(1), 39-55.
- Zhang, R., You, Z., Wang, H., Chen, X., Si, C., & Peng, C. (2018). Using bio-based rejuvenator derived from waste wood to recycle old asphalt. *Construction and building materials*, 189, 568-575.
- Zhang, R., You, Z., Wang, H., Ye, M., Yap, Y. K., & Si, C. (2019). The impact of bio-oil as rejuvenator for aged asphalt binder. *Construction and building materials*, 196, 134-143.
- Zhu, H., Xu, G., Gong, M., & Yang, J. (2017). Recycling long-term-aged asphalts using bio-binder/plasticizer-based rejuvenator. *Construction and building materials*, 147, 117-129.

CHAPTER 5 INVESTIGATING MOLECULAR-LEVEL FACTORS THAT AFFECT THE DURABILITY OF RESTORED AGED ASPHALT BINDER

A version of this paper published in the Journal of Cleaner Production

Rajib, A. I., Pahlavan, F., & Fini, E. H. (2020). Investigating Molecular-Level Factors That Affect the Durability of Restored Aged Asphalt Binder. *Journal of Cleaner Production*, 122501.

5.1 Abstract

This paper examines the durability of restored aged asphalt in terms of its susceptibility to moisture and aging. The study is motivated by the increasing use of modifiers called rejuvenators that are added to paving mixtures containing reclaimed asphalt pavements to restore the original rheological properties of asphalt binder that have been lost during service life. Although several test methods have been proposed to quantify the restoration capability of rejuvenators, not much attention has been given to the side-effects that the rejuvenators may impart to the resulting mix. Due to the specific chemical composition of certain rejuvenators, they may negatively impact the durability of the mixture, especially pertaining to its resistance to moisture damage and aging. This paper examines several rejuvenators that are all effective at restoring aged asphalt binder's rheological properties, to highlight plausible side effects that may be overlooked when selection criteria are based solely on the restoration capacity of rejuvenators. Our laboratory experiments and computational analysis geared toward the use of rheometry and density functional theory

showed that while all studied rejuvenators restored the rheological properties of aged asphalt binders, they had very different durability in terms of resistance to aging and moisture damage. Results obtained from the dynamic shear rheometer showed the rejuvenators with the highest restoration capacity did not have the best durability. Computational analysis showed that while the restoration capacity of rejuvenators is related to their penetration into and peptizing of asphaltene nanoaggregates, durability is mainly related to their polarizability values. Rejuvenators with lower polarizability showed better resistance to aging and moisture damage. The outcome of the study enables additive manufacturers and formulators to produce effective rejuvenators without compromising the long-term durability of restored asphalt binder. It also helps road authorities develop selection metrics that account for durability along with rheological properties, to prevent non-durable rejuvenators from entering the market. Accordingly, the study results promote recycling and resource conservation by providing an in-depth understanding of the relation between rejuvenators' chemical structure and the durability of restored aged asphalt binder.

Keywords: Durability, rheology, polarizability, moisture damage, aging, restoration, rejuvenation

5.2 Introduction

Many rejuvenators have been found to be promising at revitalizing the properties of aged asphalt binder (Oldham et al., 2019; Pahlavan et al., 2019). Therefore, their use is

becoming more prevalent in the asphalt industry to facilitate the use of a high content of reclaimed asphalt pavement (RAP) and recycled asphalt shingles (RAS). Studies show that rejuvenators produced from different sources perform differently; the efficacy of a rejuvenator depends on its source and chemical composition (Fini et al., 2017; Haghshenas et al., 2016). Moreover, the performance of a rejuvenator depends on the method of incorporating it into the binder (Ma et al., 2020). Bio-based modifiers have been shown to be effective candidates to rejuvenate aged asphalt binder (Cao et al., 2018; Cavalli et al., 2018; Oldham et al., 2015). In addition, considering that most bio-based modifiers are made from waste biomass, their use has additional economic and environmental benefits (Hajj et al., 2009; NAPA, 2016; Oldham et al., 2019; Zhou et al., 2020). Revitalizing aged asphalt binder's properties required a lower dose of bio-modifiers produced from organic sources (waste vegetable oil, organic oil, or tall oil) compared to a modifier based on petroleum (waste engine oil) (Zaumanis et al., 2015). A comparison between the efficacy of waste cooking oil and waste engine oil showed waste cooking oil can restore aged asphalt binder's original rheological properties more effectively (Li et al., 2019). Adding bio-oil derived from waste wood chips to aged asphalt binder showed an increase in viscous components and a decrease in stiffness (Zhang et al., 2018). Also, introducing bio-oil from sawdust improved aged asphalt binder's resistance to cracking at low temperature (Zhang et al., 2019). Bio-binder produced from swine manure has been shown to improve the cracking resistance of asphalt binder and improve the low-temperature performance of bio-asphalt mixtures

(Hill et al., 2013; Oldham et al., 2019). Improved cracking resistance was also achieved by adding waste cooking oil to aged asphalt binder (Ahmed & Hossain, 2020). A bio-rejuvenator produced from swine manure was found to restore the thermo-mechanical properties of aged asphalt by disrupting the strong molecular interactions between oxidized asphaltene molecules (Pahlavan et al., 2018). The restoration was more noticeable when a hybrid bio-rejuvenator produced from algae and swine manure was used, further promoting the deagglomeration of oxidized asphaltenes (Pahlavan et al., 2019). Although there has been extensive research showing the capacity of rejuvenators to restore the properties of aged asphalt, little research has been done to evaluate rejuvenators' plausible negative side effects, especially on pavement durability. Therefore, it is necessary to evaluate rejuvenators not only on their rheological restoration capacity but also on their effect on the durability of pavement, including resistance to damage from moisture and aging.

Moisture can cause serious damage to asphalt mixtures by promoting adhesion and cohesion failure. Considering that some of the above highly effective rejuvenators contain hydrophilic and water-soluble compounds, their introduction to asphalt may increase its propensity to moisture damage. For instance, it has been shown that the bio-rejuvenator derived from waste cooking oil is effective at restoring the rheological properties of aged asphalt binder (Ahmed & Hossain, 2020), but it also makes asphalt binder highly susceptible to moisture damage (Hosseinnezhad et al., 2019).

A study performed on a mixture containing RAP and a bio-rejuvenator made from a natural plant extract showed improved resistance to moisture damage, as indicated by increases in the storage-modulus ratio and loss-modulus ratio of moisture-conditioned samples (Hajj et al., 2013). In another study, three rejuvenators (naphthene-based, liquid plant-based, or made from waste cooking oil) were tested as modifiers to a mixture containing a high RAP content; all three were effective in revitalizing the original mechanical properties of the asphalt mixture, but they negatively affected the resistance of the asphalt mixture to moisture damage, as evidenced by a reduction in indirect tensile strength (Ziari et al., 2019).

Therefore, it is not adequate to qualify rejuvenators solely on their capacity to restore the original rheological properties of aged asphalt binder. Depending on their chemical compositions, rejuvenators can impart unwanted properties that can negatively impact the performance of the asphalt mixture. For example, many rejuvenators produced from different biomasses are quite promising in restoring the original physicochemical and rheological properties of aged asphalt binder, but they may reduce the resulting mixtures' resistance to moisture damage. The reduced resistance to moisture damage is attributed to the rejuvenators having highly polarizable water-soluble constituents. The same problem applies to the aging trajectory of rejuvenated bitumen, with some rejuvenators being too susceptible to oxidation. A study by Hosseinnezhad et al. showed that bio-modifiers' resistance to aging is highly source-dependent (Fini et al., 2017; Hosseinnezhad et al., 2019; Zadshir et al., 2018).

The effect of ultraviolet (UV) exposure on bitumen has been studied by placing a thin layer of bitumen in a UV chamber for different durations and studying the evolution of the bitumen's physicochemical properties (Hosseinnezhad et al., 2019; Hung et al., 2019; Zadshir et al., 2019). Researchers have also studied the role of UV aging on a loose asphalt mixture by placing the loose bituminous mixture in a UV chamber for 7, 14, or 28 days (Li et al., 2020). After the UV aging, the binder was extracted and recovered from the asphalt mixture to examine the binder's physical, rheological, and self-healing properties (Li et al., 2020). It has been documented that the composition of asphalt highly affects its long-term durability (Fini et al., 2020). Considering the variations in the chemical composition of rejuvenators, the durability of restored aged asphalt binder is hypothesized to vary regardless of the rejuvenators' capacity to restore the rheological properties of asphalt binder. Accordingly, it is crucial to provide an in-depth understanding of the factors affecting the durability of restored aged asphalt, to prevent non-durable rejuvenators from entering the market and compromising pavement's long-term performance. This study compares the durability of three rejuvenators that are highly effective at restoring the rheological properties of aged asphalt binder. The durability qualification test was performed after specimens were exposed to extensive moisture conditioning and ultraviolet (UV) aging. The study further relates the durability of restored aged asphalt binder to molecular-level indicators using quantum-level calculations via density functional theory analysis.

5.3 Experiment Plan

Figure 5-1 shows the detailed experiment plan including binder-level tests, mixture tests, and computational modeling. The test methods are described in later sections.

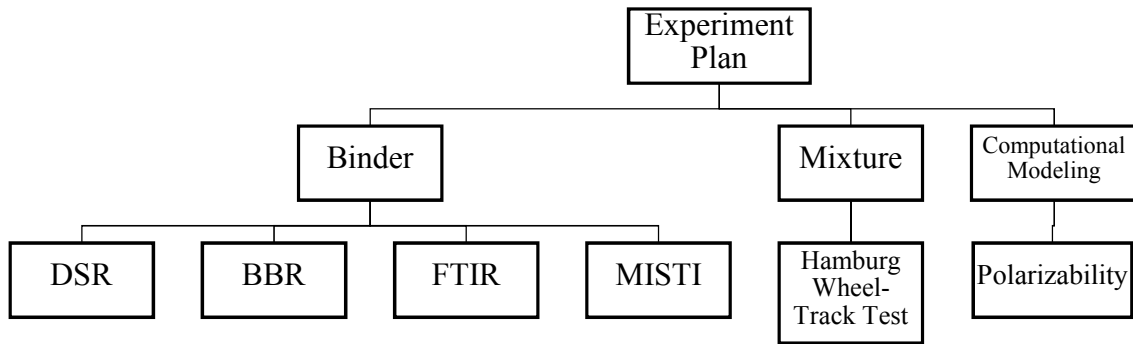


Figure 5-1 Experiment Plan of the Study

5.4 Materials and Methods

The City of Phoenix (Arizona) provided an asphalt mixture sample (described in a later section) containing 25% RAP. The binder was extracted and recovered following (ASTMD5404, 2017). First, the loose mixture was placed in a centrifuge bowl and dissolved in trichloroethylene solvent for 60 minutes, to allow the solvent to extract the binder. Next, the centrifuge machine was used to extract all the binder with solvent from the bowl. After that, the binder was recovered from the solvent using RotoVap equipment. The binder (25% RAP and 75% PG 64-16 virgin binder) extracted and recovered from the mixture was designated as the control specimen and labeled as CN for binder-level tests. The properties of PG 64-16 asphalt are given in Table 5-1-a. To make

the rejuvenated samples, the binder was heated at 135°C for 30 minutes to ensure it was sufficiently liquid, then each of the three rejuvenators was separately added to the binder at 5% by weight of binder and mixed by hand with a spatula for 5 minutes. The rejuvenated samples were labeled based on the origin of their rejuvenator: Rej-AI, made from a plant extract; Rej-SO, made from soy oil; and Rej-Swilgae, made from a co-liquefied 1:1 ratio (by weight) of swine manure and algae bio-oil. The properties of the rejuvenator samples are shown in Table 5-1-b.

Table 5-1 General Asphalt Binder Properties for PG 64-16 Used in this Study

Specific Gravity @15.6 °C	1.022
Flash point °C	>230
Mass change after RTFO	-0.106
Apparent Viscosity @ 135 °C, Pa.s	0.428
Stiffness (MPa) @-6°C @ 60s	117.0

Table 5-2 Description of Rejuvenated Samples

Sample	Saturates (%)	Aromatics (%)	Resin (%)	Asphaltene (%)	Molecules present in the sample (GC-MS)
Rej-AI	0.44	72.49	26.36	0.71	9,12-Octadecadienoic acid, n-Hexadecanoic acid,

					Octadecanoic acid, Hexadecanoic acid, ethyl ester,
Rej-SO	1.45	89.16	8.57	0.82	Linoelaidic acid, Decadienal
Rej-Swilgae	0.83	0.25	72.7	26.25	p-Cresol, Phenol, 1-Ethyl-2-pyrrolidinone

5.4.1 Preparation of Mixture Samples Containing RAP

The asphalt mixture containing RAP was collected from the City of Phoenix (Arizona) plant. The mixture has a nominal maximum aggregate size of $\frac{3}{4}$ inch, and it contains 25% RAP and 75% PG 64-16 virgin binder. The amount of binder content was 5% by weight of the mixture. This mixture sample was designated as the control sample and labeled as CN-Mix. The rejuvenated mixture samples were prepared by spraying the rejuvenator (5% by weight of total binder content) on the control sample (CN-Mix). The rejuvenated mixture samples were prepared using each of the rejuvenators and labeled as Rej-Al-Mix, Rej-SO-Mix, and Rej-Swilgae-Mix.

5.4.2 Compaction Procedure

The loose mixture aggregates were heated to the compaction temperature of 144°C and kept in the oven at 144°C for 2 hours. After that, they were compacted using a Servopac Superpave Gyrotory (SSG) compactor to a diameter of 150 mm and a fixed height of 60

mm, by following (ASTMD6925-15, 2015). The applied pressure was 600 kPa with a gyration angle of 1.16° and a gyration speed of 30 gyrations per minute.

5.4.3 Ultraviolet Aging Procedure and Extraction of Rejuvenated RAP Containing Binder

After the Hamburg wheel-track test (described in a later section), the samples were heated at 135°C for 30 min and specimens were dismantled to a loose mix. 500 gm of loose bituminous mixtures from each sample were placed in pans to develop a 2 cm thickness and placed in a UV-aging simulation chamber for 50 hours, 100 hours, or 200 hours, following the method used by (Li et al., 2020). The UV irradiation intensity of the UV chamber was 1.45 w/m^2 . The mixture aggregates were mixed every 24 h during the process of UV aging. After the UV aging, the binder was extracted and recovered from the loose aggregate according to the process described earlier. The recovered binder from each sample with the different aging conditions was used in Fourier Transform Infrared (FTIR) spectroscopy analysis.

5.4.4 Dynamic Shear Rheometer (DSR)

An Anton Paar Modular Compact Rheometer MCR 302 was used to measure the elastic and viscous behavior of each sample (aged asphalt and rejuvenated asphalt) following (ASTMD7175-15, 2015). The test was conducted at 0.1% strain rate and frequency ranging from 0.1 to 100 rad/s using an 8mm parallel plate. The test was performed at a temperature ranging from 10°C to 50°C . From the measured data, the complex shear modulus (G^*) and phase angle (δ) were calculated using Equation 5-1.

$$G^* = \frac{\tau_{\max}}{\gamma_{\max}} \quad (5-1)$$

in which $\tau_{\max} = \frac{2T}{\pi r^3}$ and $\gamma_{\max} = \left(\frac{\theta r}{h} \right)$

γ_{\max} = maximum strain

τ_{\max} = maximum stress

T = maximum applied torque

r = radius of the sample

θ = deflection (rotational) angle

h = height of the sample

Using the time-temperature superposition method, master curves were developed by shifting the complex modulus and phase angle data to a reference temperature of 30°C. The corresponding elastic modulus (G') and viscous modulus (G'') results were calculated to determine the crossover values (the frequency at which G' is equal to G'') at 20°C.

5.4.5 Multiple-Stress Creep Recovery (MSCR) Test

The MSCR test was performed using an Anton Paar Modular Compact Rheometer MCR 302 with a 25 mm parallel plate spindle and at a temperature of 64°C, following (ASTMD7405-15, 2015). During this test, the asphalt binder is subjected to repeated

cycles of shear creep and recovery. The strain accumulation is tracked during repeated cycles of 1s creep loading and 9s recovery period. In this study, the accumulated strain versus the number of cycles was used to compare aged and rejuvenated specimens in terms of their strain recovery, as an indirect measure of their potential healing capacity.

5.4.6 Bending Beam Rheometer (BBR)

The creep stiffness (S) and stress relaxation capacity (m-value) at low temperature were measured for all samples through a three-point bending test using a bending beam rheometer, following (ASTMD6648-08, 2016). The test was conducted at -6°C, which is 10 degrees higher than the binder's original low grade of -16°C, to follow the standard. The stiffness and m-value were calculated using Equations 5-2 and 5-3, respectively.

$$S(t) = \frac{PL^3}{4bh^3 \delta(t)} \quad (5-2)$$

$$m(t) = \left| d \log[S(t)] / d \log(t) \right| = \left[B + 2C \log(t) \right] \quad (5-3)$$

where:

S(t) = stiffness at time t

$\delta(t)$ = deflection at time t

t = loading time

P = a constant load (0.98 N)

L = c/c distance between beam supports (102 mm)

b = beam width (12.7 mm)

h = beam thickness (6.25 mm)

B, C = regression coefficients

Delta T_c, a measure of the difference between the two critical low temperatures based on stiffness and m-value criteria, was determined in addition to the stiffness and m-value measurements. The two temperatures were determined to meet the specimen's grade requirement for a stiffness of 300 MPa and m-value of 0.3. The ΔT_c was calculated using Equation 5-4. To calculate the two temperatures, the samples were tested at -6°C and at -18°C to capture stiffness being above and below 300 MPa and m-value above and below 0.3. After that, the corresponding critical temperatures were determined by interpolation and using Equations 5-5 and 5-6.

$$\Delta T_c = T_c (\text{Stiffness}) - T_c (\text{m-Value}) \quad (5-4)$$

$$T_c (\text{Stiffness}) = T_1 + \left(\frac{(T_1 - T_2) * (\text{Log}300 - \text{Log}S_1)}{\text{Log}S_1 - \text{Log}S_2} \right) \quad (5-5)$$

$$T_c (m) = T_1 + \left(\frac{(T_1 - T_2) * (0.300 - m_1)}{m_1 - m_2} \right) \quad (5-6)$$

5.4.7 Fourier Transform Infrared (FTIR) Spectroscopy

A Bruker FT-IR spectrometer was used to characterize the functional groups of samples subjected to different UV aging levels. Before starting the test, the FTIR diamond crystal surface was cleaned with isopropanol. The background spectra were collected and

subtracted from the sample spectra. Each FTIR spectrum was collected from 400 to 4000 cm^{-1} wavenumbers with a resolution of 4 cm^{-1} and 32 scans. OMNIC software was used to analyze the peaks and estimate the area under the peaks.

5.4.8 Hamburg Wheel -Tracking Test

A Hamburg wheel-tracking device was used following (AASHTO-T324-16, 2016) to measure the rutting and moisture susceptibility of each specimen. Two specimens (150 mm diameter and 60 mm height with an air void of 7.0 ± 0.5 percent) were prepared for each scenario. These specimens were submerged in water at 60°C and subjected to 52 steel-wheel passes per minute. The test continued until either the vertical deformation under the wheel reached 20 mm or the number of wheel passes reached 20,000 passes. From the deformation data collected as a function of the number of wheel passes, the following parameters were calculated:

- The "creep slope" is the slope at the creep stage, which is related to rutting resistance.
- The "stripping slope" is the slope at the stripping stage, which is related to moisture damage.
- The "stripping inflection point" indicates the onset of moisture damage. It is the intersection of the creep slope and stripping slope regression lines.

In this study, the Troxler PMW Hamburg Wheel Tracker device was used.

5.4.9 Moisture-Induced Shear-Thinning Index (MISTI)

The Moisture-Induced Shear-Thinning Index (MISTI) is a newly developed test that specifically characterizes the susceptibility of a bitumen-stone interface to moisture damage. To create a repeatable test that is based on a fundamental material property and properly decouples chemistry-driven moisture-damage mechanisms from other concurrent phenomena such as oxidation, the interface of bitumen and stone was recreated by introducing glass beads (100 microns in diameter) into bitumen at a 1:2 weight ratio of glass beads to bitumen. Ten specimens (0.3 g each) were prepared and cast in 8-mm silicon molds; five were placed in room conditions and the other five were water conditioned for 24hr at 60°C. Figure 5-2 shows the glass beads and samples before and after water conditioning. It was observed that after 24 hr water conditioning, the sample swelled up on top, as seen in Figure 5-2. Each specimen was surface-dried and subjected to a shear sweep test (0.1 to 100 1/sec) at 64°C. The viscosity corresponding to each shear rate was calculated, and the MISTI was determined using Equation 5-7.

$$\text{MISTI} = \frac{\text{Average Slope (Viscosity vs Shear rate) of Wet Specimen}}{\text{Average Slope (Viscosity vs Shear rate) of Dry Specimen}} \quad (5-7)$$

$$\text{Viscosity} = (\text{shear strain}) / (\text{shear rate})$$



Figure 5-2 (Left) Glass Beads Used to Mix with Bitumen; (Middle) Sample Before Water Conditioning; (Right) Sample after Water Conditioning

5.4.10 Computational Modeling Using Density Functional Theory (DFT)

Theoretical calculations were performed using a density functional approach embedded in the Gaussian 09 package (Frisch et al., 2014). A combination of Becke's three-parameter hybrid exchange functional and the Lee-Yang-Parr correlation functional (B3LYP) (Becke et al., 1988) were used as the functional. In the theoretical part of the study, we deal with the characterization of the polarizability parameter as a chemical descriptor to show the "durability" of compounds in three different rejuvenators (Rej-Al, Rej-SO, and Rej-Swilgae) toward post-rejuvenation chemical and physical changes, including moisture damage and oxidative aging. Polarizability (α) was calculated for the rejuvenator components at the B3LYP/6-311G* level in terms of its x, y, z components, as shown in Equation 5-8.

$$\langle \alpha \rangle = \frac{1}{3} [\alpha_{xx} + \alpha_{yy} + \alpha_{zz}] \quad (5-8)$$

5.5 Results and Discussion

5.5.1 Dynamic Shear Rheometer (DSR) Test

Figure 5-3 shows the complex modulus versus frequency master curves for all samples.

Figure 5-3 shows that the control sample has the highest stiffness, indicated by the highest complex modulus value. All the rejuvenated samples reduced the stiffness, especially at low frequency (i.e., high temperature). The sample modified with rejuvenator Rej-A1 showed the highest reduction in complex modulus, followed by Rej-SO and Rej-Swilgae. Figure 4 shows the graphs of the phase angle versus the reduced frequency. The control had the lowest phase-angle value, and Rej-A1 performed best at increasing the phase angle. Like the complex modulus graphs, Rej-SO outperformed Rej-Swilgae at increasing the phase-angle value.

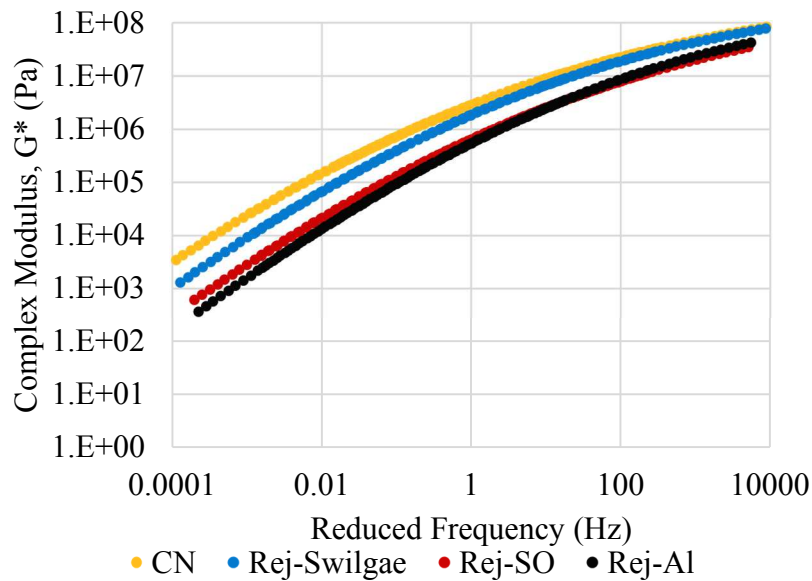


Figure 5-3 Complex Modulus Master Curves

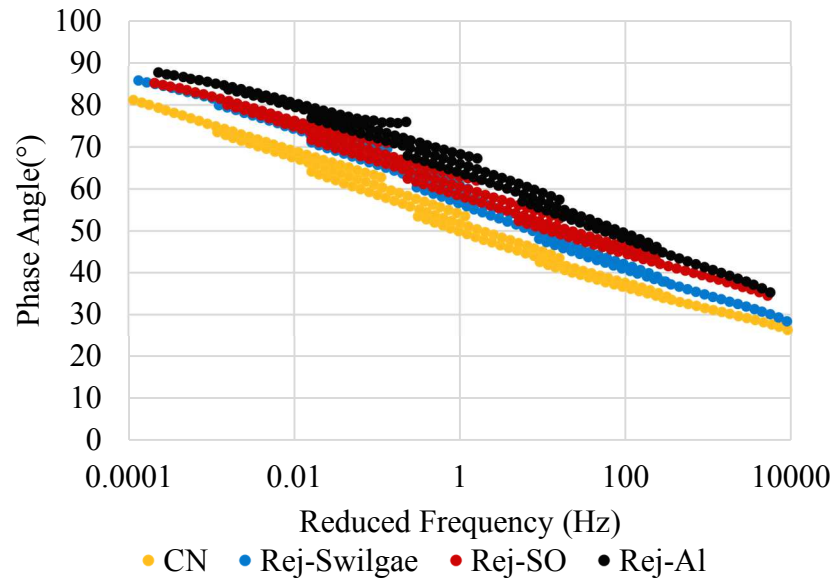


Figure 5-4 Graphs of Phase-Angle Value Versus Reduced Frequency

These graphs show the rejuvenators' efficacy in softening the stiff control sample containing RAP. Moreover, they were able to increase the phase-angle value. To justify their rejuvenation efficiency, the crossover-modulus values were calculated and are graphed in Figure 5-5.

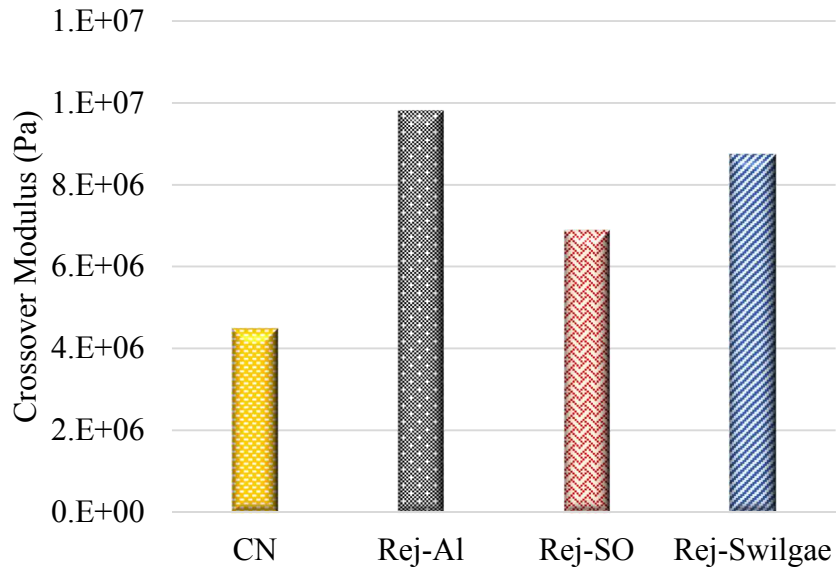


Figure 5-5 Crossover-Modulus Values for All Samples

The crossover modulus is where the viscous modulus and elastic modulus cross, making the loss factor equal to 1. A high crossover modulus value indicates the impact of a rejuvenator in both the viscous and elastic properties of stiff asphalt. The crossover modulus value for the control sample was the lowest, while Rej-Al had the highest crossover modulus value. Rej-Al increased the crossover modulus value by up to 118%. Surprisingly, Rej-Swilgae had a higher crossover modulus value compared to Rej-SO, while Rej-SO performed better in reducing the stiffness of the sample. From this analysis, Rej-Swilgae better improved both the viscous and elastic properties of the control sample, while Rej-SO was better at making the sample softer.

In addition to the crossover modulus, crossover-frequency values for all samples are graphed in Figure 5-6. Like the crossover-modulus value, a high crossover-frequency

value is good for better rejuvenation efficacy, since a high crossover-frequency value indicates improved relaxation properties of the sample. Figure 5-6 shows significant crossover-frequency increases with the addition of rejuvenators. The highest increase was found for sample Rej-AI, followed by Rej-SO and then Rej-Swilgae.

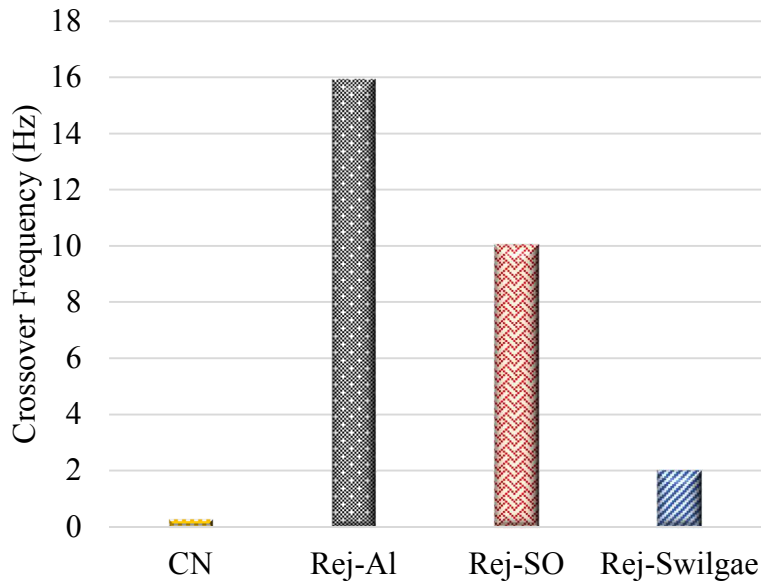


Figure 5-6 Crossover Frequency for All Samples

5.5.2 Multiple-Stress Creep Recovery (MSCR) Test

The MSCR test was conducted for all samples. Figure 5-7 shows the shear strain versus the time (from 200 cycles to 300 cycles). During this test, the asphalt binder is subjected to repeated cycles of shear creep and recovery. In this study, the accumulated strain versus the number of cycles was used to compare aged specimens and rejuvenated specimens in terms of their strain recovery, as an indirect measure of their potential

healing capacity. From Figure 5-7, the Rej-Al sample showed the highest shear strain (%) accumulation compared to all samples. At time step 300 s, the Rej-Al sample value of shear strain accumulation was more than 7 times higher than the value for the control sample. Rej-SO and Rej-Swilgae respectively showed 5 times and 2 times higher shear strain accumulation compared to the control sample. This result suggests that the rejuvenators reduced the elastic component of the specimen and made the sample more viscous. Hence, the rejuvenated samples became softer, accumulated larger strain, and showed lower recovery compared to the control (stiff) sample.

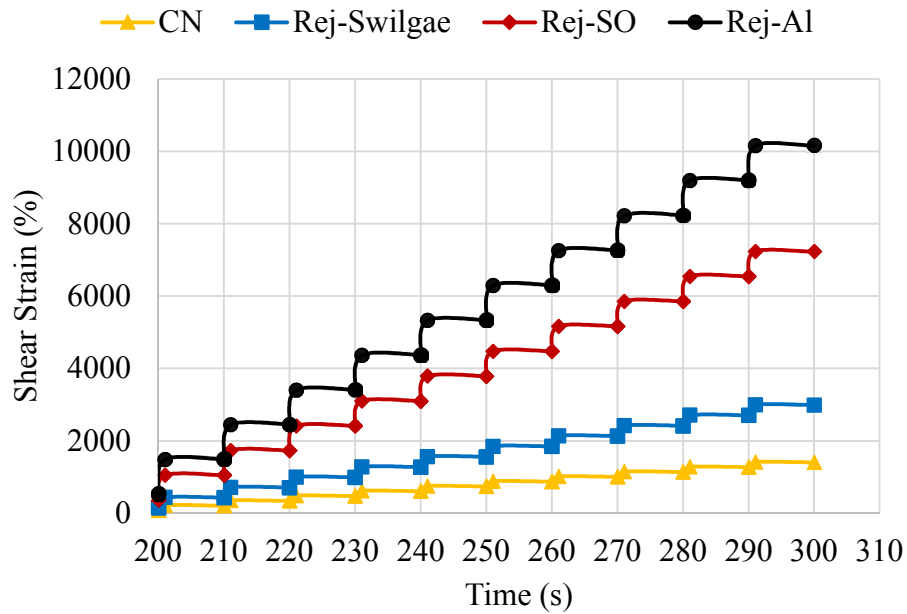


Figure 5-7 Shear Strain Versus Time at 3.2 kPa

5.5.3 Bending Beam Rheometer Test

The low-temperature cracking resistance of all rejuvenated samples was measured by measuring the deflection of the samples at -6°C . The stiffness and m-value were calculated and plotted in Figure 5-8 (a, b). Figure 5-8 (a, b) shows that all rejuvenated samples were able to have lower stiffness and higher m-values compared to the control sample. All rejuvenated samples meet the stiffness and m-value criteria at -6°C , whereas the control sample failed the m-value criterion. Among all samples, Rej-SO showed the lowest stiffness and highest m-value, meaning Rej-SO performed better at controlling the stiffening effect and stress relaxation properties of the binder. A similar trend in results was found by the addition of a bio-rejuvenator to recycled asphalt shingles (RAS), where bio-modified RAS showed lower stiffness and a higher m-value compared to non-modified RAS (Oldham et al., 2019).

In addition to low-temperature stiffness and the m-value measurement, the effect of each rejuvenator was further examined by calculating ΔT_c using Equation 5-4. The results are graphed in Figure 5-9.

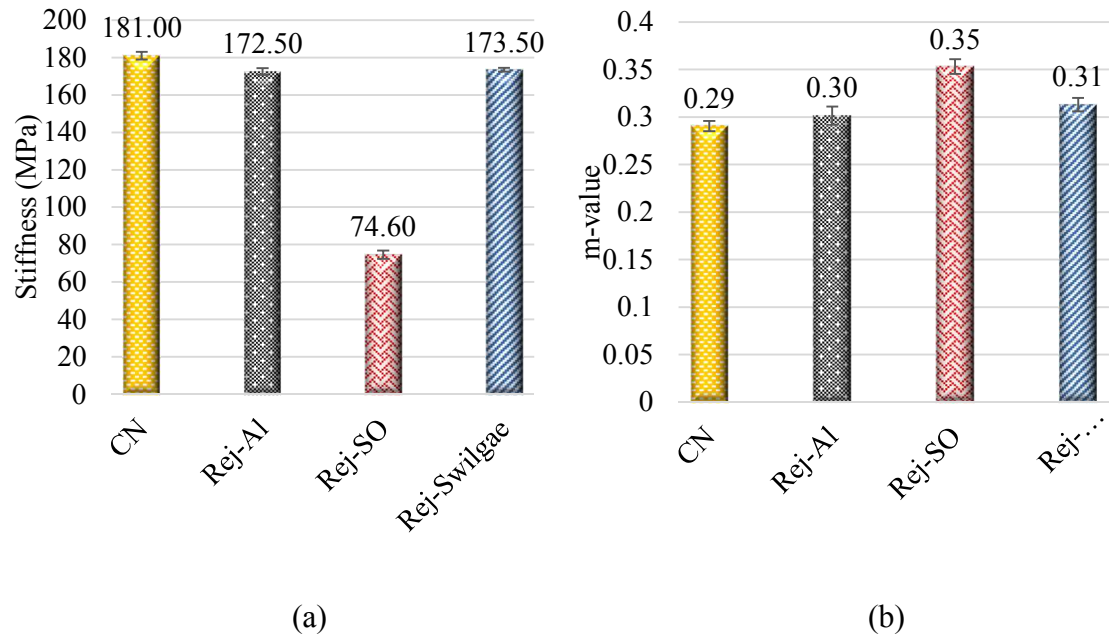


Figure 5-8 (a, b) Stiffness and m-Value Results for All Samples at -6 °C

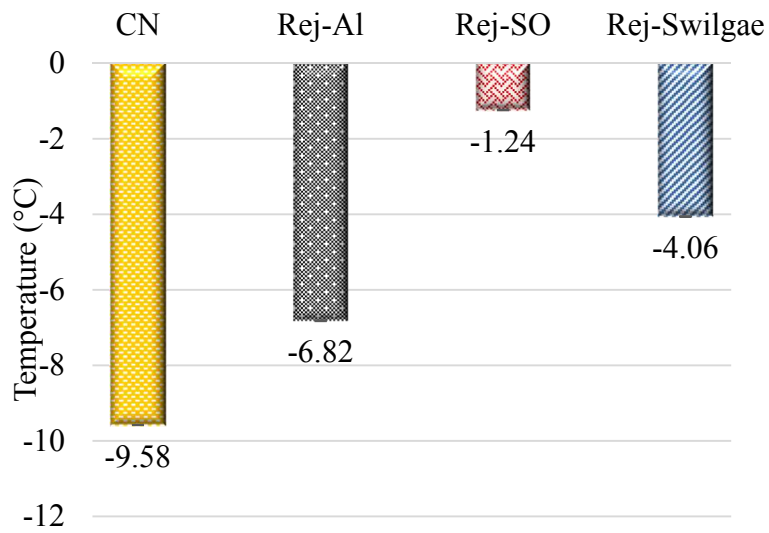


Figure 5-9 Delta T_c Values for All Samples

From Figure 5-9, the results showed that each rejuvenated sample has a ΔT_c value at a higher temperature (less negative) compared to the control sample. It was stated that a more negative change in ΔT_c suggests a higher level of aging in asphalt (Anderson, 2017). All rejuvenated samples delayed the aging effect by shifting the ΔT_c toward a less-negative value. This could be attributed to the rejuvenators' enhanced blending with aged bitumen. The lowest ΔT_c (least negative) was obtained by Rej-SO with approximately an 87% reduction of ΔT_c compared to control, followed by Rej-Swilgae and then Rej-Al. On the BBR tests, Rej-Al did not perform as well as it did on the DSR tests. While Rej-Al showed the best results in reducing stiffness at an intermediate temperature, it was not the best at low temperature in stiffness and m-value. In contrast, Rej-Swilgae showed consistent results in both the DSR and BBR test results. It showed medium performance at both intermediate and low temperatures, making it more durable than the others.

5.5.4 Fourier Transform Infrared (FTIR) Spectroscopy Test

In order to evaluate the aging phenomenon, FTIR analysis was conducted for all samples at 50-hour, 100-hour, and 200-hour aging conditions. As a measure of asphalt binder aging, the carboxyl functional group peak was measured for all samples. The background spectra were subtracted from the spectra of the samples before calculating the carbonyl index using Equation 5-9 (Hosseinnezhad et al., 2019). The results are shown in Figure 5-10.

$$\text{Carbonyl Index} = \frac{\text{Area under curve from 1680-1800}}{\text{Area under curve from 600-4000}} * 1000 \quad (5-9)$$

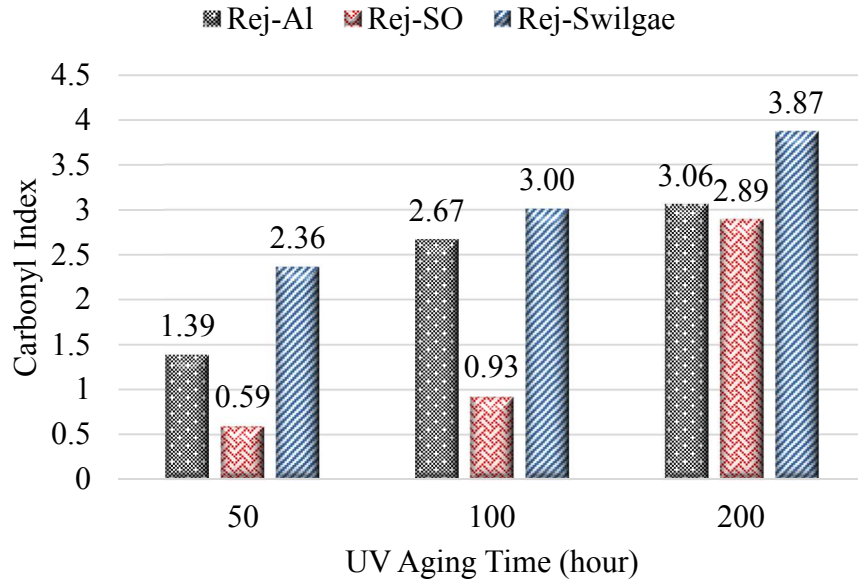


Figure 5-10 Carbonyl Index Value for All Samples Measured with FTIR

From Figure 5-10, the carbonyl index shows that all samples experienced increased carbonyl-index values after aging from 50 hours to 200 hours. In order to calculate the aging rate of each sample, the aging index was developed based on Equation 5-10; the results are shown in Figure 5-11.

$$\text{Aging Index} = \frac{\text{Carbonyl Index (200 h UV aging)} - \text{Carbonyl Index (50 h UV aging)}}{\text{Carbonyl Index (50 h UV aging)}}$$

(5-10)

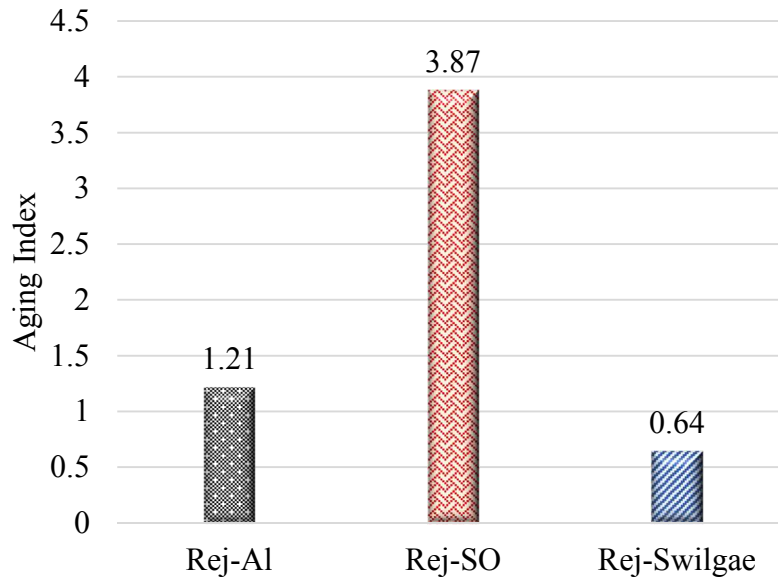


Figure 5-11 Aging Index Values for All Samples From 50 hours to 200 hours

Figure 5-11 shows that Rej-Swilgae had the lowest UV-aging index value compared to the other samples, meaning Rej-Swilgae had less damage due to UV aging. Rej-Swilgae showed 83% less aging compared to Rej-SO. The explanation for these differences in the UV-aging index is that some rejuvenators may contain residual biochar from their production (not all the biochar was filtered out); the biochar may adsorb UV and thus reduce the effects of UV aging. Similar results were obtained by some other studies where the rejuvenators produced from biomass showed aging resistance due to the presence of specific molecules in the rejuvenators (Hosseinnezhad et al., 2019; Hung et al., 2019).

5.5.5 Hamburg Wheel-Tracking Test

A Hamburg wheel-tracking test was conducted for mixture samples to evaluate the rejuvenators' effect on the samples' susceptibility to moisture damage. The results are shown in Figure 5-12.

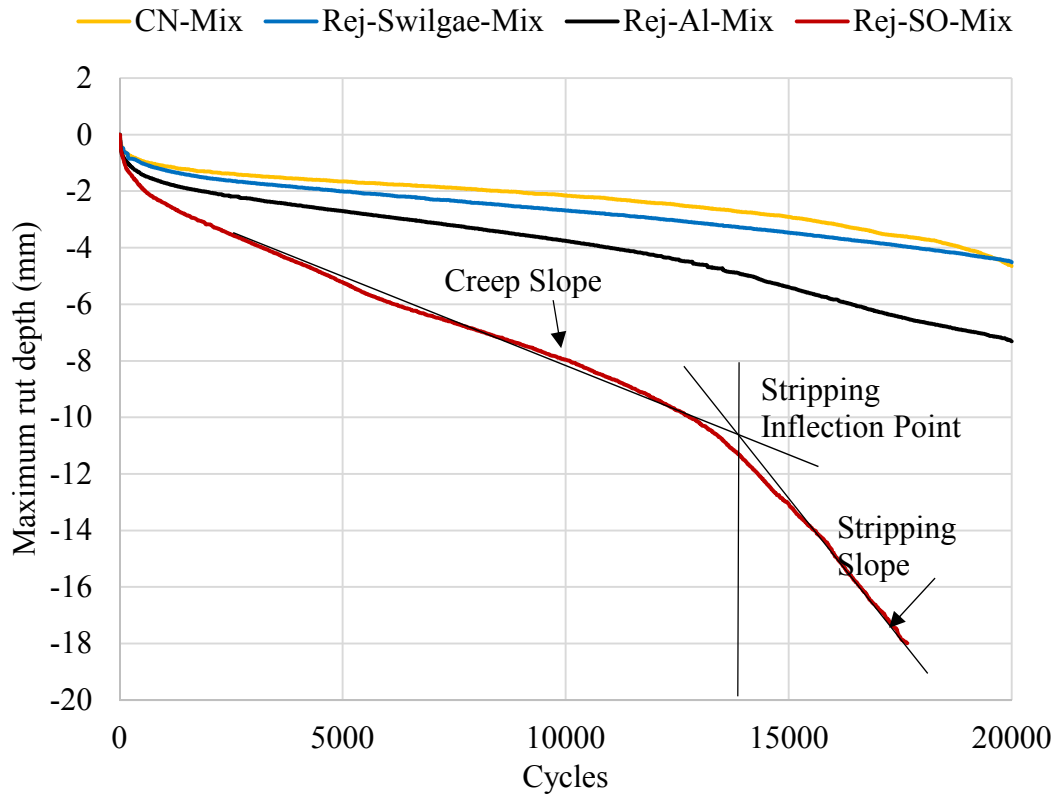


Figure 5-12 Hamburg Wheel-Tracking Test Results for All Samples

Figure 5-12 shows that not all rejuvenated samples showed moisture damage since some do not show a stripping slope and a stripping inflection point. Only Rej-SO-Mix showed moisture damage, which occurred after about 13800 cycles. From this test, the Rej-SO-Mix performed worst in susceptibility to moisture damage compared to all other samples.

5.5.6 Moisture-Induced Shear-Thinning Index (MISTI)

To develop MISTI, Rej-Al and Rej-Swilgae samples were tested to measure viscosity at different shear rates. For each sample, two scenarios were tested: a dry specimen, which was tested without moisture conditioning; and a wet specimen, which was tested after 24 hours of moisture conditioning at 60°C. Figures 5-13 (a) and 5-13 (b) show the viscosity versus shear rate for dry and wet specimens for Rej-Al and Rej-Swilgae.

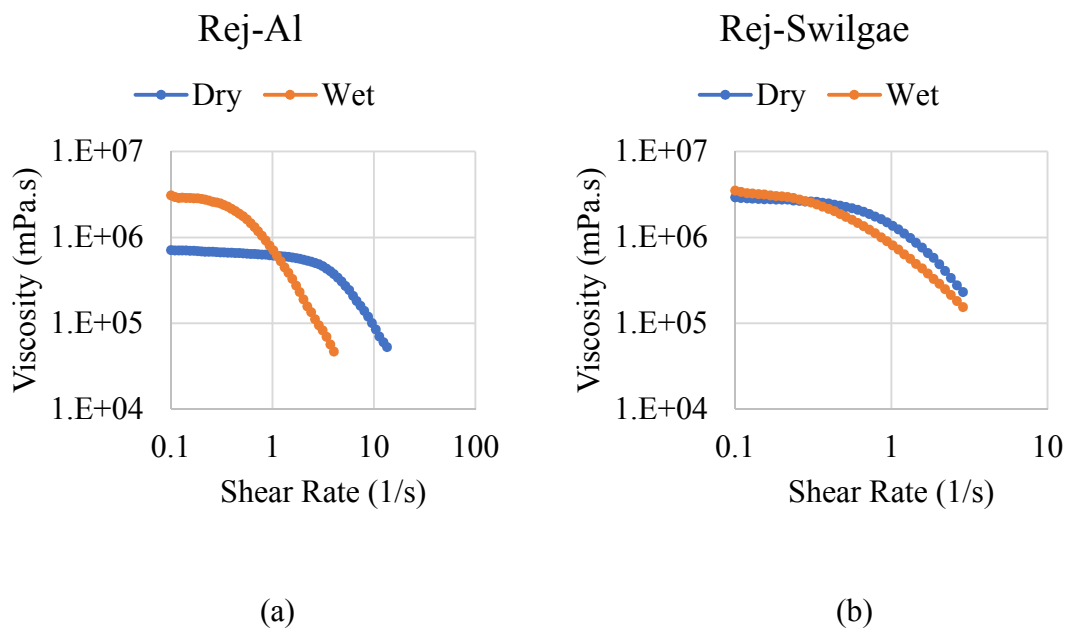


Figure 5-13 Viscosity Versus Shear Rate for Dry and Wet Specimens of (a) Rej-Al, and (b) Rej-Swilgae

In Figure 5-13 (a), sample Rej-Al shows a steeper slope after water conditioning. This phenomenon of Rej-Al could be attributed to having enhanced interaction between glass beads and bitumen. The Rej-Al graphs in Figure 5-13 (a) show increased viscosity after

water conditioning compared to the dry sample. From these results, Rej-Al is susceptible to moisture damage leading to increased viscosity. This observed behavior of Rej-Al could be explained by the fact that the Rej-Al molecules are more polarized, so they attract more water to strip the binder from glass beads, causing increased viscosity. Mousavi et al. (2016) showed that bio-modifier constituents with low polarizability showed less oxidative aging compared to constituents with high polarizability (Mousavi et al., 2016).

From Figure 5-13 (a-b), the slopes for both dry and wet tests were calculated and the MISTI was calculated using the formula in Equation 5-7. The results are shown in Figure 5-14.

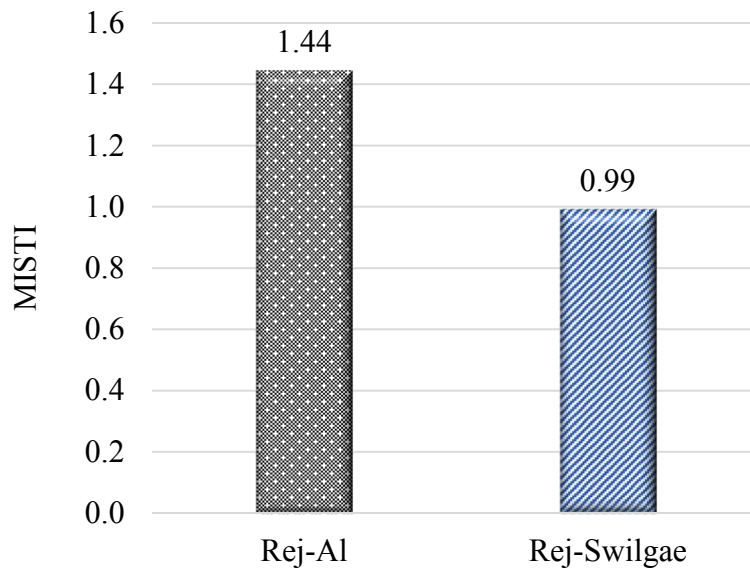


Figure 5-14 MISTI Values for Rejuvenators Rej-Al and Rej-Swilgae

Figure 5-14 shows that the MISTI value for Rej-Al is higher compared to Rej-Swilgae. A MISTI value closer to 1 is better in terms of durability issues. The difference in slope before and after water conditioning should be negligible for a well-performing rejuvenator. In terms of moisture-induced shear thinning, the Rej-Swilgae sample performed better than the Rej-Al sample.

5.5.7 DFT Evaluation of Rejuvenated Asphalt's Resistance to Post-Rejuvenation Chemical and Physical Changes

In this section, we use molecular and DFT analysis to examine the durability of the rejuvenated asphalt against moisture damage and oxidative aging. Using a computational approach, the polarizability factor is calculated for several molecules detected in each of Rej-Al, Rej-SO, and Rej-Swilgae. Polarizability is a conceptual DFT descriptor used to evaluate the reactivity of rejuvenator molecules toward oxidative agents and water. From an electronic perspective, polarizability is the response of the electron density toward an external electric field due to the proximity of other polar species. Higher polarizability for rejuvenator molecules lowers the rejuvenated asphalt's resistance to degradation when subjected to environmental factors such as oxygen-carrying components and moisture during the asphalt's service life.

For each of Rej-Al, Rej-SO, and Rej-Swilgae, Table 5-3 reports the DFT-based polarizability values of the six molecules with the highest contribution percentage detected by the mass spectrophotometer. The greatest average molecular weight for predominant molecules shown in this table is for those in Rej-SO, followed by Rej-Al,

and the least is for Rej-Swilgae. This agrees with the highest polarizability values for the Rej-SO compounds and the least polarizability values for molecules detected for Rej-Swilgae. The structural analysis of the molecules presents in Rej-SO reveals that the saturated and unsaturated hydrocarbon chains make up the major parts of the molecular structure. So, the electron densities of these molecules are easily affected by the external electric field generated due to the proximity of other species with dipoles, such as water molecules. The molecular species detected in Rej-Al are lighter than the Rej-SO molecules and have slightly lower polarizability values; the slightly lower polarizability can be explained by Rej-Al's comparatively lower content of molecules with hydrocarbon chains and loose electron density, which have higher conversion efficiency. The observed results show that the Rej-SO components have a higher propensity to interact with water molecules and oxygen, which increases the susceptibility to moisture damage and the aging of the rejuvenated product compared to the Rej-Al-rejuvenated asphalt.

In Figure 5-15, the polarizability values are compared for the first 6 compounds of each of Rej-Al, Rej-SO, Rej-Swilgae to provide insight into the durability of their respective rejuvenated asphalt binders. The lowest polarizability values in Table 5-3 are reported for Rej-Swilgae, which confirms the higher durability of the asphalt binder rejuvenated by Rej-Swilgae in comparison with either the Rej-SO or the Rej-Al modifier. The size of the main compounds in the mixed Rej-Swilgae is notably decreased compared to those in the other two rejuvenators. Therefore, the polar segments in the Swilgae molecules have a more pronounced effect on the retention of electrons within the molecular hydro-carbonic

parts. This characteristic decreases the chemical softness of the Rej-Swilgae molecules and makes electron cloud deformation more difficult, causing a lower tendency to interact with polar molecules in the environment.

Table 5-3 DFT-Based Polarizability Values for Molecular Species Identified in Rej-Al, Rej-SO, and Rej-Swilgae

Molecular Species		Formula	α (Bohr ³)	g/mol
Rej-Al				
1	9,12-Octadecadienoic acid (Z,Z)-	C ₁₈ H ₃₂ O ₂	211.85	Average MW= 183.3
2	n-Hexadecanoic acid	C ₁₆ H ₃₂ O ₂	191.75	
3	alpha.-Pinene	C ₁₀ H ₁₆	113.74	
4	alpha.-Terpineol	C ₁₀ H ₁₈ O	113.74	
5	Cyclohexene, 1-methyl-5-(1-methylethenyl)-, (R)-	C ₁₀ H ₁₆	108.97	
6	Camphene	C ₁₀ H ₁₆	105.11	
Rej-SO				
1	Cholesterol chloroformate	C ₂₈ H ₄₅ ClO ₂	321.96	Average MW=242.4
2	Linoelaidic acid	C ₁₈ H ₃₂ O ₂	212.24	

3	1,7-Dimethyl-4-(1-methylethyl) cyclodecane	C ₁₅ H ₃₀	167.06	
4	6-Dodecyne	C ₁₂ H ₂₂	137.40	
5	2,4-Decadienal	C ₁₀ H ₁₆ O	132.91	
6	Carbonic acid, propargyl cyclohexylmethyl ester	C ₁₁ H ₁₆ O ₃	125.71	
Rej-Swilgae				
1	Piperidine, 1-pentyl-	C ₁₀ H ₂₁ N	122.27	Average MW=115.3
2	Phenol, 4-ethyl-	<u>C₈H₁₀O</u>	89.04	
3	p-Cresol	C ₇ H ₈ O	76.55	
4	1-Ethyl-2-pyrrolidinone	<u>C₆H₁₁NO</u>	74.13	
5	Phenol	C ₆ H ₆ O	63.25	
6	2-Pyrrolidinone, 1-methyl-	C ₅ H ₉ NO	62.57	

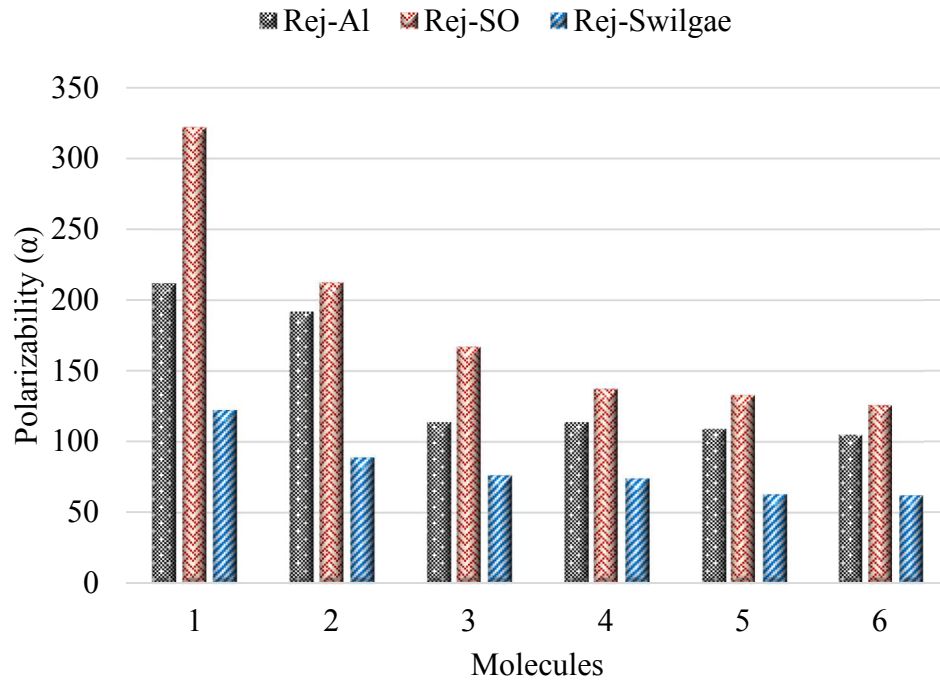


Figure 5-15 Polarizability Values for the First 6 Compounds of Each of Rej-Al, Rej-SO, and Rej-Swilgae

5.6 Conclusion

This study evaluates the durability of restored aged asphalt binders and relates their durability to molecular-level factors such as polarizability. This study shows that the high restoration capacity of a rejuvenator does not assure the durability of restored aged asphalt binder. Restoration capacity is mainly determined by rejuvenators' ability to penetrate to and peptize aged asphalt binder, while durability is related to rejuvenators' polarizability. Molecules with higher polarizability values are more prone to interact with environmental factors such as air and water, which may lead to accelerated aging and

moisture damage. This study's results show that while all studied rejuvenators performed well in revitalizing aged asphalt binder by increasing the crossover modulus and crossover frequency, the rejuvenators were not performing at the same level of improvement in resistance to moisture damage and UV aging.

From the DSR results, each rejuvenated sample showed a lower complex modulus and a higher phase-angle value compared to the control sample. Moreover, the crossover modulus and frequency values were higher than those of the control sample. In terms of crossover values, Rej-AI performed best compared to all other samples. In terms of stress relaxation and stiffness as measured by the bending beam rheometer test, Rej-SO performed the best, showing a lower ΔT_c value compared to Rej-AI and Rej-Swilgae. However, durability tests showed that the rejuvenator that was best performing at restoration was not the most durable. In fact, the moisture-induced shear-thinning test showed that Rej-AI changed significantly after 24hr conditioning in water. The Hamburg wheel-tracking test showed that Rej-SO was badly stripped and showed high susceptibility to moisture damage. The Rej-Swilgae overall was shown to have the highest durability in terms of resistance to both moisture damage and aging. Therefore, among three rejuvenators that could effectively restore aged asphalt binder's rheological properties, only one was found to be durable.

The study further related the observed durability measurement to molecular-level factors, using computational modeling. The results of computational modeling based on density functional theory showed that Rej-Swilgae had the lowest polarizability, followed by Rej-

Al, and that Rej-SO had the highest polarizability. The low polarizability values of Rej-Swilgae were reflected in its lower damage due to moisture, thus showing higher durability compared to the other rejuvenators.

It was shown that the rejuvenator that performed the best at revitalizing aged asphalt binder's rheological properties did not perform the best in terms of durability, as measured by resistance to moisture damage and aging. The outcome of the study provides insights for formulators of rejuvenators and the asphalt industry focusing on developing and selecting rejuvenators while ensuring that durability is not compromised.

Accordingly, the study results promote recycling and resource conservation by providing an in-depth understanding of the relation between rejuvenators' chemical structure and the durability of restored aged asphalt binder.

5.7 Acknowledgment

This research is sponsored by the National Science Foundation (Awards No: 1935723, and 1928807). The authors would like to acknowledge the invaluable assistance provided by Dr. Christian Hoover at Arizona State University for access to the UV chamber. The contents of this paper reflect the view of the authors, who are responsible for the facts and the accuracy of the data presented.

5.8 References

- AASHTO-T324-16. (2016). Hamburg wheel-track testing of compacted hot mix asphalt.
- Ahmed, R. B., & Hossain, K. (2020). Waste cooking oil as an asphalt rejuvenator: A state-of-the-art review. *Construction and building materials*, 230, 116985. doi:<https://doi.org/10.1016/j.conbuildmat.2019.116985>
- Anderson, R. M. (2017). Delta Tc: Concept and Use. *96th Annual Transportation Research Board Meeting, Washington, DC. Presentation.*
- ASTMD5404. (2017). Standard Practice for Recovery of Asphalt from Solution Using the Rotary Evaporator. *ASTM International, West Conshohocken, PA, 2017, www.astm.org.*
- ASTMD6648-08. (2016). Standard Test Method for Determining the Flexural Creep Stiffness of Asphalt Binder Using the Bending Beam Rheometer (BBR). *ASTM International, West Conshohocken, PA, 2016, www.astm.org.*
- ASTMD6925-15. (2015). Standard Test Method for Preparation and Determination of the Relative Density of Asphalt Mix Specimens by Means of the Superpave Gyratory Compactor. *ASTM International, West Conshohocken, PA, 2015, www.astm.org.*
- ASTMD7175-15. (2015). Standard Test Method for Determining the Rheological Properties of Asphalt Binder Using a Dynamic Shear Rheometer. *ASTM International, West Conshohocken, PA, 2015, www.astm.org.*
- ASTMD7405-15. (2015). Standard Test Method for Multiple Stress Creep and Recovery (MSCR) of Asphalt Binder Using a Dynamic Shear Rheometer. *ASTM International, West Conshohocken, PA, 2015, www.astm.org.*
- Becke, A. Density-functional thermochemistry. III. The role of exact exchange (1993) *J. Chem. Phys*, 98, 5648.
- Cao, X., Wang, H., Cao, X., Sun, W., Zhu, H., & Tang, B. (2018). Investigation of rheological and chemical properties asphalt binder rejuvenated with waste vegetable oil. *Construction and building materials*, 180, 455-463.
- Cavalli, M. C., Zaumanis, M., Mazza, E., Partl, M. N., & Poulidakos, L. D. (2018). Effect of ageing on the mechanical and chemical properties of binder from RAP treated with bio-based rejuvenators. *Composites, Part B*, 141, 174.
- Fini, E. H., Hosseinnezhad, S., Oldham, D. J., Chailleux, E., & Gaudefroy, V. (2017). Source dependency of rheological and surface characteristics of bio-modified asphalts. *Road Materials and Pavement Design*, 18(2), 408-424.

- Fini, E. H., Rajib, A. I., Oldham, D., Samieadel, A., & Hosseinezhad, S. (2020). The Role of Chemical Composition of Recycling Agents in Their Interactions with Oxidized Asphaltene Molecules. *Journal of Materials in Civil Engineering, Forthcoming*.
- Frisch, M., Trucks, G. W., Schlegel, H. B., Scuseria, G. E., Robb, M. A., Cheeseman, J. R., . . . Petersson, G. e. (2014). Gaussian~ 09 Revision D. 01.
- Haghshenas, H., Nabizadeh, H., Kim, Y.-R., & Santosh, K. (2016). Research on high-rap asphalt mixtures with rejuvenators and WMA additives.
- Hajj, E. Y., Sebaaly, P. E., & Shrestha, R. (2009). Laboratory evaluation of mixes containing recycled asphalt pavement (RAP). *Road Materials and Pavement Design, 10*(3), 495-517.
- Hajj, E. Y., Souliman, M. I., Alavi, M. Z., & Salazar, L. G. L. (2013). Influence of Hydrogreen Bioasphalt on Viscoelastic Properties of Reclaimed Asphalt Mixtures. *Transportation Research Record, 2371*(1), 13-22. doi:10.3141/2371-02
- Hill, B., Oldham, D., Behnia, B., Fini, E. H., Buttlar, W. G., & Reis, H. (2013). Low-temperature performance characterization of biomodified asphalt mixtures that contain reclaimed asphalt pavement. *Transp. Res. Rec., 2371*(1), 49.
- Hosseinezhad, S., Shakiba, S., Mousavi, M., Louie, S. M., Karnati, S. R., & Fini, E. H. (2019). Multi-scale Evaluation of Moisture Susceptibility of Bio-Modified Bitumen. *ACS Applied Bio Materials*.
- Hosseinezhad, S., Zadshir, M., Yu, X., Yin, H., Sharma, B. K., & Fini, E. (2019). Differential effects of ultraviolet radiation and oxidative aging on bio-modified binders. *Fuel, 251*, 45-56.
- Hung, A. M., Kazembeyki, M., Hoover, C. G., & Fini, E. H. (2019). Evolution of Morphological and Nanomechanical Properties of Bitumen Thin Films as a Result of Compositional Changes Due to Ultraviolet Radiation. *ACS Sustainable Chemistry & Engineering, 7*(21), 18005-18014. doi:10.1021/acssuschemeng.9b04846
- Hung, A. M., Pahlavan, F., Shakiba, S., Chang, S. L., Louie, S. M., & Fini, E. H. (2019). Preventing Assembly and Crystallization of Alkane Acids at the Silica–Bitumen Interface To Enhance Interfacial Resistance to Moisture Damage. *Industrial & Engineering Chemistry Research, 58*(47), 21542-21552.
- Lee, C., Yang, W., & Parr, R. G. (1988). Development of the Colle-Salvetti correlation-energy formula into a functional of the electron density. *Physical review B, 37*(2), 785.

- Li, H., Dong, B., Wang, W., Zhao, G., Guo, P., & Ma, Q. (2019). Effect of Waste Engine Oil and Waste Cooking Oil on Performance Improvement of Aged Asphalt. *Applied Sciences*, 9(9), 1767.
- Li, Y., Wu, S., Dai, Y., Li, C., Song, W., Li, H., . . . Shu, B. (2020). Transitions of component, physical, rheological and self-healing properties of petroleum bitumen from the loose bituminous mixture after UV irradiation. *Fuel*, 262, 116507. doi:<https://doi.org/10.1016/j.fuel.2019.116507>
- Ma, Y., Hu, W., Polaczyk, P. A., Han, B., Xiao, R., Zhang, M., & Huang, B. (2020). Rheological and aging characteristics of the recycled asphalt binders with different rejuvenator incorporation methods. *Journal of Cleaner Production*, 121249.
- Mousavi, M., Pahlavan, F., Oldham, D., Hosseinneshad, S., & Fini, E. H. (2016). Multiscale investigation of oxidative aging in biomodified asphalt binder. *J. Phys. Chem. C*, 120(31), 17224.
- NAPA. (2016). Recycled Materials and Warm-Mix Asphalt Usage. *National Asphalt Pavement Association*.
- Oldham, D. J., Fini, E. H., & Chailleux, E. (2015). Application of a bio-binder as a rejuvenator for wet processed asphalt shingles in pavement construction. *Construction and building materials*, 86, 75-84.
- Oldham, D. J., Rajib, A. I., Onochie, A., & Fini, E. H. (2019). Durability of bio-modified recycled asphalt shingles exposed to oxidation aging and extended sub-zero conditioning. *Constr. Build. Mater.*, 208, 543.
- Pahlavan, F., Hung, A., & Fini, E. H. (2018). Evolution of molecular packing and rheology in asphalt binder during rejuvenation. *Fuel*, 222, 457-464.
- Pahlavan, F., Samieadel, A., Deng, S., & Fini, E. (2019). Exploiting Synergistic Effects of Intermolecular Interactions To Synthesize Hybrid Rejuvenators To Revitalize Aged Asphalt. *ACS Sustainable Chemistry & Engineering*, 7(18), 15514-15525.
- Zadshir, M., Hosseinneshad, S., & Fini, E. H. (2019). Deagglomeration of oxidized asphaltenes as a measure of true rejuvenation for severely aged asphalt binder. *Construction and building materials*, 209, 416-424.
- Zadshir, M., Hosseinneshad, S., Ortega, R., Chen, F., Hochstein, D., Xie, J., . . . Fini, E. H. (2018). Application of a Biomodifier as Fog Sealants to Delay Ultraviolet Aging of Bituminous Materials. *J. Mater. Civ. Eng.*, 30(12), 04018310.
- Zaumanis, M., Mallick, R. B., & Frank, R. (2015). Evaluation of different recycling agents for restoring aged asphalt binder and performance of 100% recycled asphalt. *Mater. Struct.*, 48(8), 2475.

- Zhang, R., You, Z., Wang, H., Chen, X., Si, C., & Peng, C. (2018). Using bio-based rejuvenator derived from waste wood to recycle old asphalt. *Construction and building materials*, 189, 568-575.
- Zhang, R., You, Z., Wang, H., Ye, M., Yap, Y. K., & Si, C. (2019). The impact of bio-oil as rejuvenator for aged asphalt binder. *Construction and building materials*, 196, 134-143.
- Zhou, T., Kabir, S.F., Cao, L., Luan, H., Dong, Z., Fini, E.H., 2020. Comparing Effects of Physisorption and Chemisorption of Bio-oil onto Rubber Particles in Asphalt. *Journal of Cleaner Production*, 123112.
- Ziari, H., Moniri, A., Bahri, P., & Saghafi, Y. (2019). Evaluation of performance properties of 50% recycled asphalt mixtures using three types of rejuvenators. *Petroleum Science and Technology*, 1-7.

CHAPTER 6 ECONOMIC STUDY

6.1 Size of the Asphalt Global Market

According to Transparency Market Research, the global asphalt market is mainly dominated by paving products, which account for more than 50% of the consumption of asphalt. It is also predicted that the demand for asphalt in roofing products will grow consistently in the coming years (Transparency Market Research, 2020). The global asphalt market was valued at \$71.9 billion in 2017; the largest geographic region was the Asia Pacific, accounting for \$30.6 billion or 42.6% of the global market (The Business Reserach Company, 2018). It is estimated that the global asphalt market will reach \$112.01 billion by 2026, with a compound annual growth rate of 4.7% (Figure 6-1).

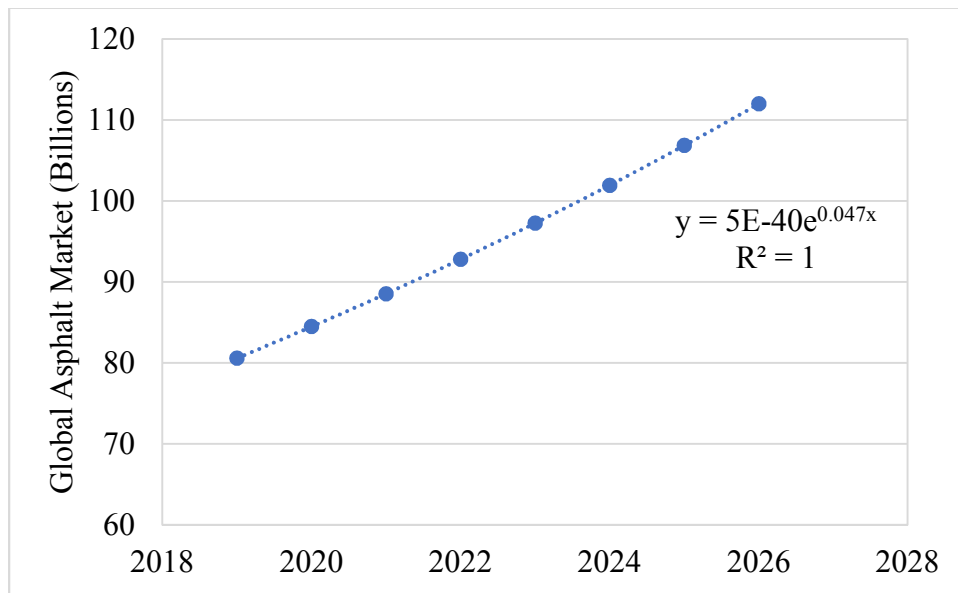


Figure 6-1 Size of Global Asphalt Market: Data for 2019-2020; Projections for 2021-2026 (Reports And Data, 2019)

6.2 Market for Recycled Asphalt

The global asphalt price is increasing and the supply from crude oil sources is being depleted, so the demand for recycled asphalt is expanding. Recycled materials including RAS, RAP, and ground tire rubber (GTR) are being used across the U.S. to meet the demand for asphalt (Figure 6-2).

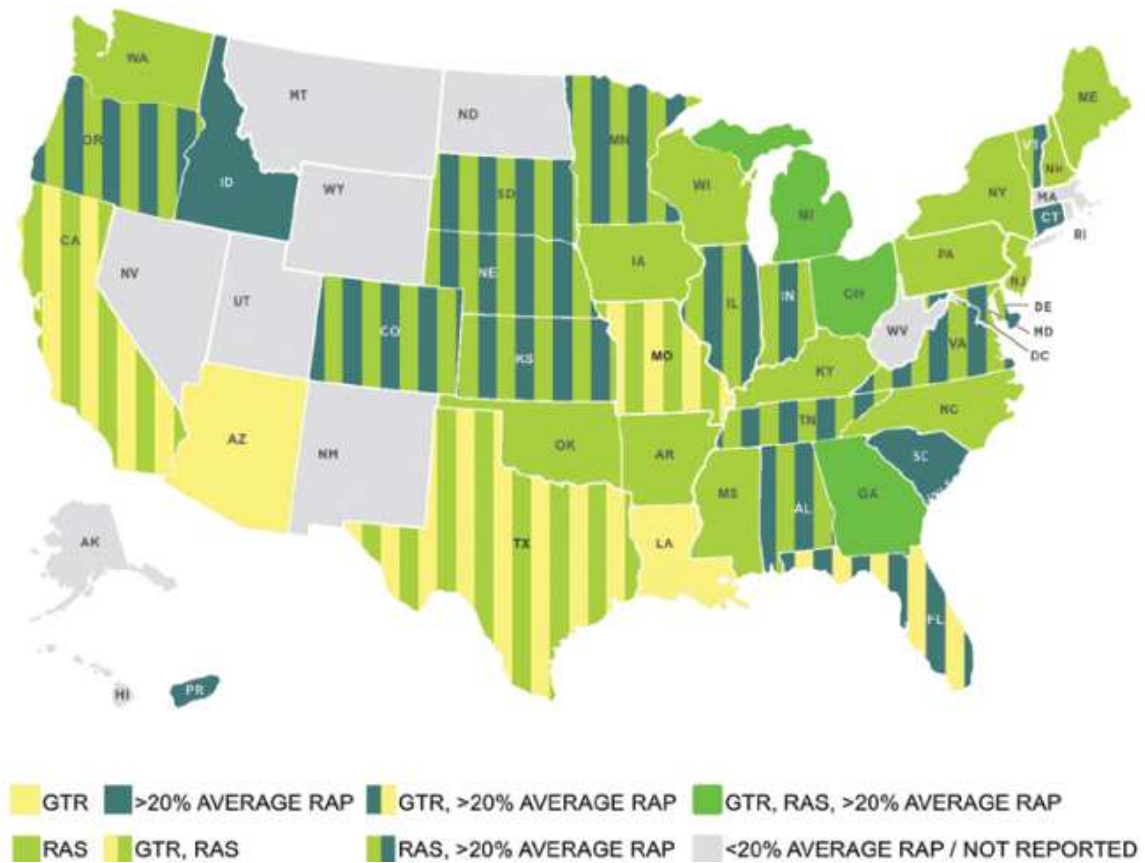


Figure 6-2 Reported Use of RAP, RAS, and GTR Across the U.S. (NCAT, Spring 2014)

6.3 Asphalt Recycling Agents

With the increased application of reclaimed asphalt pavements and recycled asphalt shingles in the asphalt pavement industry, the demand for recycling agents is expanding. Currently, there are various types of recycling agents available in the market (Table 6-1). However, a clear indicator to compare efficacy of recycling agents (Pahlavan et al., 2020) and measures to check for their effect on durability (Rajib et al., 2020) is highly missing.

Table 6-1 Types of Rejuvenators (NCAT, Spring 2014)

Category	Examples	Description
Paraffinic Oils	Waste Engine Oil (WEO) Waste Engine Oil Bottoms (WEOB) Valero VP 165® Storbit®	Refined used lubricating oils
Aromatic Extracts	Hydrolene® Reclamite® Cyclogen L® ValAro 130A®	Refined crude oil products with polar aromatic oil components
Naphthenic Oils	SonneWarmix RJ™ Ergon HyPrene®	Engineered hydrocarbons for asphalt modification
Triglycerides & Fatty Acids	Waste Vegetable Oil Waste Vegetable Grease Brown Grease Delta S*	Derived from vegetable oils *has other key chemical elements in addition to triglycerides and fatty acids
Tall Oils	Sylvaroad™ RP1000 Hydrogreen®	Paper industry byproducts

		Same chemical family as liquid antistrip agents and emulsifiers
Chemically balanced biomass	Swilgae	Animal waste and algae

6.4 A Bio-based Sustainable Rejuvenator

The proposed rejuvenator in this study is Rej-Swilgae, which is made from a co-liquefied 1:1 ratio of swine manure bio-oil and algae bio-oil. The effectiveness of Rej-Swilgae as a potential rejuvenator is discussed in the previous chapter. Rej-Swilgae is made from swine manure as an alternative to storing the swine manure in lagoons. Swine manure lagoons have detrimental environmental effects when the lagoons are poorly managed. For instance, water quality problems arise when nutrient uptake of the land is surpassed, and excess nutrients make their way to nearby surface and ground water resources (Kunz et al., 2009). Added to the above issue is the challenges associated to the inadequate manure storage and handling facilities (Laguë, 2020). It has been reported that leachate, runoff, leakage, and overflow from manure storage sites causes major environmental problems (Hatfield et al., 1998). Swine manure is rich in nutrients that pollute water bodies. When swine manure enters water streams, the nutrients contained in the swine manure give rise to the growth of aquatic plants; as a result, the water quality deteriorates

(Hatfield et al., 1998). Moreover, odor generated from swine manure is a source of air pollution (Wing et al., 2008).

In addition to a bio-oil from swine manure, the other component of Rej-Swilgae is a bio-oil from algae. Algae blooms remain a big problem for water bodies, as the algae become toxic to the water. It was reported that Lake Erie (Figure 6-3) experiences a harmful alga bloom every year and it continues to become worse (NSF Media, 2018).



Figure 6-3 A Freshwater Harmful Algal Bloom Turned Lake Erie a Bright Blue Green

(NSF Media, 2018)

Moreover, the number of algae blooms is expanding rapidly across the U.S. Figure 6-4 shows the current algae bloom locations across the U.S. (EWG, 2020)

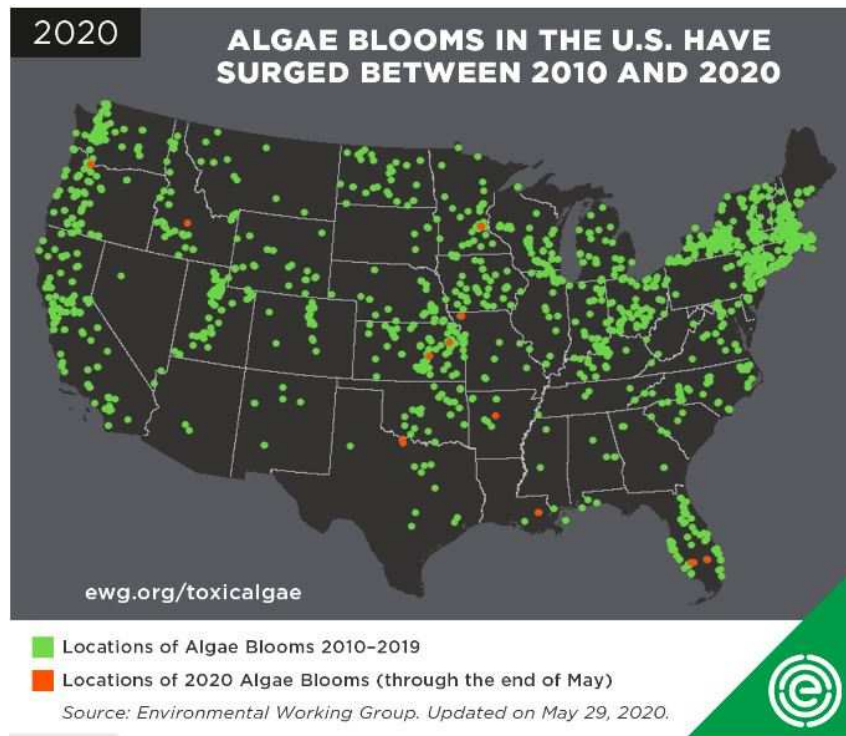


Figure 6-4 Algae Blooms Across the U.S. (EWG, 2020)

These algae blooms consist of cyanobacteria that produce the liver toxin microcystin. The blooms are expected to become worse as water bodies continue to be enriched by nitrogen and other nutrients from farm field runoff. That process causes more algae to grow, which sinks to the bottom when they die and contribute to oxygen depletion of the water (NSF Media, 2018). Another alternative source of algae is from algal biofuel production where the heavy residue after upgrading the bio-crude to fuel is disposed of. The latter application of heavy residue as rejuvenator can promote sustainability of biofuel production.

From the above discussion, swine manure and algae blooms are problems for the environment; when the leachate from manure storage comes to water bodies, the amount of algae production increases. Thus, a potential solution to the above-mentioned problems is required to reduce the amount of swine manure storage as well as algal bloom.

A rejuvenator such as Rej-Swilgae produced from swine manure and algae biomass is one of the potential value-added products of these wastes. The application of Rej-Swilgae in the recycling of aged asphalt could be a viable approach that promotes sustainability in the pavement industry. At the same time, it could solve many problems related to hog production, algal bloom, and the recycling of aged asphalt. It was reported that a rejuvenator produced from swine manure costs about \$0.54/gal. (National Hog Farmer, 2012), and the cost of co-liquified swine manure and algae-based rejuvenator is yet to be reported.

6.5 References

- EWG. (2020). News Reports of Algae Blooms, 2010 to Present. Retrieved from https://www.ewg.org/interactive-maps/algal_blooms/map/#.WzJO-9gzq7Y
- Hatfield, J., Brumm, M., & Melvin, S. (1998). Swine manure management. *Agricultural uses of municipal, animal, and industrial byproducts*, 44, 78-90.
- Kunz, A., Miele, M., & Steinmetz, R. L. R. (2009). Advanced swine manure treatment and utilization in Brazil. *Bioresource technology*, 100(22), 5485-5489.
- Laguë, C. (2020). CHALLENGES AND OPPORTUNITIES IN LIVESTOCK MANURE MANAGEMENT Retrieved from <https://pdfs.semanticscholar.org/6fc5/45f76877b3c4f95719a891f5112cd28686c6.pdf>
- National Hog Farmer. (2012). Making Asphalt from Swine Manure. Retrieved from <https://www.nationalhogfarmer.com/environment/making-asphalt-swine-manure>
- NCAT. (Spring 2014). Asphalt Technology News. Retrieved from <http://www.eng.auburn.edu/research/centers/ncat/info-pubs/newsletters/atnspring2014.pdf>
- NSF Media. (2018). Research reveals harmful algal blooms' daily cycles. Retrieved from https://www.nsf.gov/discoveries/disc_summ.jsp?cntn_id=299409
- Pahlavan, F., Rajib, A., Deng, S., Lammers, P., & Fini, E. H. (2020). Investigation of Balanced Feedstocks of Lipids and Proteins To Synthesize Highly Effective Rejuvenators for Oxidized Asphalt. *ACS Sustainable Chemistry & Engineering*.
- Rajib, A. I., Pahlavan, F., & Fini, E. H. (2020). Investigating Molecular-Level Factors That Affect the Durability of Restored Aged Asphalt Binder. *Journal of Cleaner Production*, 122501.
- Reports And Data. (2019). Bitumen Market To Reach USD 112.01 Billion By 2026. Retrieved from <https://www.globenewswire.com/news-release/2019/04/11/1802979/0/en/Bitumen-Market-To-Reach-USD-112-01-Billion-By-2026-Reports-And-Data.html>
- The Business Reserach Company. (2018). Asphalt Global Market Report 2018. Retrieved from <https://www.thebusinessresearchcompany.com/report/asphalt-global-market-report-2018>
- Transparency Market Research. (2020). Asphalt Market - Global Industry Analysis, Size, Share, Growth, Trends and Forecast, 2013 - 2019. Retrieved from <https://www.transparencymarketresearch.com/asphalt-market.html>

Wing, S., Horton, R. A., Marshall, S. W., Thu, K., Tajik, M., Schinasi, L., & Schiffman, S. S. (2008). Air pollution and odor in communities near industrial swine operations. *Environmental health perspectives*, 116(10), 1362-1368.

CHAPTER 7 CONCLUSIONS AND RECOMMENDATIONS

In general, this study discussed the rejuvenation mechanisms of differently sourced rejuvenators in revitalizing asphalts aged to various degree. This study develops the rheology-based indicators which relate to the molecular level phenomenon in the rejuvenation mechanism. Crossover modulus and crossover frequency are the rheology-based indicators that differentiated the rejuvenators from recycling agents. Moreover, the chemistry of the rejuvenator's is reflected in the rejuvenation efficiency and durability. Finally, based on the learning of chemistry, a chemically balanced rejuvenator, for instance, a balanced feedstock of lipid and protein is synthesized with superior rejuvenation properties.

These findings provide insight for developing effective rejuvenators without compromising the long-term durability of restored asphalt binder. In summary, the following conclusions are drawn, based on each chapter's results.

7.1 Rejuvenation Mechanism of Severely Aged Asphalt

In this study, the rejuvenation mechanism of severely aged asphalt binder such as those found in Recycled Asphalt Shingles (RAS) was studied. RAS was modified with a bio-rejuvenator produced from swine manure. The efficacy of bio-modified RAS was evaluated after oxidation and extended sub-zero conditioning of RAS. It was found that bio-modification improves the RAS properties that facilitate the recycling of RAS in new-pavement construction. Bio-modification reduced the viscosity of RAS-modified

asphalt and reduced its activation energy. The latter could be attributed to the bio-rejuvenator's reducing the intermolecular interaction of asphalt binder. Moreover, bio-modification reduced the agglomerates of RAS-oxidized particles, which was reflected in the lower activation energy of bio-modified RAS. Bio-modification further delayed the physical hardening of RAS-modified asphalt, which was evidenced by a higher fracture energy and failure strain of bio-modified RAS after 72 hours of conditioning at -18 °C. This result can be explained as bio-modification's delay of the molecular association and self-assembly of alkane chains in oxidized asphalt. The outcome of this study shows that the durability and performance of recycled asphalt shingles can be improved through bio-modification to facilitate its application as a sustainable construction practice.

7.2 Effect of Chemical Composition of Recycling Agents

The performance of recycling agents or rejuvenators in restoring aged asphalt depends on their chemical structures. In this study, thorough computational modeling and laboratory experiments were conducted to evaluate the rejuvenators' efficacy. It was found that some rejuvenators increased both the crossover modulus and crossover frequency, while others increased either the crossover modulus or the crossover frequency. The increased crossover modulus and crossover frequency, which is the point where storage modulus and loss modulus intersect, is a measure of rejuvenation efficacy. From computational modeling results, it was found that the effective rejuvenator's molecules are highly effective at deagglomerating oxidized asphaltenes. Moreover, this rejuvenator's molecules interact with oxidized asphalt in such a way that it restores the molecular

conformation in asphalt and reduces the size of asphaltene nanoaggregates. Based on this study's results, the efficacy of a recycling agent in the deagglomeration of oxidized asphaltenes was shown by a concurrent increase in both the crossover modulus and the crossover frequency; these two rheology-based indicators can be used together to distinguish recycling agents that can accurately be called rejuvenators.

7.3 Source Dependence of a Rejuvenator's Efficacy

In this study, a rejuvenator's efficacy was evaluated for both laboratory-prepared aged asphalt binder and field-reclaimed asphalt pavement. A total of eight differently sourced rejuvenators were used in this study. Both binder-level tests and mixture-level tests were performed to evaluate the efficacy of differently sourced rejuvenators. Moreover, a molecular-level investigation was performed to further explain laboratory observations. The source-dependency of the effectiveness of the rejuvenator was evaluated, based on the crossover modulus and the crossover frequency. While some rejuvenators only softened the binder, others revitalized both the viscous and elastic components of the aged binder, which was shown by increased values of the crossover modulus and the crossover frequency. Molecular simulation results indicated the selected molecules from a rejuvenator have the potential to peptize oxidized asphaltene and reduce the nano-aggregates' size. The effect of rejuvenators on mixture properties was reflected in a reduction of the number of gyratory compaction and a reduction in the crack propagation rate compared to aged mixture counterparts.

7.4 Durability Study of Rejuvenated Aged Asphalt

This study focused on the durability of the aged asphalt that was restored by using a chemically balanced rejuvenator. When a rejuvenator shows ability to restore aged asphalt, the rejuvenator's side effects on durability must be evaluated. In this study, laboratory experiments and computational modeling were performed to analyze the plausible side effects of rejuvenators. Results showed that a rejuvenator that is effective in restoring rheological properties of aged asphalt is not necessarily durable.

Computational analysis showed that while the restoration capacity of rejuvenators is related to their penetration into and peptizing of asphaltene nanoaggregates, durability is mainly related to their polarizability values. Rejuvenators with lower polarizability showed better resistance to aging and moisture damage. The outcome of the study facilitates the production of effective rejuvenators without compromising the long-term durability of the restored asphalt binder.

7.5 Recommendations

Based on the findings of this study, the following recommendations are made:

1. Study results showed significant source dependency and importance of the role of rejuvenators composition on its efficacy and durability. This in turn warrants future efforts to establish specifications including durability criteria.

2. Synthesis of highly effective rejuvenators from a balanced feedstock showed to be promising in this study, a cost-benefit analysis of the use of such rejuvenator is recommended for future study.
3. Simultaneous increase in both crossover modulus and crossover frequency values showed to properly differentiate recycling agents from rejuvenators. The extent of difference from those unaged values is referred to rejuvenating index (RI); This in turn warrants future efforts to establish passing thresholds for RI to facilitate and promote selection of effective rejuvenators.
4. This study used a 10% dosage of rejuvenators (by weight of asphalt binder) to evaluate the effects of rejuvenators. Future study is recommended to determine optimum dosage of various rejuvenators for aging level based on the passing threshold of RI.
5. This study used 25% reclaimed asphalt pavement (RAP) to evaluate rejuvenators' effectiveness. It is recommended that future studies evaluate rejuvenators' efficacy on mixtures containing 100% RAP.
6. Considering the significant positive economic and environmental effects of recycling of aged asphalt with rejuvenators, a complete life-cycle assessment of recycling with rejuvenators is recommended.
7. Most of the rejuvenation study was done in binder-level characterization. A robust mixture-level characterization should be conducted to expand the database of the rejuvenation study.

REFERENCES

- AASHTO-M320-05. (2002). Standard Specification for Performance Graded Asphalt Binder. *American Association of State Highway and Transportation Officials, Washington, D.C.*
- AASHTO-T315. (2012). Standard Method of Test for Determining the Rheological Properties of Asphalt Binder Using a Dynamic Shear Rheometer (DSR). *American Association of State Highway and Transportation Officials, Washington, DC.*
- AASHTO-T324-16. (2016). Hamburg wheel-track testing of compacted hot mix asphalt.
- AASHTO-TP91. (2015). Standard Method of Test for Determining Asphalt Binder Bond Strength by Means of the Binder Bond Strength (BBS) Test. *American Association of State Highway and Transportation Officials, Washington, DC.*
- AASHTOT315, T. (2012). 315 (2012).“*Standard Method of Test for Determining the Rheological Properties of Asphalt Binder Using a Dynamic Shear Rheometer (DSR).*” *American Association of State Highway and Transportation Officials, Washington, DC.*
- Abbas, A. R., Mannan, U. A., & Dessouky, S. (2013). Effect of recycled asphalt shingles on physical and chemical properties of virgin asphalt binders. *Construction and building materials, 45*, 162-172.
- Ahmed, R. B., & Hossain, K. (2020). Waste cooking oil as an asphalt rejuvenator: A state-of-the-art review. *Construction and building materials, 230*, 116985. doi:<https://doi.org/10.1016/j.conbuildmat.2019.116985>
- Al-Mansoori, T., Norambuena-Contreras, J., Micaelo, R., & Garcia, A. (2018). Self-healing of asphalt mastic by the action of polymeric capsules containing rejuvenators. *Construction and building materials, 161*, 330-339.
- Al-Qadi, I. L., Aurangzeb, Q., Carpenter, S. H., Pine, W. J., & Trepanier, J. (2012). *Impact of high RAP contents on structural and performance properties of asphalt mixtures* (0197-9191). Retrieved from
- Anderson, D. A., Christensen, D. W., Bahia, H. U., Dongre, R., Sharma, M. G., Antle, C. E., & Button, J. (1994). Binder characterization and evaluation, volume 3: Physical characterization. *Strategic Highway Research Program, National Research Council, Report No. SHRP-A-369.*
- Anderson, M. (2017). Delta Tc: Concept and Use. *Transportation Research Board Annual Meeting, Washington, DC, January 2017.*
- Anderson, R. M. (2017). Delta Tc: Concept and Use. *96th Annual Transportation Research Board*

Meeting, Washington, DC. Presentation.

- Apeageyi, A. K., Grenfell, J. R., & Airey, G. D. (2014). Moisture-induced strength degradation of aggregate–asphalt mastic bonds. *Road Materials and Pavement Design*, 15(sup1), 239-262.
- ASTM, D. (2007). 3279 Standard Test Method for n-Heptane Insolubles. *Annual Book of Standards*.
- ASTMD2872-12e1. (2012). Standard Test Method for Effect of Heat and Air on a Moving Film of Asphalt (Rolling Thin-Film Oven Test). *ASTM International, West Conshohocken, PA, 2012, www.astm.org*.
- ASTMD3279. (2007). Standard Test Method for n-Heptane Insolubles. *Annual Book of Standards*.
- ASTMD4402. (2015). *Standard test method for viscosity determination of asphalt at elevated temperatures using a rotational viscometer*. Paper presented at the American Society for Testing and Materials.
- ASTMD5404. (2017). Standard Practice for Recovery of Asphalt from Solution Using the Rotary Evaporator. *ASTM International, West Conshohocken, PA, 2017, www.astm.org*.
- ASTMD6373-13. (2013). Standard Specification for Performance Graded Asphalt Binder. *ASTM International, West Conshohocken, PA, 2013, www.astm.org*.
- ASTMD6521-13. (2013). Standard Practice for Accelerated Aging of Asphalt Binder Using a Pressurized Aging Vessel (PAV). *ASTM International, West Conshohocken, PA*.
- ASTMD6648-08. (2016). Standard Test Method for Determining the Flexural Creep Stiffness of Asphalt Binder Using the Bending Beam Rheometer (BBR). *ASTM International, West Conshohocken, PA, 2016, www.astm.org*.
- ASTMD6723. (2012). Standard Test Method for Determining the Fracture Properties of Asphalt Binder in Direct Tension (DT). *West Conshohocken, PA; ASTM International, 2012. doi:https://doi.org/10.1520/D6723-12*
- ASTMD6925-15. (2015). Standard Test Method for Preparation and Determination of the Relative Density of Asphalt Mix Specimens by Means of the Superpave Gyratory Compactor. *ASTM International, West Conshohocken, PA, 2015, www.astm.org*.
- ASTMD7175-15. (2015). Standard Test Method for Determining the Rheological Properties of Asphalt Binder Using a Dynamic Shear Rheometer. *ASTM International, West Conshohocken, PA, 2015, www.astm.org*.

- ASTMD7405-15. (2015). Standard Test Method for Multiple Stress Creep and Recovery (MSCR) of Asphalt Binder Using a Dynamic Shear Rheometer. *ASTM International, West Conshohocken, PA, 2015, www.astm.org.*
- Bajpai, P. (2020). Top Factors That Affect the Price of Oil. Retrieved from <https://www.investopedia.com/articles/investing/072515/top-factors-reports-affect-price-oil>.
- Bahia, H. U. M. (1992). Low-temperature isothermal physical hardening of asphalt cements.
- Becke, A. Density-functional thermochemistry. III. The role of exact exchange (1993) *J. Chem. Phys, 98*, 5648.
- Begley, J., & Landes, J. (1972). The J integral as a fracture criterion *Fracture Toughness: Part II*: ASTM International.
- Bowers, B. F., Huang, B., & Shu, X. (2014). Refining laboratory procedure for artificial RAP: A comparative study. *Construction and building materials, 52*, 385-390.
- Cao, W., Wang, Y., & Wang, C. (2019). Fatigue characterization of bio-modified asphalt binders under various laboratory aging conditions. *Construction and building materials, 208*, 686-696.
- Cao, X., Wang, H., Cao, X., Sun, W., Zhu, H., & Tang, B. (2018). Investigation of rheological and chemical properties asphalt binder rejuvenated with waste vegetable oil. *Construction and building materials, 180*, 455-463.
- Cavalli, M. C., Zaumanis, M., Mazza, E., Partl, M. N., & Poulidakos, L. D. (2018). Effect of ageing on the mechanical and chemical properties of binder from RAP treated with bio-based rejuvenators. *Composites, Part B, 141*, 174.
- Cavalli, M. C., Zaumanis, M., Mazza, E., Partl, M. N., & Poulidakos, L. D. (2018). Effect of ageing on the mechanical and chemical properties of binder from RAP treated with bio-based rejuvenators. *Composites Part B: Engineering, 141*, 174-181.
- Chen, J.-S., Lee, C.-T., & Lin, Y.-Y. (2018). Characterization of a Recycling Agent for Restoring Aged Bitumen. *Journal of Materials in Civil Engineering, 30*(8), 05018003.
- Dinh, B. H., Park, D.-W., & Le, T. H. M. (2018). Effect of rejuvenators on the crack healing performance of recycled asphalt pavement by induction heating. *Construction and building materials, 164*, 246-254.
- Dony, A., Ziyani, L., Drouadaine, I., Pouget, S., Faucon-Dumont, S., Simard, D., . . . Boulange, L. (2016). *MURE National Project: FTIR spectroscopy study to assess ageing of asphalt mixtures*. Paper presented at the Proceedings of the E&E congress.

- Elkashaf, M. E. (2017), Using soybean-derived materials to rejuvenate reclaimed asphalt pavement (RAP) binders and mixtures. *Graduate Theses and Dissertations*. 15514. <https://lib.dr.iastate.edu/etd/15514>
- Elkashaf, M., Jones, D., Jiao, L., Williams, R. C., & Harvey, J. (2019). Using thermal analytical techniques to study rejuvenators and rejuvenated reclaimed asphalt pavement (RAP) binders. *Energy & Fuels*.
- Elkashaf, M., Podolsky, J., Williams, R. C., & Cochran, E. W. (2018). Introducing a soybean oil-derived material as a potential rejuvenator of asphalt through rheology, mix characterisation and Fourier Transform Infrared analysis. *Road Materials and Pavement Design*, 19(8), 1750-1770.
- Elkashaf, M., Williams, R. C., & Cochran, E. (2018). Effect of Asphalt Binder Grade and Source on the Extent of Rheological Changes in Rejuvenated Binders. *Journal of Materials in Civil Engineering*, 30(12), 04018319.
- Elseifi, M. A., Salari, S., Mohammad, L. N., Hassan, M., Daly, W. H., & Dessouky, S. (2012). New approach to recycling asphalt shingles in hot-mix asphalt. *Journal of Materials in Civil Engineering*, 24(11), 1403-1411.
- EWG. (2020). News Reports of Algae Blooms, 2010 to Present. Retrieved from https://www.ewg.org/interactive-maps/algal_blooms/map/#.WzJO-9gzq7Y
- Figueroa, A. S., Velasquez, R., Reyes, F. A., & Bahia, H. (2013). Effect of water conditioning for extended periods on the properties of asphalt binders. *Transportation Research Record*, 2372(1), 34-45.
- Fini, E. H., Al-Qadi, I. L., Abu-Lebdeh, T., & Masson, J.-F. (2011). Use of surface energy to evaluate adhesion of bituminous crack sealants to aggregates. *American Journal of Engineering and Applied Sciences*, 4(2).
- Fini, E. H., Hosseinneshad, S., Oldham, D. J., Chailleux, E., & Gaudefroy, V. (2017). Source dependency of rheological and surface characteristics of bio-modified asphalts. *Road Materials and Pavement Design*, 18(2), 408-424.
- Fini, E. H., Kalberer, E. W., Shahbazi, A., Basti, M., You, Z., Ozer, H., & Aurangzeb, Q. (2011). Chemical characterization of biobinder from swine manure: Sustainable modifier for asphalt binder. *J. Mater. Civ. Eng.*, 23(11), 1506.
- Fini, E., Rajib, A. I., Oldham, D., Samieadel, A., & Hosseinneshad, S. (2020). Role of Chemical Composition of Recycling Agents in Their Interactions with Oxidized Asphaltene Molecules. *Journal of Materials in Civil Engineering*, 32(9), 04020268.
- Frisch, M., Trucks, G. W., Schlegel, H. B., Scuseria, G. E., Robb, M. A., Cheeseman, J. R., . . . Petersson, G. e. (2014). Gaussian~ 09 Revision D. 01.

- Gevrenov, J. (2008). Utilization of recycled asphalt shingles in hot-mix asphalt. *Recycling Shingles into Roads, US EPA Perspective. Presentation Made at the Missouri Showcase.*
- Gong, M., Yang, J., Zhang, J., Zhu, H., & Tong, T. (2016). Physical–chemical properties of aged asphalt rejuvenated by bio-oil derived from biodiesel residue. *Construction and building materials, 105*, 35-45.
- Haghshenas, H., Nabizadeh, H., Kim, Y.-R., & Santosh, K. (2016). Research on high-rap asphalt mixtures with rejuvenators and WMA additives.
- Hajj, E. Y., Sebaaly, P. E., & Shrestha, R. (2009). Laboratory evaluation of mixes containing recycled asphalt pavement (RAP). *Road Materials and Pavement Design, 10*(3), 495-517.
- Hajj, E. Y., Souliman, M. I., Alavi, M. Z., & Salazar, L. G. L. (2013). Influence of Hydrogreen Bioasphalt on Viscoelastic Properties of Reclaimed Asphalt Mixtures. *Transportation Research Record, 2371*(1), 13-22. doi:10.3141/2371-02
- Hansen, K. R., & Newcomb, D. E. (2011). Asphalt pavement mix production survey on reclaimed asphalt pavement, reclaimed asphalt shingles, and warm-mix asphalt usage: 2009-2010. *Information Series, 138*, 21.
- Hasan, M. R. M., You, Z., Porter, D., & Goh, S. W. (2015). Laboratory moisture susceptibility evaluation of WMA under possible field conditions. *Construction and building materials, 101*, 57-64.
- Hatfield, J., Brumm, M., & Melvin, S. (1998). Swine manure management. *Agricultural uses of municipal, animal, and industrial byproducts, 44*, 78-90.
- Hesp, S. A. M., & Subramani, S. (2009). *Another look at the bending beam rheometer for specification grading of asphalt cements.*
- Hill, B., Oldham, D., Behnia, B., Fini, E. H., Buttlar, W. G., & Reis, H. (2013). Low-temperature performance characterization of biomodified asphalt mixtures that contain reclaimed asphalt pavement. *Transp. Res. Rec., 2371*(1), 49.
- Hosseinnezhad, S., Kabir, S.F., Oldham, D., Mousavi, M., Fini, E.H., 2019. Surface functionalization of rubber particles to reduce phase separation in rubberized asphalt for sustainable construction. *Journal of Cleaner Production 225*, 82-89.
- Hosseinnezhad, S., Shakiba, S., Mousavi, M., Louie, S. M., Karnati, S. R., & Fini, E. H. (2019). Multi-scale Evaluation of Moisture Susceptibility of Bio-Modified Bitumen. *ACS Applied Bio Materials.*
- Hosseinnezhad, S., Zadshir, M., Yu, X., Yin, H., Sharma, B. K., & Fini, E. (2019). Differential effects of ultraviolet radiation and oxidative aging on bio-modified binders. *Fuel, 251*, 45-56.

- Huang, S.-C., Qin, Q., Grimes, W. R., Pauli, A. T., & Glaser, R. (2014). Influence of rejuvenators on the physical properties of RAP binders. *Journal of Testing and Evaluation*, 43(3), 594-603.
- Hung, A. M., Kazembeyki, M., Hoover, C. G., & Fini, E. H. (2019). Evolution of Morphological and Nanomechanical Properties of Bitumen Thin Films as a Result of Compositional Changes Due to Ultraviolet Radiation. *ACS Sustainable Chemistry & Engineering*, 7(21), 18005-18014. doi:10.1021/acssuschemeng.9b04846
- Hung, A. M., Mousavi, M., Pahlavan, F., & Fini, E. H. (2017). Intermolecular Interactions of Isolated Bio-Oil Compounds and Their Effect on Bitumen Interfaces. *ACS Sustainable Chemistry & Engineering*, 5(9), 7920-7931.
- Hung, A. M., Pahlavan, F., Shakiba, S., Chang, S. L., Louie, S. M., & Fini, E. H. (2019). Preventing Assembly and Crystallization of Alkane Acids at the Silica–Bitumen Interface To Enhance Interfacial Resistance to Moisture Damage. *Industrial & Engineering Chemistry Research*, 58(47), 21542-21552.
- Jennings, P., Desando, M., Raub, M., Moats, R., Mendez, T., Stewart, F., . . . Smith, J. (1992). NMR spectroscopy in the characterization of eight selected asphalts. *Fuel science & technology international*, 10(4-6), 887-907.
- Ji, J., Yao, H., Suo, Z., You, Z., Li, H., Xu, S., & Sun, L. (2017). Effectiveness of vegetable oils as rejuvenators for aged asphalt binders. *Journal of Materials in Civil Engineering*, 29(3), D4016003.
- Kabir, S.F., Mousavi, M., Fini, E.H., 2020. Selective adsorption of bio-oils' molecules onto rubber surface and its effects on stability of rubberized asphalt. *Journal of Cleaner Production* 252, 119856.
- Khan, M. K., Sarkar, B., Zeb, H., Yi, M., & Kim, J. (2017). Simultaneous breaking and conversion of petroleum emulsions into synthetic crude oil with low impurities. *Fuel*, 199, 135-144.
- Kriz, P., Stastna, J., & Zanzotto, L. (2008). Glass transition and phase stability in asphalt binders. *Road Materials and Pavement Design*, 9(sup1), 37-65.
- Kunz, A., Miele, M., & Steinmetz, R. L. R. (2009). Advanced swine manure treatment and utilization in Brazil. *Bioresource technology*, 100(22), 5485-5489.
- Kupareva, A., Mäki-Arvela, P. i., Grénman, H., Eränen, K., Sjöholm, R., Reunanen, M., & Murzin, D. Y. (2012). Chemical characterization of lube oils. *Energy & Fuels*, 27(1), 27-34.
- Laguë, C. (2020). CHALLENGES AND OPPORTUNITIES IN LIVESTOCK MANURE MANAGEMENT Retrieved from

- <https://pdfs.semanticscholar.org/6fc5/45f76877b3c4f95719a891f5112cd28686c6.pdf>
- Lee, C., Yang, W., & Parr, R. G. (1988). Development of the Colle-Salvetti correlation-energy formula into a functional of the electron density. *Physical review B*, 37(2), 785.
- Lei, Z., Bahia, H., & Yi-qiu, T. (2015). Effect of bio-based and refined waste oil modifiers on low temperature performance of asphalt binders. *Construction and building materials*, 86, 95-100.
- Lesueur, D. (2009). The colloidal structure of bitumen: Consequences on the rheology and on the mechanisms of bitumen modification. *Advances in colloid and interface science*, 145(1-2), 42-82.
- Levine, B. G., Stone, J. E., & Kohlmeyer, A. (2011). Fast analysis of molecular dynamics trajectories with graphics processing units—Radial distribution function histogramming. *Journal of computational physics*, 230(9), 3556-3569.
- Li, D. D., & Greenfield, M. L. (2014). Chemical compositions of improved model asphalt systems for molecular simulations. *Fuel*, 115, 347-356.
- Li, H., Dong, B., Wang, W., Zhao, G., Guo, P., & Ma, Q. (2019). Effect of Waste Engine Oil and Waste Cooking Oil on Performance Improvement of Aged Asphalt. *Applied Sciences*, 9(9), 1767.
- Li, J., Xiao, F., Zhang, L., & Amirhanian, S. N. (2019). Life cycle assessment and life cycle cost analysis of recycled solid waste materials in highway pavement: A review. *Journal of Cleaner Production*, 233, 1182-1206.
- Li, Y., Wu, S., Dai, Y., Li, C., Song, W., Li, H., . . . Shu, B. (2020). Transitions of component, physical, rheological and self-healing properties of petroleum bitumen from the loose bituminous mixture after UV irradiation. *Fuel*, 262, 116507. doi:<https://doi.org/10.1016/j.fuel.2019.116507>
- Liu, X., Cao, F., Xiao, F., & Amirhanian, S. (2018). BBR and DSR Testing of Aging Properties of Polymer and Polyphosphoric Acid-Modified Asphalt Binders. *Journal of Materials in Civil Engineering*, 30(10), 04018249.
- Loeber, L., Muller, G., Morel, J., & Sutton, O. (1998). Bitumen in colloid science: a chemical, structural and rheological approach. *Fuel*, 77(13), 1443-1450.
- Lowry, E., Sedghi, M., & Goual, L. (2017). Polymers for asphaltene dispersion: Interaction mechanisms and molecular design considerations. *Journal of Molecular Liquids*, 230, 589-599.
- Lu, X., & Isacson, U. (2002). Effect of ageing on bitumen chemistry and rheology. *Construction and building materials*, 16(1), 15-22.

- Ma, Y., Hu, W., Polaczyk, P. A., Han, B., Xiao, R., Zhang, M., & Huang, B. (2020). Rheological and aging characteristics of the recycled asphalt binders with different rejuvenator incorporation methods. *Journal of Cleaner Production*, 121249.
- Marasteanu, M., Austin, J., & Moon, K. H. (2012). Recycling Asphalt Roofing Shingles in Asphalt Pavements. *CURA Reporter*, 42(1).
- Marasteanu, M., Buttlar, W., Bahia, H., Williams, C., Moon, K. H., Teshale, E. Z., . . . Paulino, G. (2012). Investigation of low temperature cracking in asphalt pavements national pooled fund study–phase II.
- Maupin, G. W. (2010). Investigation of the use of tear-off shingles in asphalt concrete (No. VTRC 10-R23). Virginia Transportation Research Council.
- Mirhosseini, A. F., Kavussi, A., Tahami, S. A., & Dessouky, S. (2018). Characterizing temperature performance of bio-modified binders containing RAP binder. *Journal of Materials in Civil Engineering*, 30(8), 04018176.
- Mogawer, W., Bennert, T., Daniel, J. S., Bonaquist, R., Austerman, A., & Booshehrian, A. (2012). Performance characteristics of plant produced high RAP mixtures. *Road Materials and Pavement Design*, 13(sup1), 183-208.
- Mogawer, W. S., Booshehrian, A., Vahidi, S., & Austerman, A. J. (2013). Evaluating the effect of rejuvenators on the degree of blending and performance of high RAP, RAS, and RAP/RAS mixtures. *Road Materials and Pavement Design*, 14(sup2), 193-213.
- Moghadas Nejad, F., Azarhoosh, A., Hamed, G. H., & Roshani, H. (2014). Rutting performance prediction of warm mix asphalt containing reclaimed asphalt pavements. *Road Materials and Pavement Design*, 15(1), 207-219.
- Mohammadafzali, M., Ali, H., Sholar, G. A., Rilko, W. A., & Baqersad, M. (2018). Effects of Rejuvenation and Aging on Binder Homogeneity of Recycled Asphalt Mixtures. *Journal of Transportation Engineering, Part B: Pavements*, 145(1), 04018066.
- Morgan, T., Alvarez-Rodriguez, P., George, A., Herod, A., & Kandiyoti, R. (2010). Characterization of Maya crude oil maltenes and asphaltenes in terms of structural parameters calculated from nuclear magnetic resonance (NMR) spectroscopy and laser desorption– mass spectroscopy (LD– MS). *Energy & Fuels*, 24(7), 3977-3989.
- Mousavi, M., Pahlavan, F., Oldham, D., Hosseinneshad, S., & Fini, E. H. (2016). Multiscale investigation of oxidative aging in biomodified asphalt binder. *The Journal of Physical Chemistry C*, 120(31), 17224-17233.

- NAPA. (1996). Pavements, Recycling Hot-Mix Asphalt National Asphalt Pavement Association (NAPA). Information Series 123.–Lanham (MD), 1996.–28 p.
- NAPA. (2016). Recycled Materials and Warm-Mix Asphalt Usage. *National Asphalt Pavement Association*.
- National Hog Farmer. (2012). Making Asphalt from Swine Manure. Retrieved from <https://www.nationalhogfarmer.com/environment/making-asphalt-swine-manure>
- Nayak, P., & Sahoo, U. C. (2017). Rheological, chemical and thermal investigations on an aged binder rejuvenated with two non-edible oils. *Road Materials and Pavement Design*, 18(3), 612-629.
- NCAT. (Spring 2014). Asphalt Technology News. Retrieved from <http://www.eng.auburn.edu/research/centers/ncat/info-pubs/newsletters/atnspring2014.pdf>
- NCDOT. (2018). Monthly Terminal Asphalt Binder & Fuel FOB Prices. *North Carolina Department of Transportation Business Partner Resources*.
- Noureldin, A. S., & Wood, L. E. (1989). Variations in molecular size distribution of virgin and recycled asphalt binders associated with aging. *Transportation Research Record*(1228).
- NSF Media. (2018). Research reveals harmful algal blooms' daily cycles. Retrieved from https://www.nsf.gov/discoveries/disc_summ.jsp?cntn_id=299409
- Oldham, D. J., Fini, E. H., & Chailleux, E. (2015). Application of a bio-binder as a rejuvenator for wet processed asphalt shingles in pavement construction. *Construction and building materials*, 86, 75-84.
- Oldham, D. J., Rajib, A. I., Onochie, A., & Fini, E. H. (2019). Durability of bio-modified recycled asphalt shingles exposed to oxidation aging and extended sub-zero conditioning. *Construction and building materials*, 208, 543-553. doi:<https://doi.org/10.1016/j.conbuildmat.2019.03.017>
- Oldham, D., Qu, X. Q., Wang, H., & Fini, E. H. (2020). Investigating Change of Polydispersity and Rheology of Crude Oil and Bitumen Due to Asphaltene Oxidation. *Energy & Fuels*.
- Ongel, A., & Hugener, M. (2015). Impact of rejuvenators on aging properties of bitumen. *Construction and building materials*, 94, 467-474.
- Pahlavan, F., Hung, A., & Fini, E. H. (2018). Evolution of molecular packing and rheology in asphalt binder during rejuvenation. *Fuel*, 222, 457-464.
- Pahlavan, F., Hung, A. M., Zadshir, M., Hosseinneshad, S., & Fini, E. H. (2018). Alteration of π -Electron Distribution To Induce Deagglomeration in Oxidized

- Polar Aromatics and Asphaltenes in an Aged Asphalt Binder. *ACS Sustainable Chem. Eng.*, 6(5), 6554.
- Pahlavan, F., Mousavi, M., Hung, A. M., & Fini, E. H. (2018). Characterization of oxidized asphaltenes and the restorative effect of a bio-modifier. *Fuel*, 212, 593-604.
- Pahlavan, F., Samieadel, A., Deng, S., & Fini, E. (2019). Exploiting Synergistic Effects of Intermolecular Interactions To Synthesize Hybrid Rejuvenators To Revitalize Aged Asphalt. *ACS Sustainable Chemistry & Engineering*, 7(18), 15514-15525.
- Pahlavan, F., Rajib, A., Deng, S., Lammers, P., & Fini, E. H. (2020). Investigation of Balanced Feedstocks of Lipids and Proteins To Synthesize Highly Effective Rejuvenators for Oxidized Asphalt. *ACS Sustainable Chemistry & Engineering*.
- Plimpton, S. (1995). Fast parallel algorithms for short-range molecular dynamics. *Journal of computational physics*, 117(1), 1-19.
- Puello, J., Afanasjeva, N., & Alvarez, M. (2013). Thermal properties and chemical composition of bituminous materials exposed to accelerated ageing. *Road Materials and Pavement Design*, 14(2), 278-288.
- Qin, Q., Schabron, J. F., Boysen, R. B., & Farrar, M. J. (2014). Field aging effect on chemistry and rheology of asphalt binders and rheological predictions for field aging. *Fuel*, 121, 86-94.
- Rajib, A. I., Pahlavan, F., & Fini, E. H. (2020). Investigating Molecular-Level Factors That Affect the Durability of Restored Aged Asphalt Binder. *Journal of Cleaner Production*, 122501.
- Reports And Data. (2019). Bitumen Market To Reach USD 112.01 Billion By 2026. Retrieved from <https://www.globenewswire.com/news-release/2019/04/11/1802979/0/en/Bitumen-Market-To-Rreach-USD-112-01-Billion-By-2026-Reports-And-Data.html>
- Rice, J. R. (1968). A path independent integral and the approximate analysis of strain concentration by notches and cracks. *Journal of applied mechanics*, 35(2), 379-386.
- Romero, P., Youtcheff, J., & Stuart, K. (1999). Low-temperature physical hardening of hot-mix asphalt. *Transportation Research Record: Journal of the Transportation Research Board*(1661), 22-26 %@ 0361-1981.
- Samieadel, A., Høgsaa, B., & Fini, E. H. (2018). Examining the Implications of Wax-Based Additives on the Sustainability of Construction Practices: Multiscale Characterization of Wax-Doped Aged Asphalt Binder. *ACS Sustainable Chemistry & Engineering*, 7(3), 2943-2954.

- Samieadel, A., Høgsaa, B., & Fini, E. H. (2019). Examining the Implications of Wax-Based Additives on the Sustainability of Construction Practices: Multiscale Characterization of Wax-Doped Aged Asphalt Binder. *ACS Sustainable Chem. Eng.*, 7(3), 2943.
- Samieadel, A., Høgsaa, B., & Fini, E. H. (2019). *Investigation of Thermo-Mechanical Characteristics of Wax-doped Aged Asphalt Binder*. Retrieved from
- Samieadel, A., Oldham, D., & Fini, E. H. (2017). Multi-scale characterization of the effect of wax on intermolecular interactions in asphalt binder. *Construction and building materials*, 157, 1163-1172.
- Shen, J., Amirhanian, S., & Tang, B. (2007). Effects of rejuvenator on performance-based properties of rejuvenated asphalt binder and mixtures. *Construction and building materials*, 21(5), 958-964.
- Shen, J., Amirhanian, S. N., & Lee, S.-J. (2007). HP-GPC characterization of rejuvenated aged CRM binders. *Journal of Materials in Civil Engineering*, 19(6), 515-522.
- Stempihar, J., & Kaloush, K. (2017). A Notched Disk Crack Propagation Test for Asphalt Concrete. *MOJ Civil Eng*, 3(5), 00084.
- Su, J.-F., Schlangen, E., & Wang, Y.-Y. (2015). Investigation the self-healing mechanism of aged bitumen using microcapsules containing rejuvenator. *Construction and building materials*, 85, 49-56.
- Sun, H., Mumby, S. J., Maple, J. R., & Hagler, A. T. (1994). An ab initio CFF93 all-atom force field for polycarbonates. *Journal of the American Chemical society*, 116(7), 2978-2987.
- The Business Reserach Company. (2018). Asphalt Global Market Report 2018. Retrieved from <https://www.thebusinessresearchcompany.com/report/asphalt-global-market-report-2018>
- Tran, N. H., Taylor, A., & Willis, R. (2012). Effect of rejuvenator on performance properties of HMA mixtures with high RAP and RAS contents. *NCAT Report*, 12-05.
- Transparency Market Research. (2020). Asphalt Market - Global Industry Analysis, Size, Share, Growth, Trends and Forecast, 2013 - 2019. Retrieved from <https://www.transparencymarketresearch.com/asphalt-market.html>
- Ungerer, P., Rigby, D., Leblanc, B., & Yiannourakou, M. (2014). Sensitivity of the aggregation behaviour of asphaltenes to molecular weight and structure using molecular dynamics. *Molecular Simulation*, 40(1-3), 115-122.
- Waldman, M., & Hagler, A. T. (1993). New combining rules for rare gas van der Waals parameters. *Journal of Computational Chemistry*, 14(9), 1077-1084.

- Wang, D., Wang, L., Gu, X., & Zhou, G. (2013). Effect of basalt fiber on the asphalt binder and mastic at low temperature. *Journal of materials in civil engineering*, 25(3), 355-364 %@ 0899-1561.
- West, R. C., & Willis, J. R. (2014). *Case Studies on Successful Utilization of Reclaimed Asphalt Pavement and Recycled Asphalt Shingles in Asphalt Pavements*. Retrieved from
- West, R. C., Willis, J. R., & Marasteanu, M. O. (2013). *Improved mix design, evaluation, and materials management practices for hot mix asphalt with high reclaimed asphalt pavement content* (Vol. 752): Transportation Research Board.
- Wiehe, I. A. (2008). *Process chemistry of petroleum macromolecules*: CRC press.
- Williams, B. A., Copeland, A., & Ross, T. C. Asphalt Pavement Industry Survey on Recycled Materials and Warm-Mix Asphalt Usage: 2017; National Asphalt Pavement Association: Lanham, MD, USA, 2018; No. Information Series, 138.
- Williams, B. A., Willis, J. R., & Ross, T. C. (2019). Asphalt Pavement Industry Survey on Recycled Materials and Warm-Mix Asphalt Usage: 2018 (No. IS 138 (9e)).
- Williams, R. C., Cascione, A. A., Yu, J., Haugen, D., Marasteanu, M., & McGraw, J. (2013). Performance of recycled asphalt shingles in hot mix asphalt.
- Wing, S., Horton, R. A., Marshall, S. W., Thu, K., Tajik, M., Schinasi, L., & Schiffman, S. S. (2008). Air pollution and odor in communities near industrial swine operations. *Environmental health perspectives*, 116(10), 1362-1368.
- Yang, Z., Zhang, X., Zhang, Z., Zou, B., Zhu, Z., Lu, G., . . . Yu, H. (2018). Effect of Aging on Chemical and Rheological Properties of Bitumen. *Polymers*, 10(12).
- Yaseen, S., & Mansoori, G. A. (2018). Asphaltene aggregation due to waterflooding (A molecular dynamics study). *Journal of Petroleum Science and Engineering*, 170, 177-183.
- You, Z., Mills-Beale, J., Fini, E., Goh, S. W., & Colbert, B. (2011). Evaluation of low-temperature binder properties of warm-mix asphalt, extracted and recovered RAP and RAS, and bioasphalt. *Journal of Materials in Civil Engineering*, 23(11), 1569-1574.
- Zadshir, M., Hosseinezhad, S., & Fini, E. H. (2019). Deagglomeration of oxidized asphaltenes as a measure of true rejuvenation for severely aged asphalt binder. *Construction and building materials*, 209, 416-424.
- Zadshir, M., Hosseinezhad, S., Ortega, R., Chen, F., Hochstein, D., Xie, J., . . . Fini, E. H. (2018). Application of a Biomodifier as Fog Sealants to Delay Ultraviolet Aging of Bituminous Materials. *J. Mater. Civ. Eng.*, 30(12), 04018310.

- Zaumanis, M., & Mallick, R. B. (2015). Review of very high-content reclaimed asphalt use in plant-produced pavements: state of the art. *International Journal of Pavement Engineering*, 16(1), 39-55.
- Zaumanis, M., Mallick, R. B., & Frank, R. (2015). Evaluation of different recycling agents for restoring aged asphalt binder and performance of 100% recycled asphalt. *Materials and Structures*, 48(8), 2475-2488.
- Zaumanis, M., Mallick, R. B., & Frank, R. (2015). Evaluation of different recycling agents for restoring aged asphalt binder and performance of 100% recycled asphalt. *Mater. Struct.*, 48(8), 2475.
- Zeng, M., Li, J., Zhu, W., & Xia, Y. (2018). Laboratory evaluation on residue in castor oil production as rejuvenator for aged paving asphalt binder. *Construction and building materials*, 193, 276-285.
- Zhang, R., You, Z., Wang, H., Chen, X., Si, C., & Peng, C. (2018). Using bio-based rejuvenator derived from waste wood to recycle old asphalt. *Construction and building materials*, 189, 568-575.
- Zhang, R., You, Z., Wang, H., Ye, M., Yap, Y. K., & Si, C. (2019). The impact of bio-oil as rejuvenator for aged asphalt binder. *Construction and building materials*, 196, 134-143.
- Zhao, S., Nahar, S. N., Schmets, A. J., Huang, B., Shu, X., & Scarpas, T. (2015). Investigation on the microstructure of recycled asphalt shingle binder and its blending with virgin bitumen. *Road Materials and Pavement Design*, 16(sup1), 21-38.
- Zhou, F. (2013). Balanced RAP/RAS mix design and performance evaluation for project-specific service conditions.
- Zhou, T., Kabir, S.F., Cao, L., Luan, H., Dong, Z., Fini, E.H., 2020. Comparing Effects of Physisorption and Chemisorption of Bio-oil onto Rubber Particles in Asphalt. *Journal of Cleaner Production*, 123112.
- Zhu, H., Xu, G., Gong, M., & Yang, J. (2017). Recycling long-term-aged asphalts using bio-binder/plasticizer-based rejuvenator. *Construction and building materials*, 147, 117-129.
- Ziari, H., Moniri, A., Bahri, P., & Saghafi, Y. (2019). Evaluation of performance properties of 50% recycled asphalt mixtures using three types of rejuvenators. *Petroleum Science and Technology*, 1-7.

APPENDIX A

PREVIOUSLY PUBLISHED WORK

Chapters 2, 3, 4 and 5 are all studies that have been submitted for peer review and chapter 2, and 5 are published in the journal. The references are given below:

1. Oldham, D. J., Rajib, A. I., Onochie, A., & Fini, E. H. (2019). Durability of bio-modified recycled asphalt shingles exposed to oxidation aging and extended sub-zero conditioning. *Constr. Build. Mater.*, 208, 543.
2. Fini, E. H., Rajib, A. I., Oldham, D., Samieadel, A., & Hosseinnzhad, S. (2020). Role of Chemical Composition of Recycling Agents in Their Interactions with Oxidized Asphaltene Molecules. *Journal of Materials in Civil Engineering*.
3. Rajib, A. I., Samieadel, A., Zalgout, A., Kaloush, K., Sharma, B., Fini, E. H., (2020). Evaluating Efficacy of Asphalt Rejuvenators via a Multi-scale Characterization. *Journal of Road Materials and Pavement Design*.
4. Rajib, A. I., Pahlavan, F., & Fini, E. H. (2020). Investigating Molecular-Level Factors That Affect the Durability of Restored Aged Asphalt Binder. *Journal of Cleaner Production*, 122501.

Reference 1 (chapter 2) paper, Amirul Rajib wrote the introduction of the paper and build the manuscript. He ran the laboratory experiment for the rotational viscometer to measure the viscosity. He analyzed and prepared the necessary plots for viscosity analysis. He also calculated the shear susceptibility and activation energy of the studied samples. Daniel Oldham and Albert Onochie prepared the other sections of the paper. Dr. Fini provided guidelines and interpretation of the results. His contribution to that study made the foundation of the paper. This contribution was significant enough. The outcome of the

study perfectly fits this dissertation which focused on the rejuvenation mechanism of severely aged asphalt such as Recycled Asphalt Shingles (RAS).

Reference 4 (chapter 5) paper, Amirul Rajib performed all the laboratory experiments and write-up of the manuscript. Farideh Pahlavan performed the computational modeling analysis of the study. Dr. Elham H. Fini provided the research topic and guidance for conducting the research and results interpretation.

APPENDIX B

COAUTHOR PERMISSION FOR PREVIOUSLY PUBLISHED WORK

All coauthor has granted their permission for the use of the previously published or future publishable work to be used for the dissertation of Amirul Rajib.

BIOGRAPHICAL SKETCH

Amirul Islam Rajib grew up in Homna, Comilla, Bangladesh. He received his elementary and secondary education from Homna Govt. Primary School and Homna Govt. High School. He received his higher secondary education from Tejgaon College, Dhaka. He received his Bachelor of Science Degree in Civil Engineering from Khulna University of Engineering and Technology (KUET) in June 2011. He received his Master of Science Degree in Civil Engineering from North Carolina Agricultural and Technical State University in May 2016. He started his Ph.D. work in 2016 at NC A&T State and accompanied his PhD advisor to Arizona State University in 2019. His research under the supervision of Dr. Elham Fini focuses on the rejuvenation mechanism of aged asphalt binder. During his Ph.D. studies, Amirul Rajib has authored and co-authored 6 technical articles in prestigious journals such as Journal of Cleaner Production, ACS Sustainable Chemistry and Engineering, and Construction and Building Materials. During his Ph.D. studies at ASU, he received Engineering Graduate Fellowship from The Ira A. Fulton Schools of Engineering.